Research into the use of Multibeam Backscatter for Seabed Classification in the Outer Thames Estuary

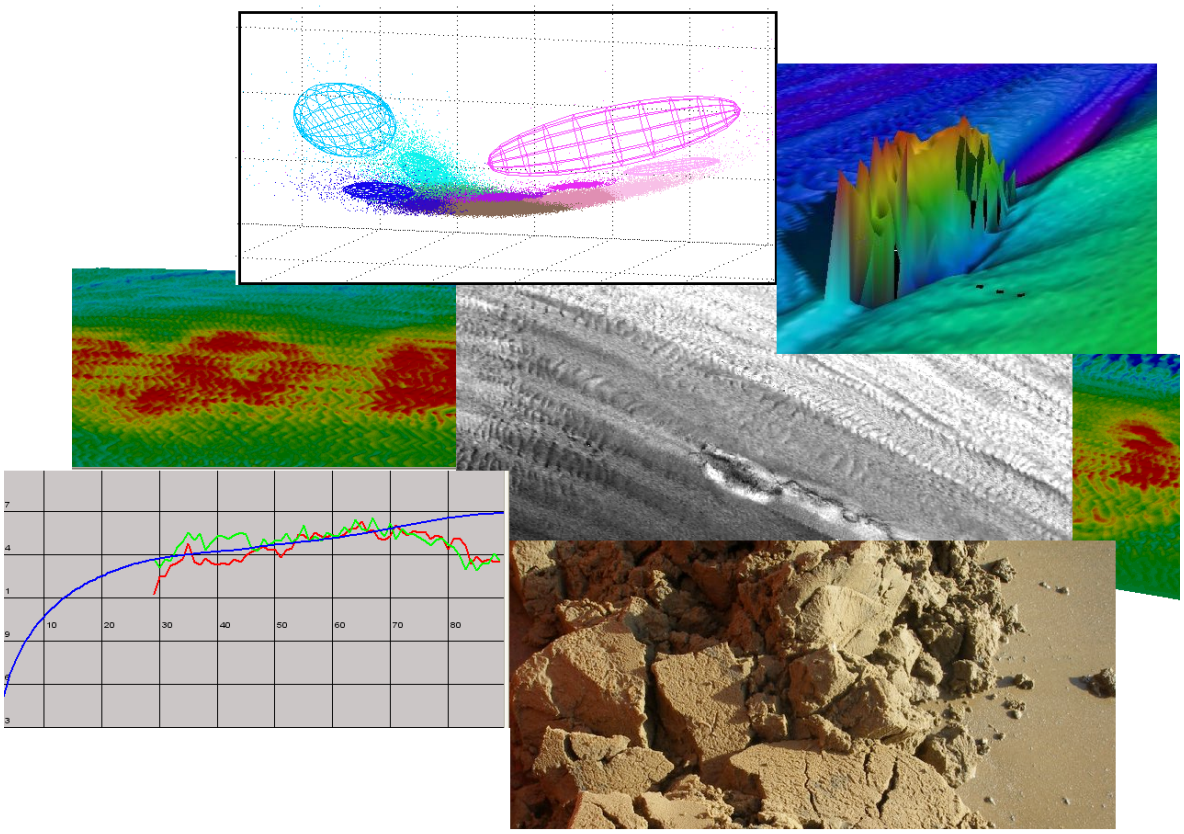

Siddhi Joshi

MSc Hydrographic Surveying

Civil, Environmental and Geomatic Engineering

University College London

Table of Contents

Acknowledgements

This project has been carried out working with the Port of London Authority and Cefas, and has been funded by the Marine Aggregate Levy Sustainability Fund (MALSF) MSc bursary scheme. It has resulted after a great effort to obtain results, process data and researching a range of topics to help understand this new and developing area of science.

I would like to thank all the staff of the Port of London Authority Hydrographic Department for their support and for making data collection in the North Edinburgh Channel possible, including John Dillon-Leetch, Alex Mortley and Jim Powell. I would like to thank Dr. Jonathan Iliffe, the academic supervisor, for providing advice throughout the year and Prof. Paul Leonard for the moral support.

Thanks also go to Kate Francis, Patricia Falconer, Alison Challiss and Koen Vanstaen of Cefas for guidance. Also thanks to Jason Sadler of the Geodata Institute, Southampton and Vince Grove and Charlotte Brown of Gardline for providing the Thames REC data. I would like to thank Glenda Wyatt and Chris Elliott of Quester Tangent Corporation, British Columbia, for their continuous support throughout my endeavours and the excellent customer service. Some data processing using the Geocoder software has been courtesy of Duncan Mallace of Net Survey and Luciano Fonseca of the University of New Hampshire. Special thanks also go to Dave Maddock of Hypack and Larry Mayer for the help with Geocoder. Other thanks include to Bob Foster-Smith of Envision Mapping, Rob Clark of the Sussex Sea Fisheries Committee, Chris Malzone of Reson and Kimberly Bridge of Hanson Marine for answering my questions. Also, special thanks to Dr. Jian Guo Liu and Dr. Philippa Mason of Imperial for allowing me to do the “Image Processing and GIS” course during the first term. Finally, I would also like to thank my family for their patience and understanding throughout.

List of Figures

Figure 14: The ARA parameter are extracted from different domains to help summarise the key properties which are affected by backscatter strength (from Fonseca, 2006).

Figure 15: Map of the Port of London Authority limits, with the North Edinburgh Channel, Princes Channel (after PLA, 2004).

Figure 16: The North Edinburgh Channel Sand Placement Plan, with the cells where material has been dumped highlighted. The restricted area in the west is in a biologically sensitive area and that on the east is the exclusion zone for the Hawksdale.

Figure 17 and 18: Data Collection for the first survey took place aboard the Yantlet with the second and third surveys aboard the Verifier (from PLA, 2008b).

Figures 19 and 20: Bathymetric editing in Hysweep shows the Hawksdale wreck and the stepped terraces in the North Edinburgh Channel.

Figures 21 and 22: Multibeam Bathymetry from before and after the sand placement.

Figure 23: A multibeam bathymetric difference model of the North Edinburgh Channel highlights the area where dredged material has been placed.

Figure 24: The fully corrected Reson 8125 multibeam beam averaged-backscatter mosaic clearly shows the area of relocation in the centre.

Figure 25: The fully corrected Reson 8125 multibeam snippet mosaic.

Figures 26: The pseudo-sidescan mosaics were constructed in Hyscan using the Reson 8101 hsx files.

Figure 27: The corrected pseudosidescan mosaic constructed in Geocoder in Hypack 2008 using the Reson 8101 hsx files. In contrast to the Hyscan mosaic, the Geocoder mosaic allows interpretation to be possible. The relocation area clearly shows the dredged material.

Figure:28a and 28b: The Patch AVO tool allows model inversion of a 30 ping x half swath width patch. The outer domain is not considered as it has a negligible contribution.

Figure 29: The Near Far AVO of the Reson 8125 data shows highlight features on the seabed, with lower values from the deeper region in the east. The area where sand placement has occurred is showing medium backscatter values in this domain.

Figure 30: The Far AVO of the Reson 8125 data shows highlight different features on the seabed. The area where sand placement has occurred is showing the highest backscatter values in this domain, with the outer south east area with low values in the far domain.

Figure 31: Patch AVO results for Grab 1, from the area potentially containing clay in the sand placement grid.

Figure 32: Patch AVO results for Grab 2, from the area of relocated sediment, as indicated by the bathymetry.

Figure 33: Patch AVO results for Grab 3, from the area of relocated sediment, based on the area of fine sand in the sand placement grid.

Figure 34: Patch AVO results for Grab 4, from the outer south east area (QTC class 13).

Figure 35: Patch AVO results for Grab 5, from the QTC class 7 located just west of the south eastern class.

Figure 36: Patch AVO results for Grab 6, from QTC class 6 located in towards the north of the area of relocation.

Figure 37 and 38: An image of the Hawksdale wreck in the Multiview Image viewer and FFV (Full Feature Vector) editing in the FFV Editor bathymetry editing mode is shown.

Figure 39: The 14 clusters from the North Edinburgh Channel are shown in the QTC feature space or Q Space.

Figure 40: The Track plot of the classification with the rectangles output as an ascii .seabed file. Similarity colours are where a colour scale is assigned to each class depending on the distance that cluster from another cluster in feature space. This allows similar classes to be of a similar colour etc.

Figure 41: QTC Classification map with the Sand Placement Grid shows the presence of classes corresponding to the relocation area. There is also an eastward movement of these "relocated sediment" classes, in relation to the sand placement grid.

Figure 42: The results of the Particle size distribution shown as pie charts to show the compositions of the grab samples as being predominantly sand, with variable amounts of gravels (or gravel sized shell material), silts and clays.

Figure 43: The QTC unsupervised classification map with groundtruthing based on the analysis of the grab samples

Figures 44, 45 and 46: The predicted errors of interpolation using the ArcGIS Geostatistical Analyst.

Figure 47, 48 and 49: The images representing the Q values output from the QTC unsupervised classification, for Q1, Q2 and Q3 respectively.

List of Tables

ABSTRACT

Multibeam systems collect both bathymetry and backscatter data and can be used for seabed classification. Two different approaches to seabed classification, the image-based method and the angular response characterisation approach have been studied and subsequently compared. Seabed classification methods are one way of characterising the seabed and have many applications in the field of seabed mapping. This study has used the Quester Tangent Corporation (QTC) image-based method and the newer Geocoder software's angular response characterisation approach to characterise two areas affected by dredging activities. The QTC approach divides the region into discrete classes, which are subsequently identified by groundtruthing. Geocoder is able to make remote estimates of the physical properties of the seafloor using the Angular Range Analysis (ARA) method.

First, the North Edinburgh Channel sand placement site, monitored by the Port of London Authority, is studied. Results include different types of multibeam backscatter mosaics, partially stacked backscatter, angular response curves and remote estimates of the grain size. Overall, Geocoder results here show good agreement with groundtruthing. The QTC unsupervised classification approach is used to identify and monitor the classes in the area of relocation. This effectively distinguishes between the coarser relocated material and classes in the North Edinburgh Channel seabed.

Geocoder ARA results from the second site; the Thames Regional Environmental Characterisation survey area, has been studied and compared with the QTC classification. Results suggest that the QTC method can more effectively discriminate between areas affected by aggregate extraction in this region. The Geocoder software however shows great potential, allowing quantitative information about the grain size, acoustic impedance and seafloor roughness to be determined using multibeam data. Both approaches have their merits and can be used as part of seabed characterisation studies in a wide range of applications.

Chapter 1: Introduction

1.1: General Overview

Recent developments in multibeam backscatter processing techniques have increased the potential of using multibeam data for seabed characterisation. Seabed classification is based on the idea that different bottom types such as sand, mud and clay give varying backscatter strength. The main aim is to divide the area into regions of different bottom types, depending on the properties of the acoustic return. Therefore, the ultimate goal of seabed classification is accurate seabed characterisation (Blondel, 2002, Figure 1).

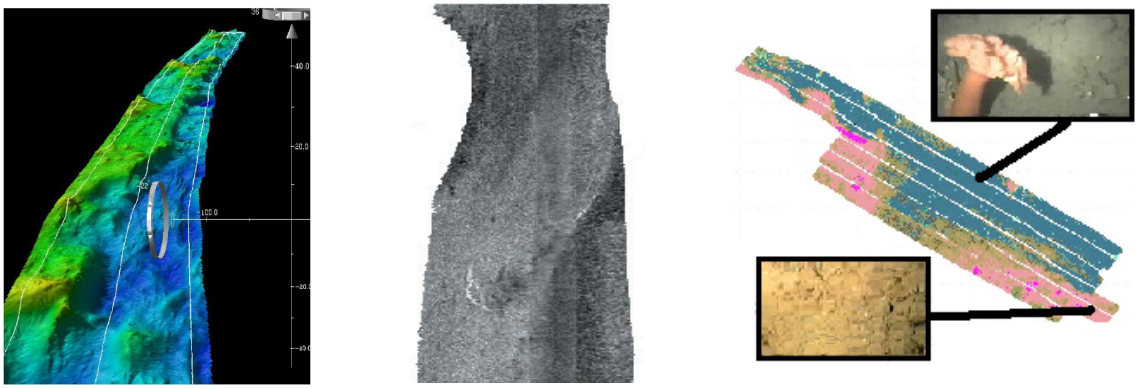

Figure 1a,b and c: Multibeam systems collect bathymetry and backscatter data, which can be used to derive classification maps, aiding the process of seabed characterisation.

One well established approach is to adapt traditional remote sensing image processing methods to quantitatively analyse the backscatter intensity data. After image segmentation, and classification, acoustic imagery can be used to discriminate between areas with different morphological properties (Pouliquen et. al. 2002). The functionality of Geographic Information Systems (GIS) can be used to integrate data from different sources, for example, integrating with groundtruthing data. This allows classification maps derived from multibeam data to help characterise the seabed and more effectively manage its use.

Another newer approach is the angular response characterisation method. In contrast with the image-based approach, this uses the information about the composition of the seafloor recorded in the backscatter angular response. Parameters extracted from the backscatter strength versus angle of incidence curves are used to model the received backscatter in terms of the physical factors affecting backscatter strength, with the use of a backscatter model (Fonseca, 2006).With inversion of this backscatter model, it is possible to obtain remote estimates of the physical properties of the seabed (Hughes-Clarke, 1997).

$$Modelling: \; Y = T(X)$$

$$Characterisation: \; \hat{X} = T^{-1}(Y)$$

Equation 1a and 1b: The generic approach used in geoacoustic inversion for seabed characterisation (after Fonseca, 2006). Y = Observations or Parameters extracted from the angular response curves, T = Backscatter Model, X = Observables or Physical properties of the seafloor

This approach has previously had limited application due to problems with unambiguous inversion of the backscatter model. However, by modifying this process and imposing constraints on the model inversion, new techniques have been developed which allow quantitative estimates of the mean grain size, acoustic impedance and roughness of the seabed to be obtained (Fonseca and Mayer, 2007). This project ultimately aims to study these two approaches of seabed classification in detail and to compare them, assessing their merits and limitations. Two leading commercially available software used in this project are:

- The Quester Tangent Corporation's (QTC) suite of seabed classification software from Vancouver Island. This image-based classification approach uses a range of algorithms, including textural analysis and clustering (Preston et. al. 2004, Figure 2a).

- The newer Geocoder mosaicking and seabed characterisation software, developed at the University of New Hampshire's Centre for Coastal and Ocean Mapping, which uses the angular response characterisation method (Fonseca and Mayer, 2007), Figure 2b).

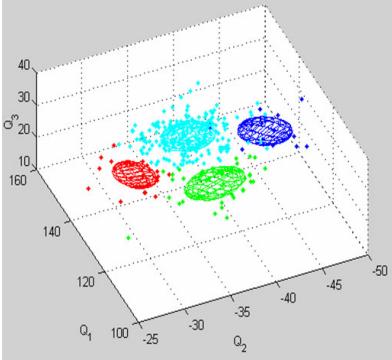

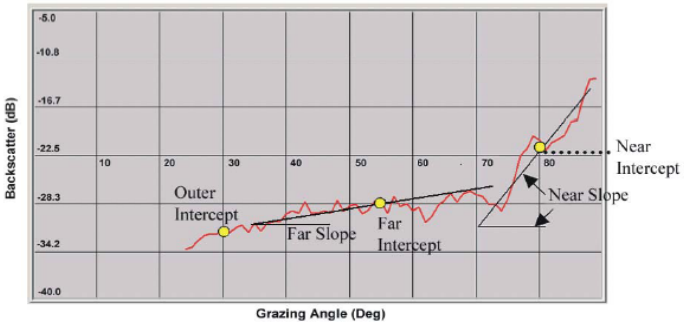

Figures 2a and 2b: The QTC software texture-based approach and Geocoder's Angular Range Analysis approach are two different methods of backscatter analysis.

1.2: New Applications of Multibeam Data

Multibeam backscatter is still considered to be a by-product of a multibeam survey, with bathymetry being the primary information (Figure 3). New methods of backscatter analysis have however increased the range of applications for which multibeam systems can be used. For example, an important application of hydrographic surveying is to monitor areas affected by dredging activities. Bathymetric surveys routinely take place at different stages of the dredging process to monitor the volume of material extracted. More recently, there has been increased need to manage the environment in a sustainable way, with legislation in place to minimise the adverse impacts of aggregate extraction (Gubbay, 2005). New software tools available have allowed seabed characterisation using multibeam data to be possible at different stages of the dredging process, enabling monitoring of these impacts. Hence, seabed mapping techniques provide a relatively new method of assessing the impact of anthropogenic activities on a broader scale (Boyd et. al, 2006).

Such alternative use of multibeam data is a growing area of hydrography, with new applications of seabed characterisation using acoustics being discovered. Some other important applications of seabed classification and multibeam backscatter data include:

- **Marine geological mapping:** Multibeam backscatter as well as sidescan sonar imagery has commonly been used to discriminate between seabeds of different compositions and to monitor geological processes (de Moustier, 1993, Johnson and Helferty, 1990, Blondel and Parsons, 1998). Backscatter strength has also been found to correlate with the sediment grain size and this is an important link to a wide range of related applications (Collier and Brown, 2005, Hughes-Clarke, 1996).
- **Benthic habitat mapping and fisheries applications:** Seabed classification techniques are extensively used for habitat mapping of a range of species including sponge reefs, maerl beds, cold water corals, reef building worms and eel grass habitats. Habitat mapping is a useful way of giving biological information a spatial component, as well as for environmental monitoring, fish stock assessments and conservation purposes.
- **Military applications:** Seabed classification is also a method of mine detection and is used as part of mine countermeasure and planning operations (Blondel, 2000).
- **Archaeological applications:** Multibeam backscatter imagery can be used to image shipwrecks and other archaeological structures for monitoring purposes and in principle in any survey where sidescan sonar is currently being used.

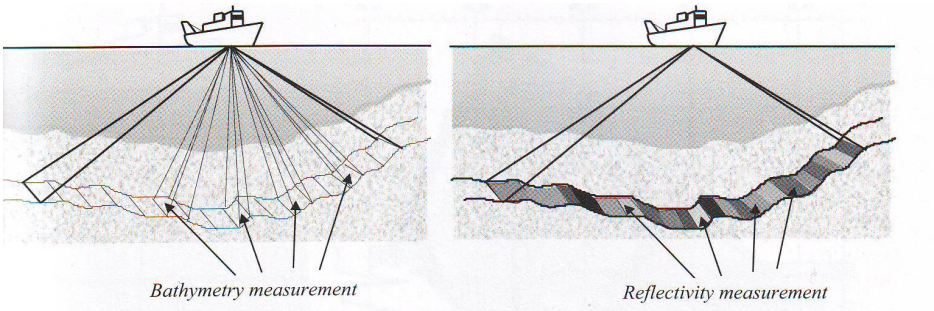

Figure 3a and 3b: Multibeam systems collect both bathymetry and backscatter data, which can be considered as a reflectivity measurement (from Lurton, 2002)

1.3: Snippet data and Sidecan sonar imagery

Multibeam backscatter mosaics can be used for qualitative seabed characterisation in a similar way to sidescan sonar imagery. As technology advances, new multibeam systems are showing a marked increase in the resolution of the backscatter data. A recent development in the field of multibeam backscatter includes the introduction of snippet data (Meurling, 2008). Snippet data is raw backscatter time-series data for each beam footprint and each ping (Lockhart et. al., 2001). This has seen multibeam imagery rival that of sidescan sonar. Hence, there is the need to compare the findings of the different types of multibeam backscatter data, including snippet data and pseudo-sidescan backscatter. Although sidescan sonar has been the traditionally preferred method of object detection, surveys including sidescan can be slower to perform, due to the constraints involved in towing the instrument (Brissette et. al. 1998). Multibeam backscatter has the advantage of providing georeferenced imagery data and has the great potential to replace sidescan sonar as an imaging tool in the future.

1.4: Scope and Study Area

This study aims to review the two different approaches to seabed classification and compare the results obtained using the QTC software and the Geocoder software. Literature relevant to a range of related topics has been researched to help explain the theory behind multibeam backscatter and seabed classification. The principal application examined includes seabed characterisation of areas affected by dredging activities.

The main study site is a licensed dredge disposal area monitored by the Port of London Authority, the North Edinburgh Channel (PLA, 2004). The North Edinburgh Channel is a sand placement area, where material has been disposed following dredging in the nearby Princes Channel. Data from two monitoring surveys following relocation has been examined, assessing the angular response characterisation and the image-based classification approach individually in detail.

The second dataset studied is from a series of licensed aggregate extraction sites monitored by Defra as part of the Thames Regional Environmental Characterisation (REC) surveys (Brown and Grove, 2008, Figure 4). Marine aggregate extraction involves the removal of sand and gravel from the seabed, for use by the construction industry and for beach replenishment. Seabed mapping techniques play an important role in assessing the impacts of aggregate extraction. Hence, developing methods that can accurately characterise the seabed has many applications in this industry. The REC data has been used to compare Geocoder's Angular Range Analysis (ARA) method with the QTC classification method.

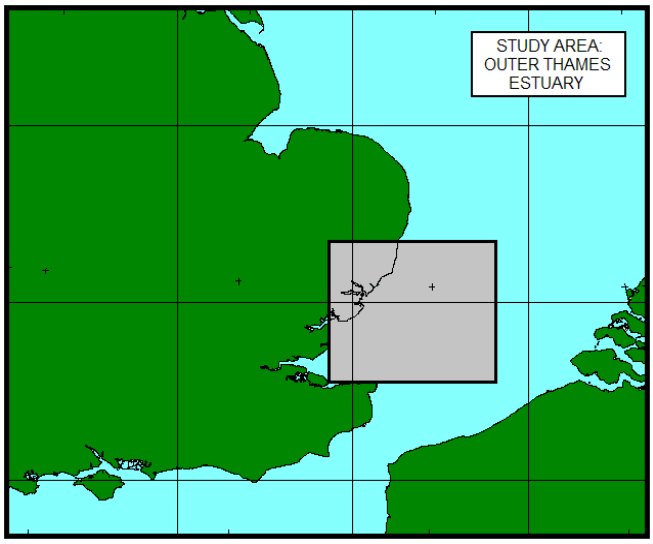

Figure 4: This study is based in the Outer Thames Estuary, studying the North Edinburgh Channel, a sand placement area and some licensed areas of aggregate extraction.

1.5: Structure of this Thesis

Chapter 1 has introduced the topic and the problems examined by this study, Chapter 2 reviews the theory behind seabed characterisation using multibeam backscatter. It discusses the physical processes affecting the measurement and the corrections which need to be made before interpretation of backscatter mosaics. The different types of acoustic backscatter data are also reviewed. Chapter 3 reviews the use of unsupervised and supervised classification methods for seabed characterisation. More specifically, the Geocoder Angular Range Analysis (ARA) method and the QTC method are discussed.

Chapter 4 focuses on seabed characterisation of the North Edinburgh Channel and presents the results obtained from the QTC unsupervised and a supervised classification method, and Geocoder results in detail. It also compares the backscatter mosaics from different types of backscatter data acquired by Reson multibeam systems. Chapter 5 then extends this theme by presenting Geocoder's Angular Range Analysis (ARA) results with the QTC method applied to the same multibeam data set, in a licensed area of aggregate extraction. An assessment of the accuracy of the remote estimate of the grain size obtained using the Geocoder software has been made, by comparing with extensive groundtruthing. Chapter 6 then discusses the key findings of this project and evaluates the study as a whole, assessing the merits and potential of each method for accurate seabed characterisation.

Chapter 2: Multibeam Backscatter

2.1: Factors affecting Backscatter Strength

The theory relating to multibeam backscatter is a complex subject and this chapter attempts to explain and summarise the key ideas relevant to seabed characterisation. The reader should also consult the section on Backscatter Models in Appendix 1 for further information. The backscatter signal recorded by a multibeam system provides a raw measurement of the amount of energy received back at the sonar source. In order to understand the information provided by this measurement, it is necessary to be aware of the factors affecting backscatter strength. Multibeam backscatter varies primarily with the angle of incidence, the physical processes occurring at the seabed and the intrinsic nature of the seafloor (Blondel and Murton, 1997). Other factors also affecting the backscattered return are the frequency of the sonar system and the seabed slope (Lurton, 2002).

The backscattered return is strongest at the nadir and weakest at the grazing angles. This is because the acoustic pulse ensonifies a larger area of the seabed at normal incidence angles, whereas a smaller area is ensonified by a pulse incoming at more oblique angles. Traditionally, a correction is applied to correct for the angular dependence when mosaicking the backscatter data, as this can lead to along-track artefacts being present in the final backscatter mosaic. Nevertheless, the angular response of backscatter at a particular frequency has been found to vary with seabed type (de Moustier, 1991, Hughes-Clarke et. al. 1997). The shape of the backscatter strength versus angle of incidence curve can be used to differentiate areas with different physical properties (Figure 5 and 6).

Another key factor affecting backscatter strength is the interface roughness. The acoustic wave is subject to a different type of scattering process, depending on the degree of roughness of the seabed with respect to the wavelength of the incoming sound (Lurton, 2002). The type of scattering process also varies with the angle of incidence. At oblique and grazing angles the wave is subject to Bragg scattering, where microscale roughness plays an important role (Parnum et. al. 2004). Assuming such microscale roughness, the

Rayleigh-Rice perturbation theory becomes applicable in this domain. Specular backscattering due to facets dominates at the nadir, where the tangent plane (Kirchhoff) approximation is valid (Lurton, 2002). The composite roughness theory is another such approximation, which separates the type of roughness into longer and shorter wavelengths. Shorter wavelengths of roughness result in interface scattering and longer wavelengths result in change in the grazing angle (Jackson et. al. 1986).

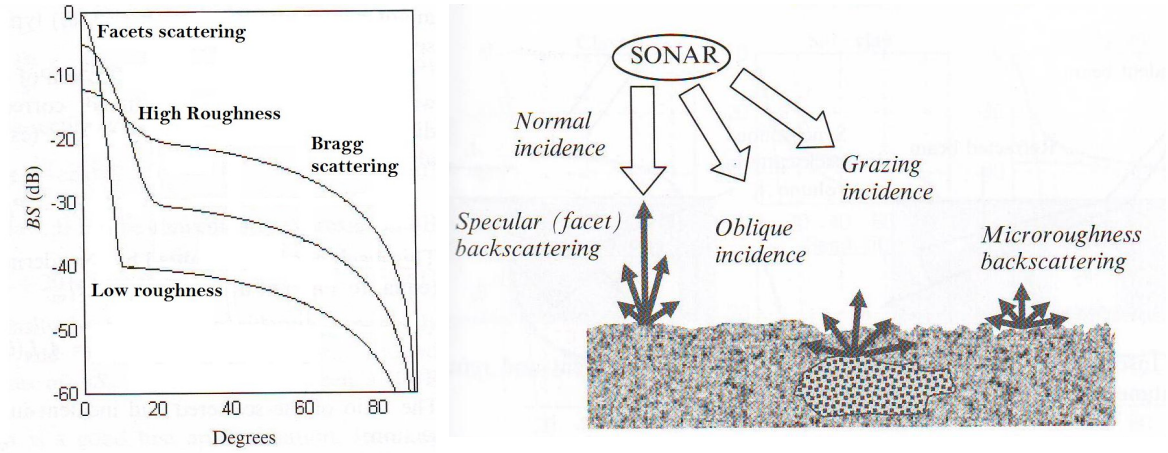

Figure 5 and 6: The shape of the backscatter strength versus angle of incidence curve varies with the degree of roughness of the seafloor (as well as its intrinsic properties). This is because the acoustic wave is subject to a different type of scattering process. The physical process occurring at the seabed also depends on the angle of incidence. Facet scattering dominates at normal angles, interface scattering with volume scattering contributions at oblique incidences and microscale roughness at grazing angles (after Lurton, 2002).

Some of the energy also enters into the seafloor and may be subject to volume scattering due to heterogeneities in the surface sediment (Urick, 1967). The contribution due to volume scattering depends on the acoustic attenuation (and therefore sediment type) as well as the frequency (Jackscon et. al., 1986). Low frequencies penetrate deeper into the sediment whereas high frequencies are absorbed, with a smaller volume scattering contribution. A seabed composed of hard material and one composed of a soft material gives a different strength of return and the intrinsic nature of the seabed also affects the backscatter strength (Blondel and Murton, 1997). The acoustic impedance is the product of

density and the speed of sound. There is an impedance contrast at the sediment-water interface due to the changing medium. Hence, a seafloor composed of a hard material with high density, would give strong impedance, where as one composed of a soft material would give weaker impedance (Collier and Brown, 2005). This is the key physical property that needs to be studied for seabed characterisation, as it can allow determination of the mean grain size (Fonseca and Mayer, 2007).

2.2: Backscatter Data Corrections

For accurate seabed characterisation, the quality of the backscatter data must be maintained to a consistent standard as this data is the raw measurement used in all subsequent analysis (Fonseca and Calder, 2005). Additionally, when producing backscatter mosaics, corrections need to be applied to remove artefacts from the backscatter map. This involves correcting for radiometric and geometric distortions. These are reviewed, with a particular focus on the corrections possible using the Geocoder mosaicking software.

2.2.1. Radiometric Corrections

Radiometric corrections alter the value of the pixels. These include correcting for the power and gain settings by reapplying the Time Varying Gain (TVG) and Angle Varying Gain (AVG). The angular response and beam pattern corrections also need to be made.

Time Varying Gain (TVG) and Angle Varying Gain (AVG)

The Transmission Loss (TL) due to attenuation and beam spreading of the transmitted sound varies with the local conditions in the water column (Chu and Hufnagle, 2006). Hence, correspondingly the time-varying gain applied to amplify each received signal during acquisition also varies. This needs to be smoothed out by reapplying the TVG during processing. This is an along track correction, which can lead to the presence of banding between adjacent swaths if left uncorrected (Fonseca et. al. 2006). Similarly, re-applying the Angle-Varying Gain corrects for the angular variations in the gain in the

across-track direction (Blondel and Murton, 1997). The Geocoder software also corrects for the any changes in the pulse width and power that may have been made.

The Angular Response Correction

The angular response correction or angular gain equalisation corrects for the angular dependence of backscatter (Figure 7a and 7b). A Lambertian correction is usually made by the multibeam system during acquisition, with a flat bottom assumption and is not always effective. Geocoder does not use the simplified flat bottom assumption and calculates the across track and along track slope to obtain the true grazing angle. The software makes an improved correction, taking bathymetry into account during mosaicking (Fonseca and Calder, 2005).

As the angular dependence varies with seabed type, this correction also removes information about the composition of the seafloor recorded in the angular response curves. Nevertheless, it is still an important part of backscatter data processing, especially if using image processing based seabed classification methods such as using textural analysis. An important distinction is that the Angular Range Analysis (ARA) process in Geocoder utilises this angular information about the backscatter, whereas the QTC method performs a compensation routine to correct for this effect.

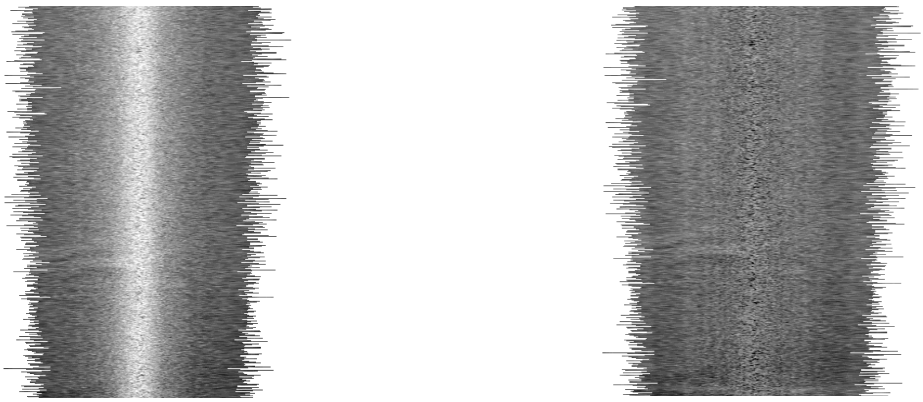

Figure 7a and 7b: The image before and after the angular dependence correction (from Beaudoin et. al. 2002).

Beam Pattern Residuals and Speckle Removal

Variations in the transmit beam pattern can be caused by small amplification differences between the elements in the sonar transducer (Fonseca and Calder, 2005). This can alter the measured angular response and therefore the beam pattern residuals need to be removed before processing of the AR curve. This can be considered to be a geometric correction, as the beam pattern is altered by the roll, pitch and heave of the vessel. Speckle is caused by constructive and destructive interference and needs to be removed before interpretation.

2.3.2. Geometric Corrections

Geometric corrections ultimately alter the position of the grey levels. The geometric corrections include the slant range correction, slope and georeferencing the mosaic.

Slant Range Correction and Slope

The slant range correction needs to be applied to map the backscatter values to ground range rather than slant range (Beaudoin et. al, 2002). Without this correction, targets in the far range will appear distorted and being wider than they actually are and targets near the nadir appears narrower than they actually are (Fish and Carr, 1990). It can be applied with a flat bottom assumption, or after co-registering the backscatter with the bathymetry, and using the true grazing angle to correct for the slope. This helps to remove distortion that may be present due to the variations in bathymetry.

Georeferencing the Mosaic

The final step in producing a multibeam backscatter map is to geocode the mosaic into a projected coordinate system. Here, the Geocoder software utilises the navigation and sensor attitude information (Fonseca and Calder, 2005).

2.3: Different Types of Backscatter Data

The resolution of the imagery depends on the type of multibeam backscatter data being acquired. New methods of logging backscatter data are quite regularly being developed and the user needs to be aware of what is actually being recorded. Previous reviews have made the distinction between three key types of Reson backscatter data (Beaudoin et. al. 2002).

- Pseudo-sidescan multibeam backscatter (Figure 8a and 8b).
- Backscatter time series data or "snippets" (Figure 8c and 8d).
- Beam-averaged intensity

As resolution of multibeam backscatter increases, it can be comparable to sidescan sonar imagery and hence this is also briefly reviewed. Other factors such as the frequency of the sonar system and transducer shape can also determine the resolution and coverage.
The so called "pseudo-sidescan" imagery is acquired using multibeam systems. It samples the seafloor using two additional receive beams produced digitally on the port and starboard side (Figures 8a and 8b, Meurling, 2008). Sampling occurs across the area of the beam which is in contact with the seafloor, at the time of ensonification. This is quite a large area due to the fan-like shape of the beam (Lockhart et. al. 2001). The resulting imagery acquired is of relatively low resolution and a larger footprint size. Still, when using this option (also known as Reson Option 33) imagery is acquired over a large swath. Whereas bathymetric data quality can be restricted to 75 degrees, backscatter data is usually also acquired beyond this angle (Wyatt, 2008) .

Multibeam "Pseudo-sidescan"

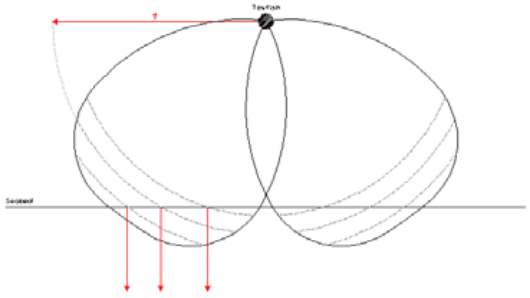

Multibeam Snippets

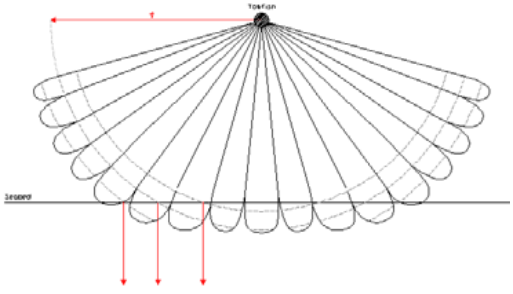

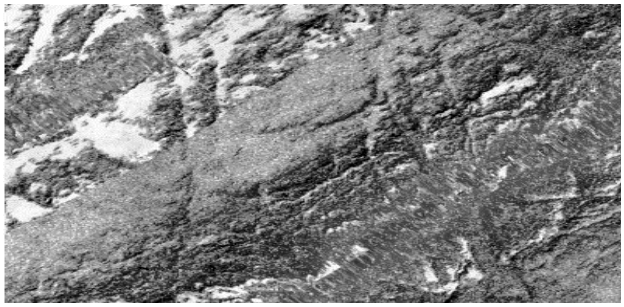
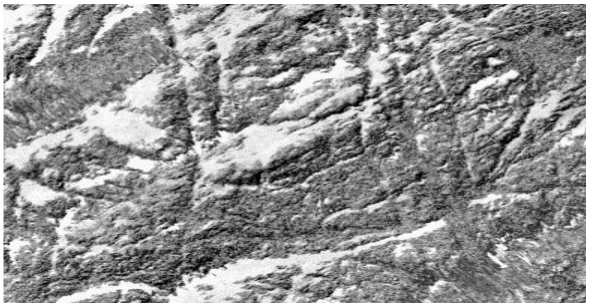

Figures 8a, 8b (left), 8c and 8d (right): Multibeam "pseudo-sidescan" imagery is acquired over a larger area (left). Snippet data is acquired over a smaller footprint and is of higher resolution as shown in the imagery (right). (from Meurling et. al. 2008, Courtesy of Reson)

Snippets or "Foot-print time series" data is the newest form of multibeam backscatter with the highest resolution. It was developed during trials by Fugro Pelagos Inc, Reson Inc and Trition Elics Inc (Lockhart et. al., 2001). Beam-formed backscatter time series is sampled and logged across each ping (along-track) and for each beam (across track) (Meurling, 2008). Snippets can result in up to 20 000 pixels per ping being acquired with a very large volume of data (Gilmour and Nelson., 2008). A disadvantage of snippets is that the volume of data acquired makes regular acquisition, processing and storage a difficult task. Services are being offered which enable virtual storage of large data sets over the internet using ArcIMS (Gilmour et. al., 2008). The snippets can be averaged across a beam to obtain beam- averaged intensity data and this has a lower resolution than snippets.

These different types of multibeam backscatter have different resolutions and can in turn be compared with sidescan sonar imagery. Although the resolution of multibeam backscatter is still not considered to be as high as that of sidescan sonar imagery, multibeam backscatter data has some key advantages. The first is that the multibeam data is georeferenced, with accompanying bathymetric data acquired by the same system. This is not possible with sidescan sonar, although bathymetric sidescan systems can also acquire georeferenced imagery. Secondly, there is far less ambiguity about the position of the sensor, as multibeam data is properly compensated for the vessel's roll, pitch, yaw and heave. The sidescan sonar does not provide this depth information, but has the advantage of

usually operating in a towed configuration. This means that it can acquire data at low grazing angles, being closer to the seabed (Blondel and Murton, 1997). This has the advantage of providing higher resolution imagery. Still, another important advantage is that multibeam systems acquire backscatter over a wider range of grazing angles and can be used for obtaining the backscatter angular response curve (Hughes-Clarke et. al. 1997). Hence, at the rate at which this technology evolves, one can be reasonably certain that multibeam backscatter has the potential to replace sidescan sonar within the next decade.

Chapter 3: Seabed Classification Methods

Seabed classification is possible using a range of methods and the use of acoustics is simply one route. Others routes include in-situ sampling methods such as geological, geotechnical sampling, and visual imagery (Blondel, 2002). The use of optical sensors has been restricted to depths less than 40m due to absorption of electromagnetic radiation by water. Most recently, processing tools have been developed to classify data acquired using airborne bathymetric LiDAR systems, (QTC, 2008). Nevertheless, acoustics remain the preferred method of imaging the seafloor as data can be acquired over a much larger area (than in-situ sampling) from almost any depth. Acoustic seabed classification is possible using a wide range of systems other than multibeam, including sidescan sonar, single beam echosounders, interferometric systems and sub-bottom profilers.

3.1: Image-based Seabed Classification

The origins of image-based seabed classification methods lie in the domain of remote sensing. Image processing methods used to classify satellite images have been adapted to be used on acoustic data. The key steps in statistical image-based classification include pre-processing of the data, feature extraction, segmentation and classification (Reed and Hussong,1989). Spectral approaches to classification have not been possible to the same extent as with classification in satellite remote sensing, due to lesser knowledge about the spectral signatures of the seabed. Therefore, many image-based seabed classification algorithms are based on spatial pattern recognition, as well as spectral approaches.

Such methods can broadly be categorised into two types; unsupervised classification and supervised classification. Unsupervised classification is also known as iterative clustering and does not require any prior knowledge of the area. Here, the image is subject to feature extraction, where algorithms are used to quantify different spatial properties of an image patch. These pixels are then subject to clustering in the N dimensional feature space and are correspondingly mapped into a particular cluster during feature space partitioning (Reed and Hussong, 1989) Clustering algorithms can vary by having different methods of seed

selection during initialization. The decision rule by which a pixel is assigned to a cluster also varies. For example, during K-means clustering, all the pixels are assigned to arbitrary cluster centres based on the minimum Euclidean distance decision rule. Following this, the cluster mean and statistics redefined in the next iteration (Lillesand et al 2008). The output is a classified symbol image, obtained by replacing the pixels with their respective cluster numbers (Liu and Mason, 2007).

Supervised classification requires the user to define a set of training areas based on prior knowledge, before the classification stage. It requires all the classes to have been identified beforehand, so that the statistics can be calculated for each training area. Pixels are then assigned to a particular class depending on how well they meet a particular decision or dissimilarity rule. For example, the minimum distance classifier assigns a pixel to the class whose cluster centre is found to be nearest (Lillesand et.al. 2008). The maximum likelihood classifier and Bayesian classifier assess the probability of each pixel belonging to all the classes and assign the pixel to the cluster with the highest probability.

An advantage of unsupervised classification is that results are not dependent on the quality of the training data set. It divides the image into acoustically distinct areas and it is able to find all the subclasses which may have been missed during the supervised training stage. Still, a potential disadvantage is that subclasses can increasingly complicate the interpretation and be difficult to identify without detailed groundtruthing.

The hybrid approach combines the benefits of unsupervised classification and those of supervised classification. A commonly used way of doing a hybrid classification is to perform unsupervised classification first. Following this, the classification output together with groundtruthing can be used to form a more accurate training dataset. Finally, a supervised classification is carried out on the raw data, using the more comprehensive training data set (Liu and Mason, 2007).

The image-based classification method is a commonly used approach and many previous studies have classified sidescan data using textural analysis algorithms for feature extraction (Reed and Hussong, 1989). Other approaches include representing backscatter as a stochastic process and using the probability density function (PDF) to assess the distribution of backscatter strength. Artificial Neural Networks have also been used, which train the system to recognise regularities (Pouliquen, 2002, Tso and Mather,2001). Some studies have attempted the supervised classification approach using intermediate PCA outputs from the Quester Tangent software (Boyd et.al,2006). More recently, Robidoux et. al. 2008 has compared the QTC method with the Geocoder's Angular Range Analysis and has found that both methods can effectively identify the sediment boundaries (Robidoux et.al.2008).

3.2: The Quester Tangent Corporation Method

The QTC method of multibeam and sidescan classification takes the image-based route and uses a range of algorithms, including textural analysis. The company has a range of seabed classification products and the QTC Multiview software has been used for unsupervised classification in this project. A key advantage of this approach is that it does not require absolute values of backscatter strength. It does require image amplitude to be uniformly proportional to backscatter strength and hence thorough cleaning need to be performed to minimise artefacts (Preston, 2004). The software can accept a wide range of data formats from many systems, including Hypack .hsx files, Simrad .all files and Reson snippet data in .xtf format. A key requirement is that the data must be the original raw data, with bathymetry and backscatter in the same file. This is because it makes use of both bathymetry and backscatter for feature extraction and only a limited amount of cleaning can be performed on resampled or processed data. The steps are shown in Figure 9. Following raw load of files line by line, the data needs to be visually assessed, by using the Image Viewer waterfall display and cleaned.

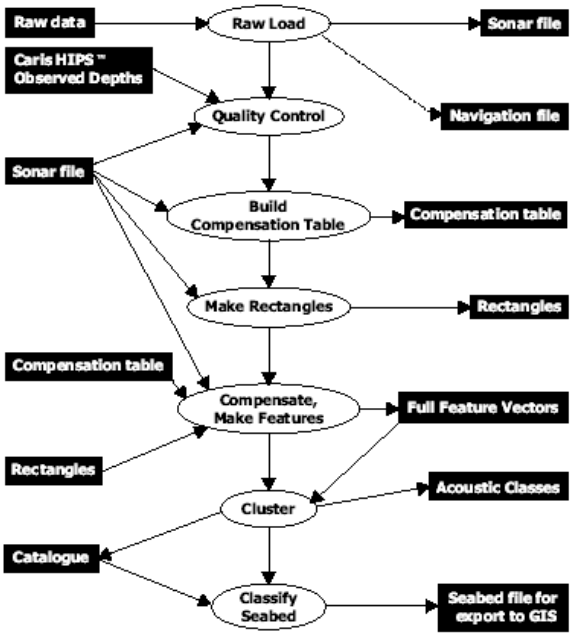

Figure 9: The steps involved in the QTC classification approach 9 from QTC,2008)

Available cleaning tools include the depth thresholding, masking by beam grazing angle and rejecting beams, as well as manual boarder edits (Figure10a). Additionally, the Hypack processed .hs2 files or the rejected flags from CARIS HIPS and SIPS can be imported for quality control. Rectangle generation is the next stage, where the rectangles of a size defined by the user are generated on the image as shown in Figure 10b. This divides the image into windows, with 132 features extracted for each rectangle. A compensation table is also developed to correct for the angular dependence, attenuation with depth and range related artefacts. It is advised that all the rectangles are generated for the whole data set, before any features are generated as this ensures a more complete compensation table (QTC,2007). The algorithms used for feature extraction include basic statistics, quantile and histogram, Grey Level Co-occurrence Matrices (GLCMs), ratios based on power spectra and fractal dimension. Basic statistics include the mean and the standard deviation of the backscatter values. GLCMs are one statistical approach to textural analysis which quantifies the spatial organisation of an image. (Haralick,1979). They are formed by examining how many times a given combination of pixels are repeated when scanning the image in different directions and used to differentiate between rough and smooth areas. The

seabed can be though of a fractal with self-similar patterns being repeated at different spatial scales. For this algorithm, the QTC software needs to uses the bathymetry as well as the backscatter (Preston, 2003). Fast Fourier Transforms are used to represent the image in the frequency domain rather than the spatial domain and are used here to obtain the power spectra of an image patch.

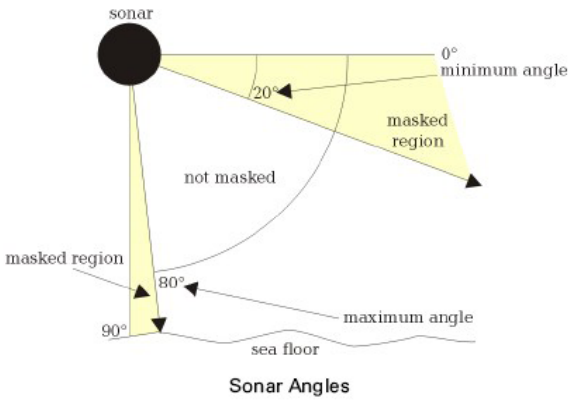

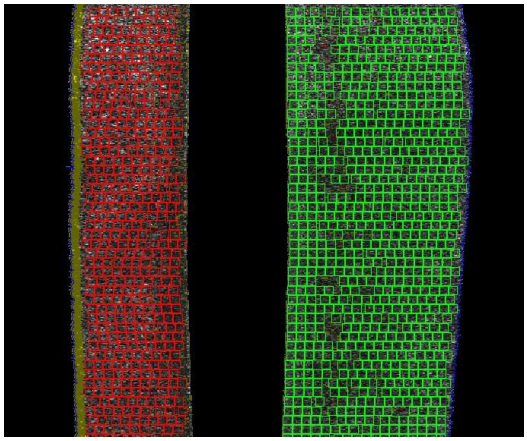

Figure 10a and 10b: Cleaning using the mask by grazing angle tool and rectangle generation.

Principal Component Analysis (PCA) and Clustering (Preston,2004)

Principal Component Analysis (PCA) then takes place to reduce the dimensionality of the data set prior to clustering. The two main clustering tools available are the Manual Cluster and Automatic Cluster Engine (ACE) in "Q space" (Figure 11). The Manual Clustering tool is based on the K- Means clustering algorithm and allows the user to split and merge the clusters and examine the score. Here, the minimum Mahalanobis distance is used as a decision rule. The second more objective clustering tool is the ACE tool, which uses "simulated annealing" for clustering in feature space. A number of iterations are performed for each number of classes. The Bayesian Information Criterion (BIC) is calculated for every iteration. This score helps to determine which model is most suitable to assign to the data. It can be used to compare the different possible model distributions, with the lowest BIC score corresponding to the most suitable number of classes. The catalogue generated is used to obtain a classified output of the survey.

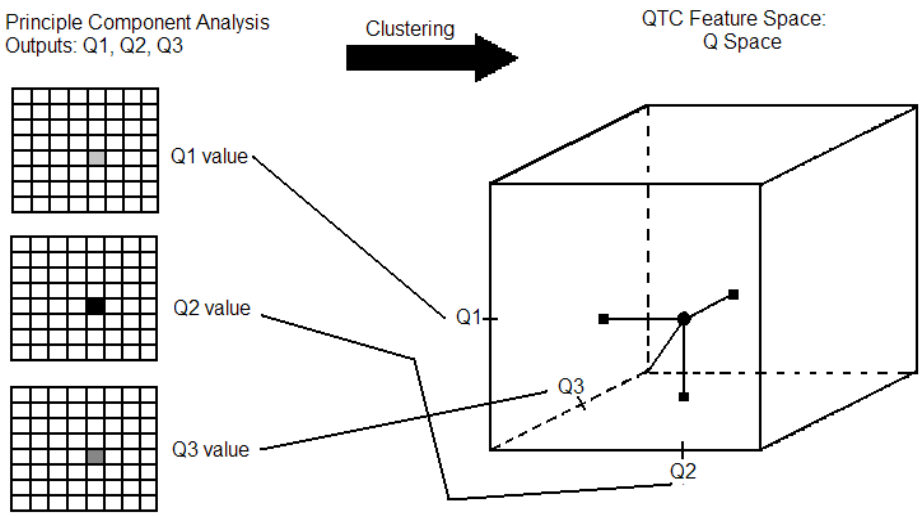

Figure 11: The QTC software carries out segmentation by clustering in feature space (Q Space) (modified after Liu and Mason, 2007)

3.3: Angular Response Characterisation

Angular response characterisation is a newer approach which makes use of the better geometric resolution and directional information provided by multibeam systems. The angular response (AR) received varies with the composition of the seafloor (Figure 12). This approach makes use of this angular dependence, rather than applying the correction which would have been carried out during mosaicking or textural analysis. An important requirement here is calibrated backscatter, with absolute values necessary. De Moustier and Alexandrou 1991, have used the curve fitting approach to compare the angular response curves from a known seabed type with the measured normalised angular response (de Moustier and Alexandrou, 1991). AR parameters can be extracted from these curves and be used to compare the different angular responses (Hughes-Clarke et.al.,1997). Note that there are two AR curves for each half of the swath width (port or starboard) and this can limit the resolution possible using this method.

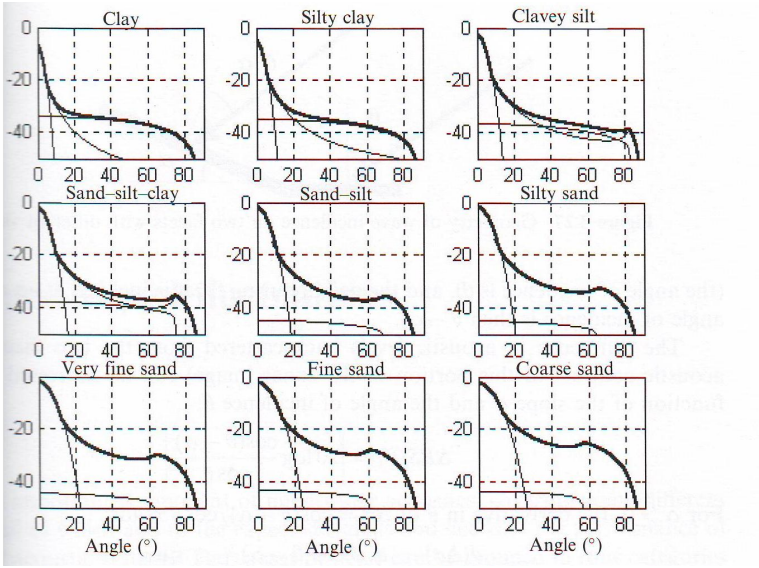

Figure 12: The angular response from seafloors composed of different material varies and can be used for seabed characterisation purposes. (from Lurton 2002).

As backscatter strength varies with the angle of incidence, the AR curve is divided into domains. The composite roughness theory briefly introduced in the previous chapter distinguishes between the three domains of the AR curve (Jackson et.al.1986). Hence, different parameters need to be extracted from each domain to represent that particular AR curve (Figure 13). The parameters which change with seabed type include the boundaries between the domains and those which quantify the shape of the curve. Backscatter however acts in a stochastic manner and hence the AR curves for simply one swath may contain unrepresentative signatures and biases (Hughes- Clarke, 1997). Therefore, the angular response is generally averaged for around 20-50 pings across half a swath width. These parameters have been used in different ways to help characterise the seafloor. One approach is to follow a route similar to that of image-based seabed classification methods and use the angular response parameters as feature vectors subject to clustering (Fonsena and Calder,2007). Another approach is to use these feature vectors for inversion of a backscatter model. This is used by the Geocoder's Angular Range Analysis (ARA).

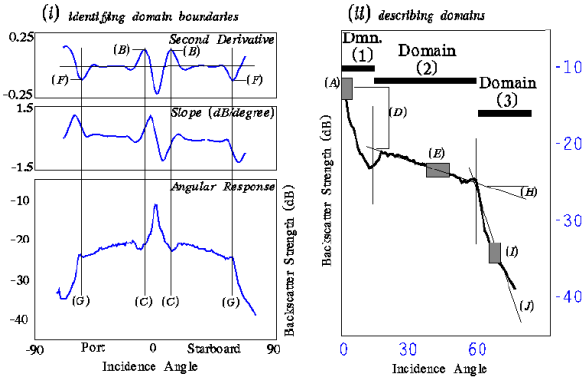

Figure 13: The AR curve can be divided into domains, with parameters extracted from each domain to represent the relevant differences (from Hughes-Clarke et.al.1997).

3.4: Geocoder's Angular Range Analysis (ARA) (Fonsena and Mayer,2007).

The Angular Range Analysis (ARA) method used by the Geocoder software is based on the Amplitude Versus Offset (AVO) method from seismic surveying (The AVO terminology is synonymous to ARA). Presently, this software is very new and is being included as part of hydrographic processing software, such as HYPACK 2008, CARIS SIPS and Fledermaus. Its release has been anticipated by many in the seabed mapping community as it is able to obtain quantitative remote estimates of the physical properties of the seabed, including the mean grain size. The mosaicking version of the software has been included in HYPACK 2008 and this is able to perform the model inversion for a single patch using the "Patch AVO" tool. The full seabed characterisation module is yet to be released. The Geocoder software at present is relatively untested and many aspects are in the developmental stage.

The Geocoder software obtains the angular response curve by stacking a series of pings in the along-track direction. Hence, this area of the seafloor represents a patch, of half a swath width in the along and across track direction. The first stage of ARA is the partial stacking of backscatter signature from different domains, helping to preserve the angular information (Fonsena and Calder,2007). This divides the return into three domains; the near, far and outer region. The ARA method then uses parameters extracted from the angular response curves as part of a geoacoustic inversion process.

The angular response parameters, known for Geocoder as ARA parameters, extracted for each domain are:

- Near mean, near slope, near intercept and near angle (Figure 14)
- Far mean, far slope, far intercept and far angle (Figure 14)
- Outer mean and the orthogonal deviation

These parameters have been linked to the different seafloor properties affecting backscatter strength. For example, the slope has been found to change with the roughness and the mean found to change with the impedance (Fonsena et.al., 2004). The orthogonal deviation, also known as the fluid factor, has been found to be linked to the contribution by volume heterogeneities. ARA parameters are extracted from the measured angular response and then subsequently compared to the modelled ARA parameters using parametric equations.

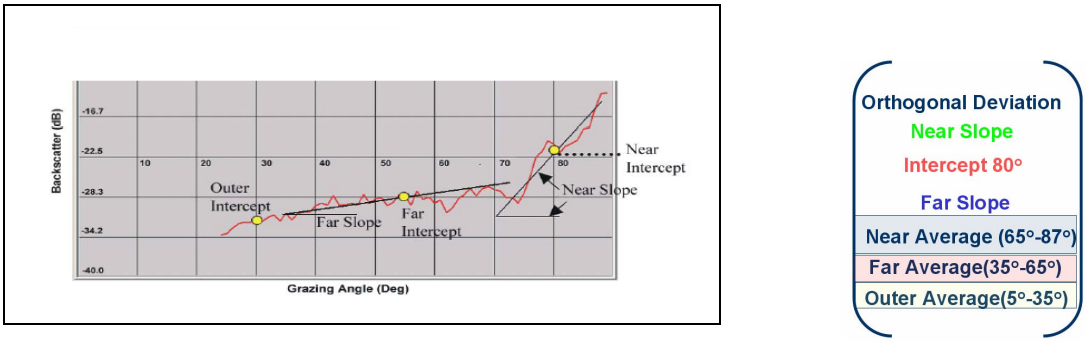

Figure 14: The ARA parameter are extracted from different domains to help summarise the key properties which are affected by backscatter strength (from Fonsena, 2006).

This technique uses a constrained iterative inversion of the Williams, 2001 Effective Density Fluid backscatter model (Williams, 2001).Inversion is carried out iteratively until convergence, by altering the modelled ARA parameters to match the measured ARA parameters. As the unambiguous inversion of an acoustic backscatter model is not feasible, the inversion is constraint. These constraints are based on Hamilton's equations, which are a "classic" set of regression equations linking the sediment geophysical backscatter model parameters with the grain size (Hamilton, 1974). Following inversion, the backscatter

model is used to make estimates of the roughness, acoustic impedance and the volume heterogeneities (acoustic attenuation), and subsequently the mean grain size. Practical application of these methods has been implemented in the following chapters.

Chapter 4: North Edinburgh Channel

4.1: The North Edinburgh Channel Sand Placement Site

The first area examined by this study is the North Edinburgh Channel. This chapter is about seabed classification using the QTC and Geocoder approach in this area. It gives background to the North Edinburgh relocation, the survey methodology, results and preliminary analysis. It helps illustrate the different things possible using the two software, with a comparison in the following chapter. This area is a sand placement site located in the Thames Estuary (Figure 15). This site was selected to be a dredge disposal site, following deepening of the Princes Channel by the Port of London Authority (PLA).

The Princes Channel Deepening (PLA, 2004)

The PLA are responsible for the maintaining navigation safety in the Thames Estuary and ensuring safe access to the port. The outer Thames estuary is a dynamic region with mobile sand banks and channels. In the 90s, the North Edinburgh Channel was previously the southern approach providing the access to Black Deep, the main deep water channel. However, as a result of migration of a mobile sand bar in the South of the channel, traffic was diverted to Fisherman's Gat and the Princes channel as an alternative route. The Fisherman's Gat is a more complex channel to navigate and more recently, there has been a double-crossing situation at the junction with Black Deep. The deepening of the Princes Channel to 8m below chart datum was proposed to minimise potential conflict between vessels. Following some beneficial use of dredged material during Phase 1, the North Edinburgh Channel was selected to be a suitable placement site in Phase 2.

The North Edinburgh Channel Characterisation and Sand Placement Plan

The North Edinburgh Channel was selected as it is one of the most dynamic channels in the PLA limits and there are strong currents in the area during both the ebb and the flood. Material placed in this area is most likely to be recycled within the estuary as it is placed in the same sedimentary cell (PLA, 2003).

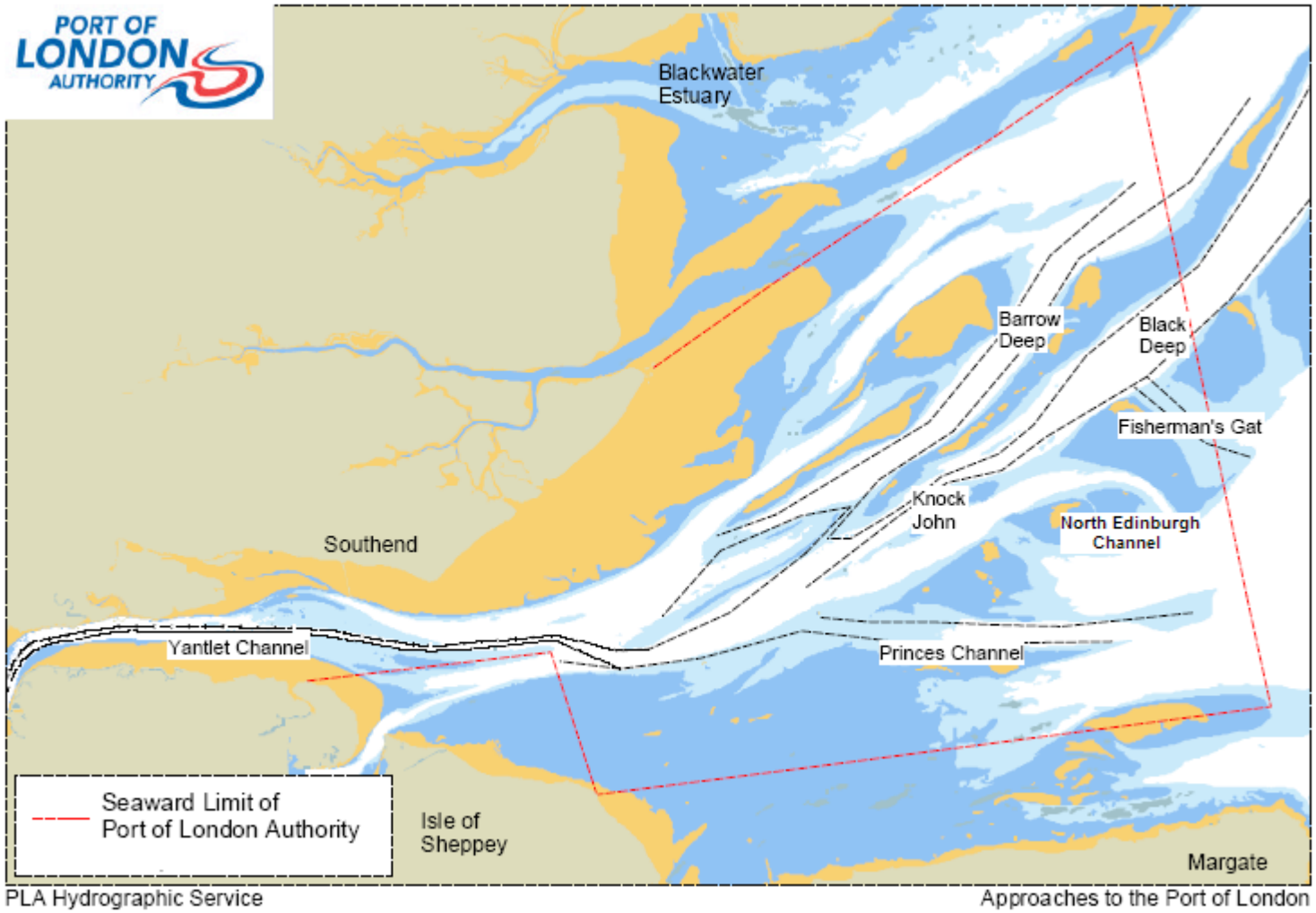

Figure 15: Map of the Port of London Authority limits, with the North Edinburgh Channel, Princes Channel (after PLA, 2004)

Previous groundtruthing characterising the seabed in the North Edinburgh Channel state that the area is composed of fine to medium sand with some silt and gravel. The Hawksdale wreck is found in the South East, with a 100m exclusion zone surrounding the wreck (PLA, 2008). Other key seabed features include the presence of stepped terraces, a Paleaolithic artefact in the North West (Wessex Archeaology,2004).

The relocation in the North Edinburgh Channel during Phase 2 involved 2.5 million m^3 of material being extracted from the Princes channel. A license for relocation of the material was granted by Defra under the Food and Environment Protection Act (FEPA) (PLA, 2008). Groundtruthing from Princes channel following extensive vibrocore samples shows that the relocated material consisted mainly of fine sands with some weak clay present in the eastern part. The clay fraction was unsuitable to be placed in the North Edinburgh Channel and was relocated to a licensed marine disposal site at South Falls (PLA, 2003). There was also the presence of shell content, which limited the possible beneficial uses of the material. The material was dredged by the dredging company using the trailing suction hopper dredger. It was relocated in the cells shown in the sand placement plan by bottom placement (Figure 16). This is more likely to contain the impact of relocation and the also allows monitoring of these impacts. This site is now subject to post relocation monitoring using multibeam, with two surveys carried out following the completion of relocation. PLA have recently been carrying out trial using snippets and data from these surveys has been studied here.

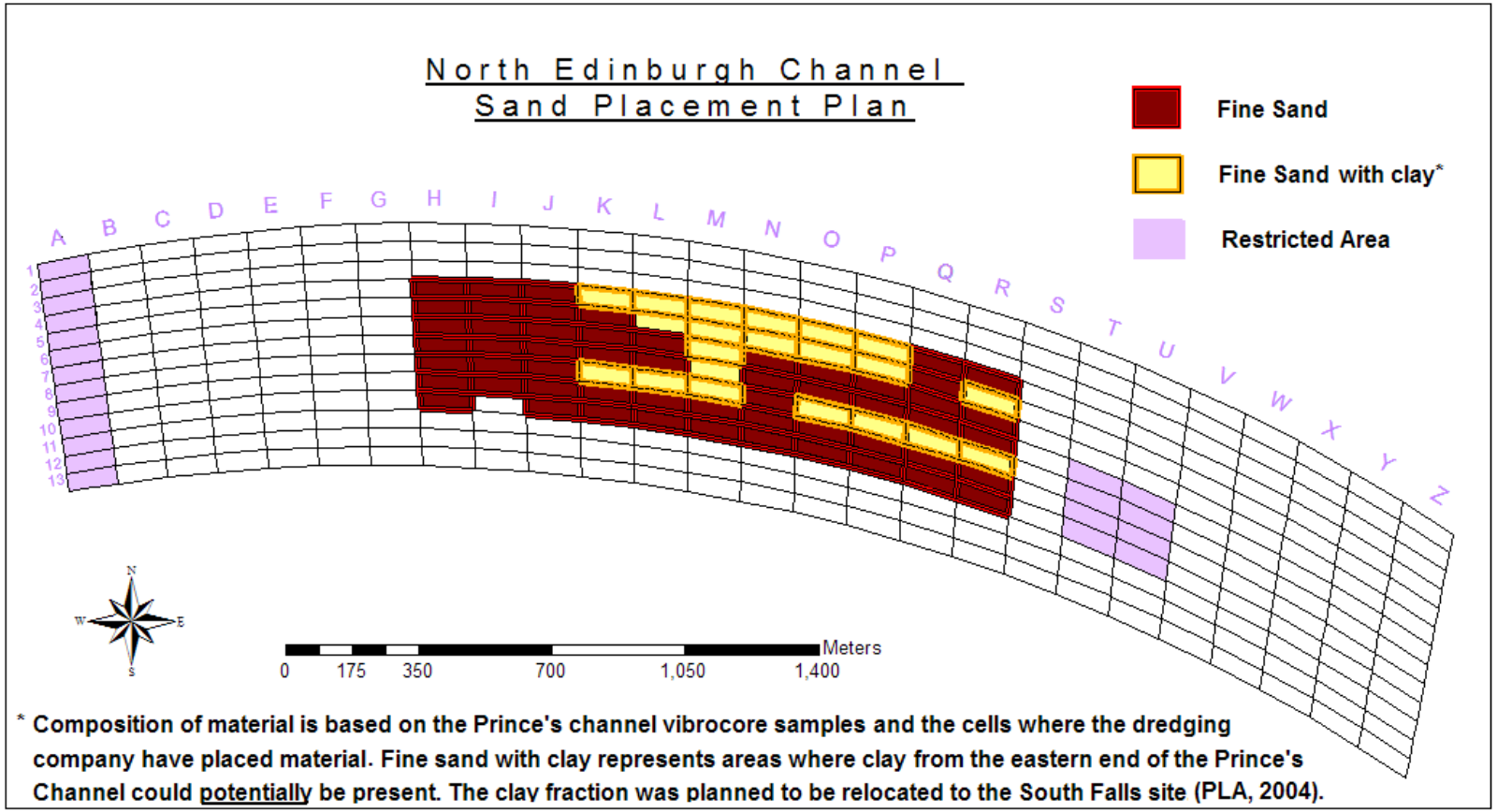

Figure 16: The North Edinburgh Channel Sand Placement Plan, with the cells where material has been dumped highlighted. The restricted area in the west is in a biologically sensitive area and that on the east is the exclusion zone for the Hawksdale.

4.2: Data Acquisition Methodology

Data collection took place in three surveys as part of the monitoring of the sand placement area. The first multibeam survey after the placement of the dredged material was the carried out on 30th May 2008 aboard the Yantlet, a 13.4m PLA survey vessel (Figures 17). The second multibeam survey and third groundtruthing survey took place on 24th July 2008 and 7th August respectively aboard the Verifier, a 20.4m vessel (Figure 18).

Figure 17 and 18: Data Collection for the first survey took place aboard the Yantlet with the second and third surveys aboard the Verifier (from PLA, 2008b).

Survey 1: Multibeam Bathymetry, Backscatter and Snippets

Twenty two lines of multibeam bathymetry, backscatter and snippets were successfully acquired using the Reson 8125 455kHz multibeam system. Four sound velocity profiles were carried out before, during and after the survey and were applied during acquisition. The Applanix POSMV motion sensor and DGPS positioning was used with 2m accuracy, with true heave. A predicted tide file was applied during acquisition and later replaced by the measured tides. Data was logged using Hypack 2008, with the hsx files containing the bathymetry and "pseudosidescan" backscatter data and binary .81x files with snippets. Data acquired was of a good overall quality, with no adverse weather conditions.

Survey 2: Multibeam Bathymetry and Backscatter

The second survey was carried out using the Reson 8101 240 kHz multibeam system with bathymetry and pseudosidescan backscatter data logged in the hsx files. Twenty lines were successfully acquired with minimal infilling necessary. The Applanix POSMV and DGPS were used. The sound velocity was measured every hour and a predicted tide file was used during the survey with measured tides reapplied during processing. An echo sounder was also used for bathymetric cross checking purposes.

Survey 3: Groundtruthing

Grab sampling was carried out using a Day grab deployed from an A frame. Six grabs were successfully collected with photographs, descriptions following visual inspection and a sample collected for analysis of the Particle Size Distribution (PSD). The locations of the grabs were selected based on the multibeam bathymetry, the sand placement grid and the QTC unsupervised classification (Table 1). All coordinates are in UTM Zone 31N, with WGS84 as the datum. Target files in Hypack were used to mark the provisional coordinates and were used as a guide during acquisition. The PSD analysis was carried out by Geolabs.

Table 1: Coordinates of the grab samples with notes referring to how they were selected.

Grab Number	Easting	Northing	Location Notes
1	383284	5713357	Sand Placement grid- fine sand with clay
2	382441	5713324	Relocated sediment based on bathymetry
3	382640	5713361	Sand Placement grid- fine sand
4	384687	5712523	Outer south east - QTC class 13 (Light Blue)
5	384154	5712740	Near south east- QTC class 7 (Green)
6	382750	5713588	Northern - QTC class 6 (Dark Blue)

4.3: Data Processing Methodology and Result Analysis

This section describes the data processing carried out and presents the results for the North Edinburgh Channel with the discussion of the findings found in Chapter 6. It includes presentation of the bathymetry, difference models, different types of backscatter mosaics, Geocoder partial stacking and Patch AVO results, QTC unsupervised classification, supervised classification using the QTC outputs and groundtruthing.

Bathymetry and Difference Model

Bathymetry was processed in Hypack 2008, with use of the multibeam editor MB MAX in Hysweep. A measured tide file, obtained from the Margate tide gauge was used to tidally correct the soundings for both surveys. The POSPAC true heave file was applied and then sounding editing took place in Hysweep during Phase 2 of editing. A filter of 63 degrees was applied to reject the soundings outside this angle on the port and starboard side. The final stage of editing in Hypack was area based editing. Following this, .hs2 files were saved and used to generate an xyz file in Fledermaus. Figure 19 and Figure 20 show two key bathymetric features in the North Edinburgh Channel (Figure 19 and Figure 20).

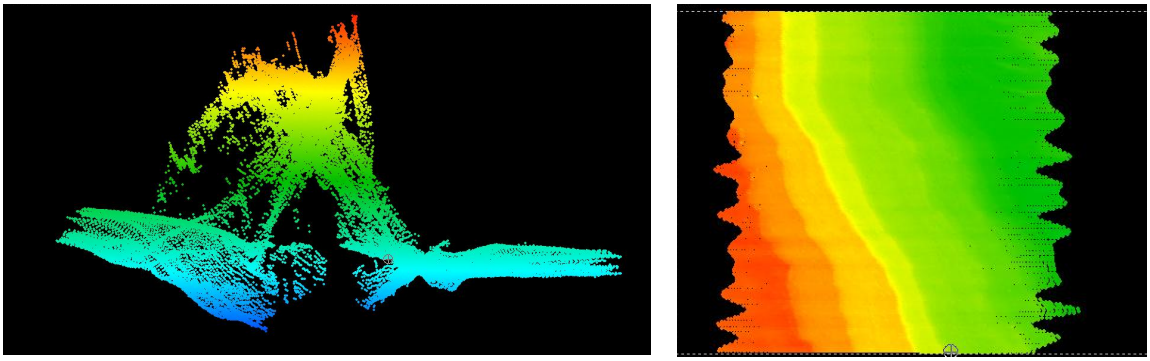

Figures 19 and 20: Bathymetric editing in Hysweep shows the Hawksdale wreck and the stepped terraces in the North Edinburgh Channel.

The area also contained the presence of numerous migrating sand waves, with a deeper area in the eastern part of the survey area. Bathymetry prior to and after the disposal of material is shown in Figure 21 and 22. A tin model with both datasets, generated in Hypack, was used to obtain a difference model of the bathymetry shown in Figure 23.

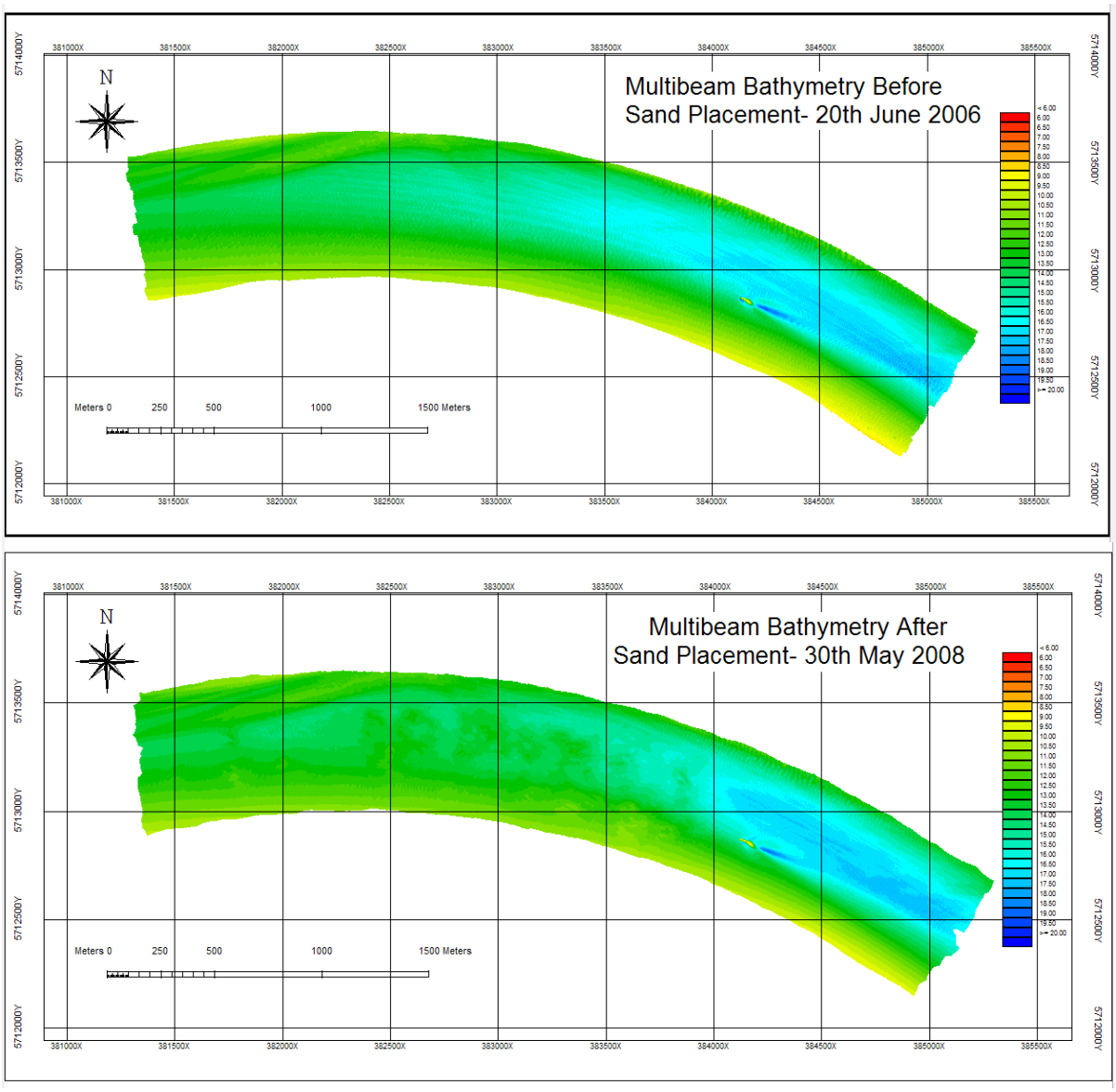

Figures 21 and 22: Multibeam Bathymetry from before and after the sand placement.

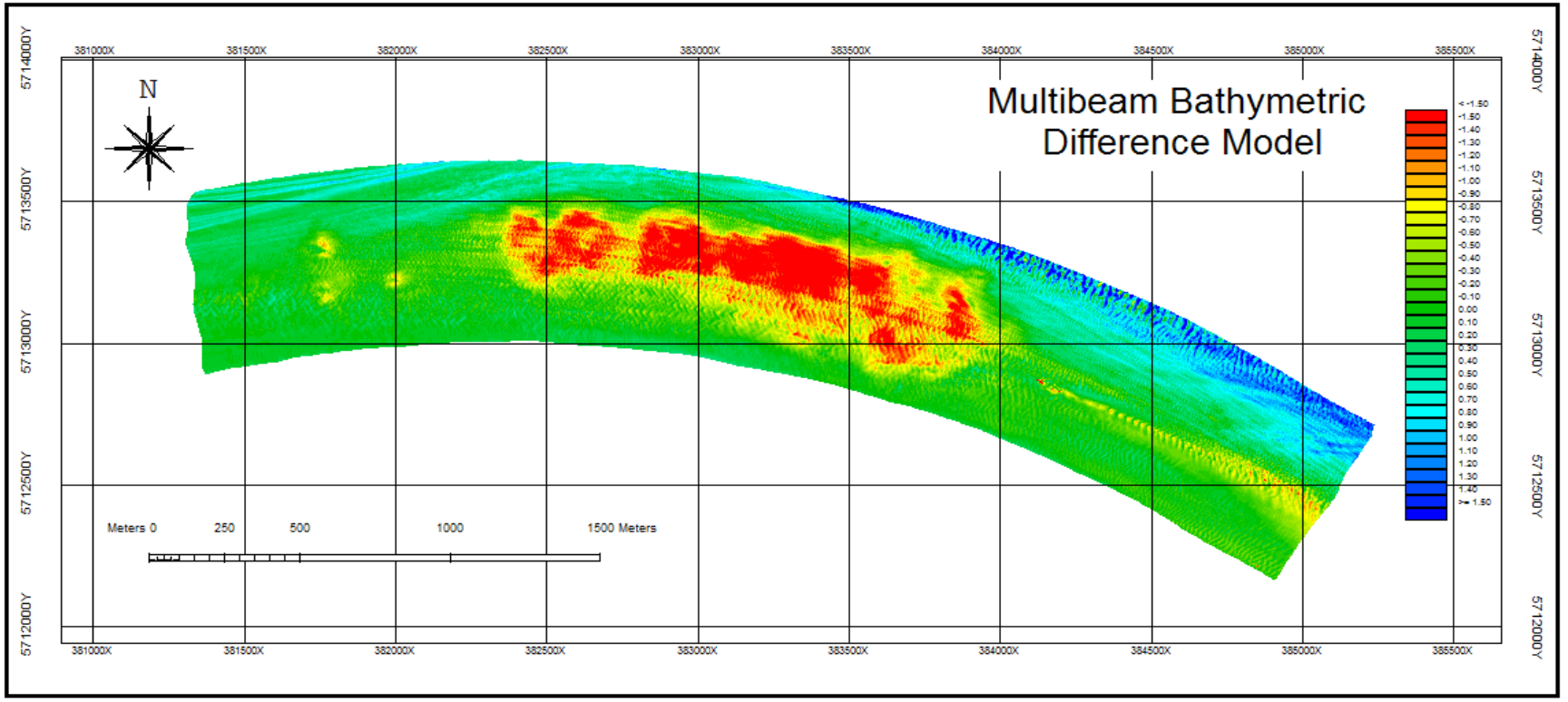

Figure 23: A multibeam bathymetric difference model of the North Edinburgh Channel highlights the area where dredged material has been placed.

Seabed characterisation using Geocoder

Backscatter mosaicking allows a preliminary interpretation and can be used for qualitative seabed characterisation. The Backscatter data from the 81x files was viewed in Hypack, using the "Load sidescan option" in Hysweep. Following the bathymetry editing of the Reson 8125 data, gsf files were saved as the required format for Geocoder. The created GSFs contained the beam averaged intensity data and the snippets time series data, incorporated by Hysweep into one file. Geocoder is also able to accept hsx and xtf files, although not all the features are presently available when using the hsx files. The Reson 8101 hsx files were loaded directly into Geocoder, to produce a pseudo-sidescan mosaic. To help illustrate the much improved mosaicking ability of Geocoder, a mosaic was constructed in Hyscan, the native Hypack sidescan and backscatter mosaicking tool.

Figure 24 and Figure 25 show the corrected backscatter mosaics from the first survey. Figures 26 and Figure 27 show the uncorrected pseudosidescan mosaic from Hyscan and the corrected mosaic from Geocoder (Figure 26 and 27). All mosaics are of 0.5m resolution. Geocoder applies most of the corrections during the load, with the slant range correction, Time Varying Gain and Angle Varying Gain (including the angular equalisation correction) applied. Beam pattern extraction was also carried out prior to the partial stacking stage, by loading a file of homogenous composition and extracting the beam pattern averaged over 1000 pings.

The partial stacking stage on the other hand preserved the angular information. It divided the backscattered return from the near-domain and that from the far-domain of the angular response curve. This is the first stage of Angular Range Analysis. Hence, the near- domain represents backscattered sound from between 65 and 87 degrees, whereas the far-domain represents the backscattered sound from between 35 and 65 degrees (Figures 29 and 30) (Fonseca and Mayer, 2007).

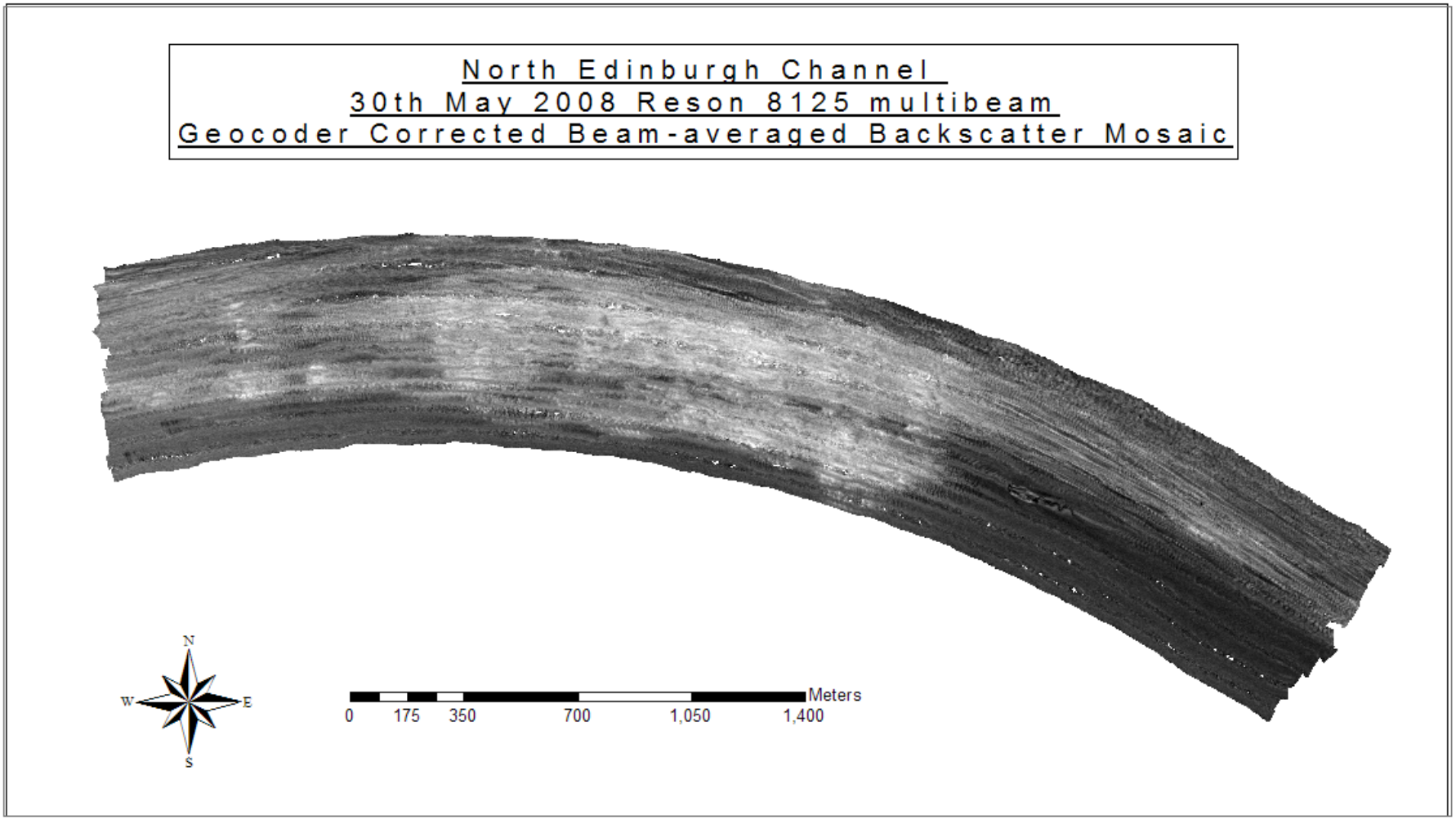

Figure 24: The fully corrected Reson 8125 multibeam beam averaged-backscatter mosaic clearly shows the area of relocation in the centre.

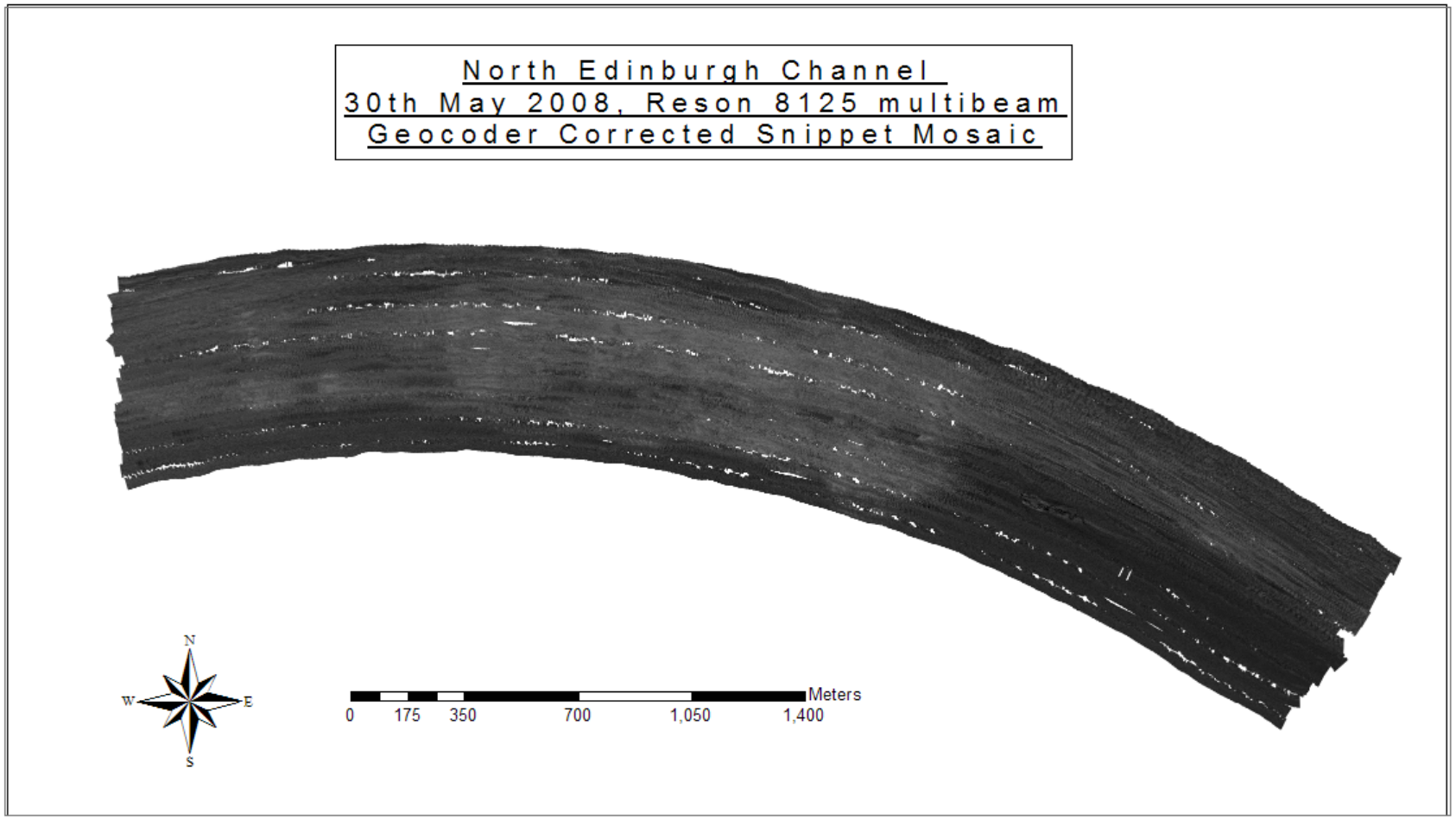

Figure 25: The fully corrected Reson 8125 multibeam snippet mosaic from the North Edinburgh Channel Survey 1 gsf files.

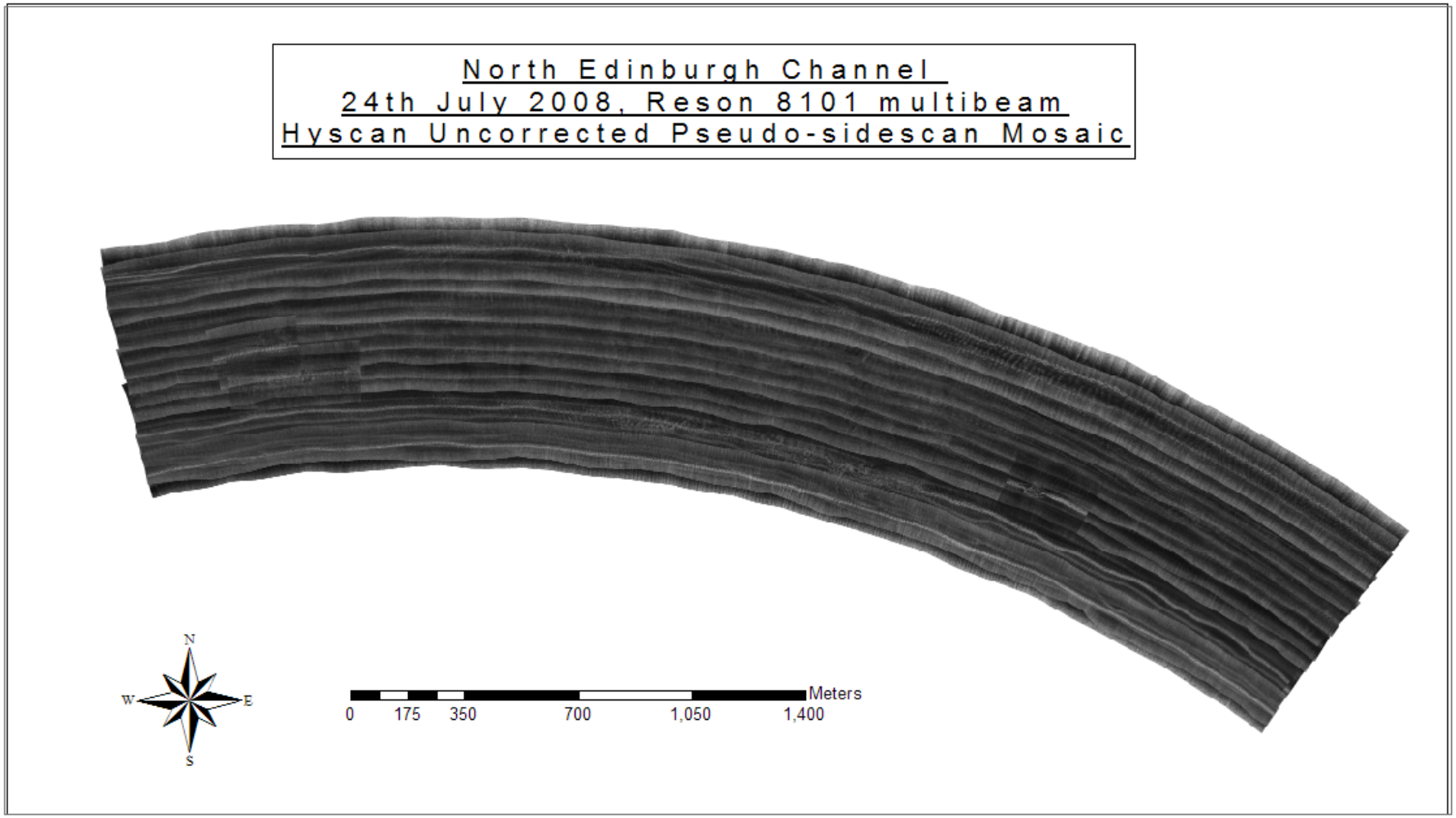

Figures 26: The pseudo-sidescan mosaics were constructed in Hyscan using the Reson 8101 hsx files.

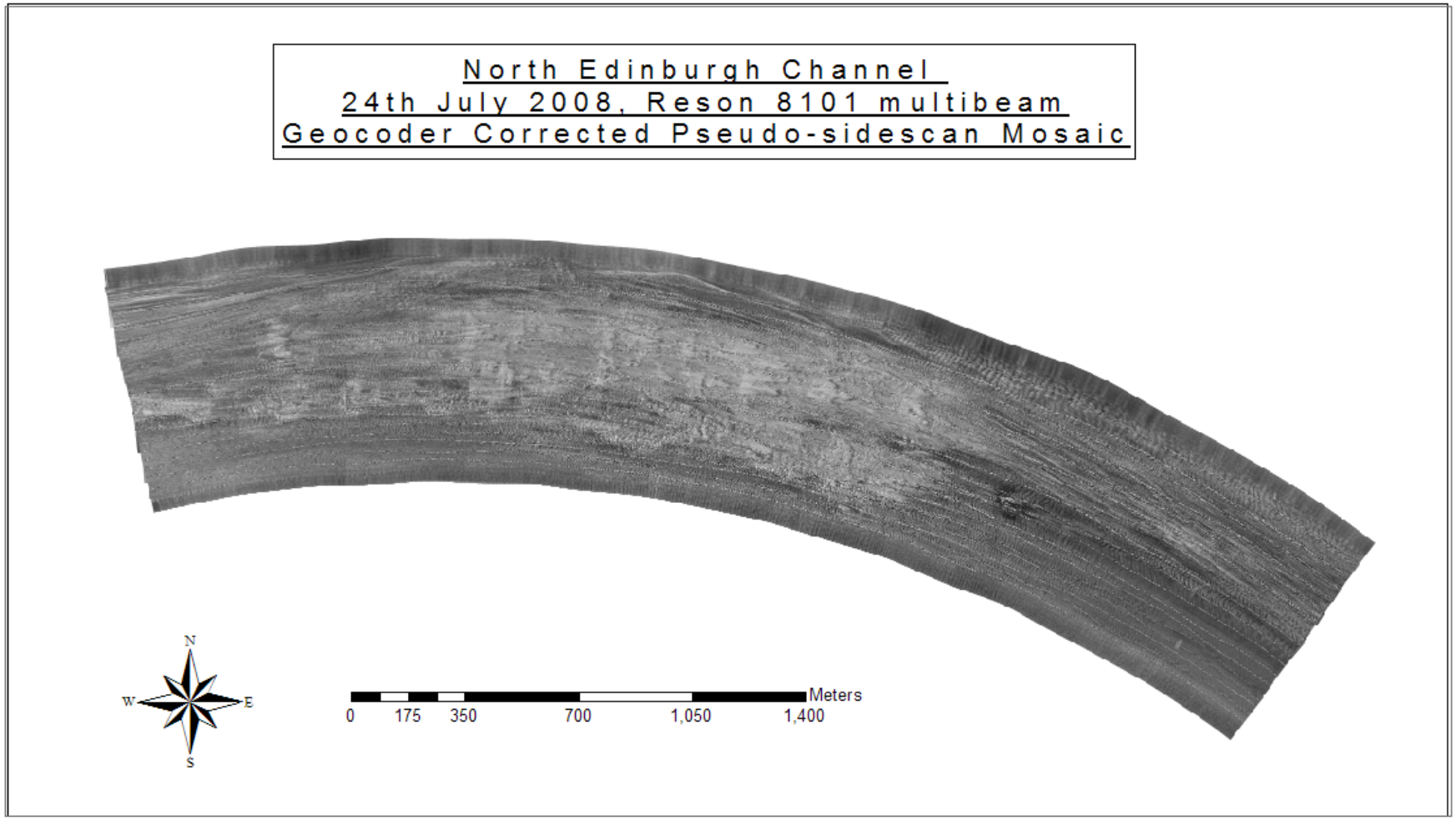

Figure 27: The corrected pseudosidescan mosaic constructed in Geocoder in Hypack 2008 using the Reson 8101 hsx files. In contrast to the Hyscan mosaic, the Geocoder mosaic allows interpretation to be possible. The relocation area clearly shows the dredged material.

The angular response curves were obtained from a seafloor patch and used to extract the ARA parameters required for Angular Range Analysis[1] of that patch, using the Patch AVO feature (Figure 28a and 28b). This was carried out at the grab locations, to compare with the measured grain size with the remote estimate of the grain size (Figures 31 to Figure 37). The blue line in these figures represents the model, with the red line representing the port side and the green representing the starboard side. An important consideration was that the seabed selected patch needed to be of homogeneous composition, as the angular response is characterised over half a swath width. Therefore, the most homogeneous side was selected for Patch AVO.

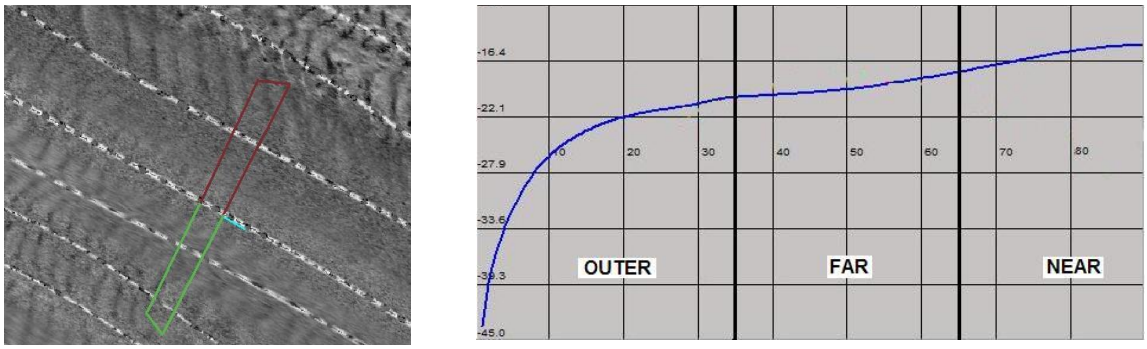

Figure:28a and 28b: The Patch AVO tool allows model inversion of a 30 ping x half swath width patch. The outer domain is not considered as it has a negligible contribution.

1 1

The full model inversion of the Reson 8125 data has not been included following advice from Luciano Fonseca, the author of the Geocoder software, regarding the limitations of the backscatter model used by Geocoder (Fonseca, 2008). This system has a frequency of 455 kHz and the present backscatter model is only able to work reliably to make remote estimates of the grain size, impedance and roughness for frequencies up to 300kHz. Although the Hypack 2008 version of Geocoder is able to accept and process the Reson 8101 (240kHz) pseudosidescan data in the Hypack's proprietary hsx format, the version of Geocoder with the seabed characterisation module is not able to read the hsx files. This highlights the fact that this is very new software and is still in its developmental stages. The Patch AVO can be carried out in Hypack 2008 and the full Angular Range Analysis is planned to be included in Hypack 2009.

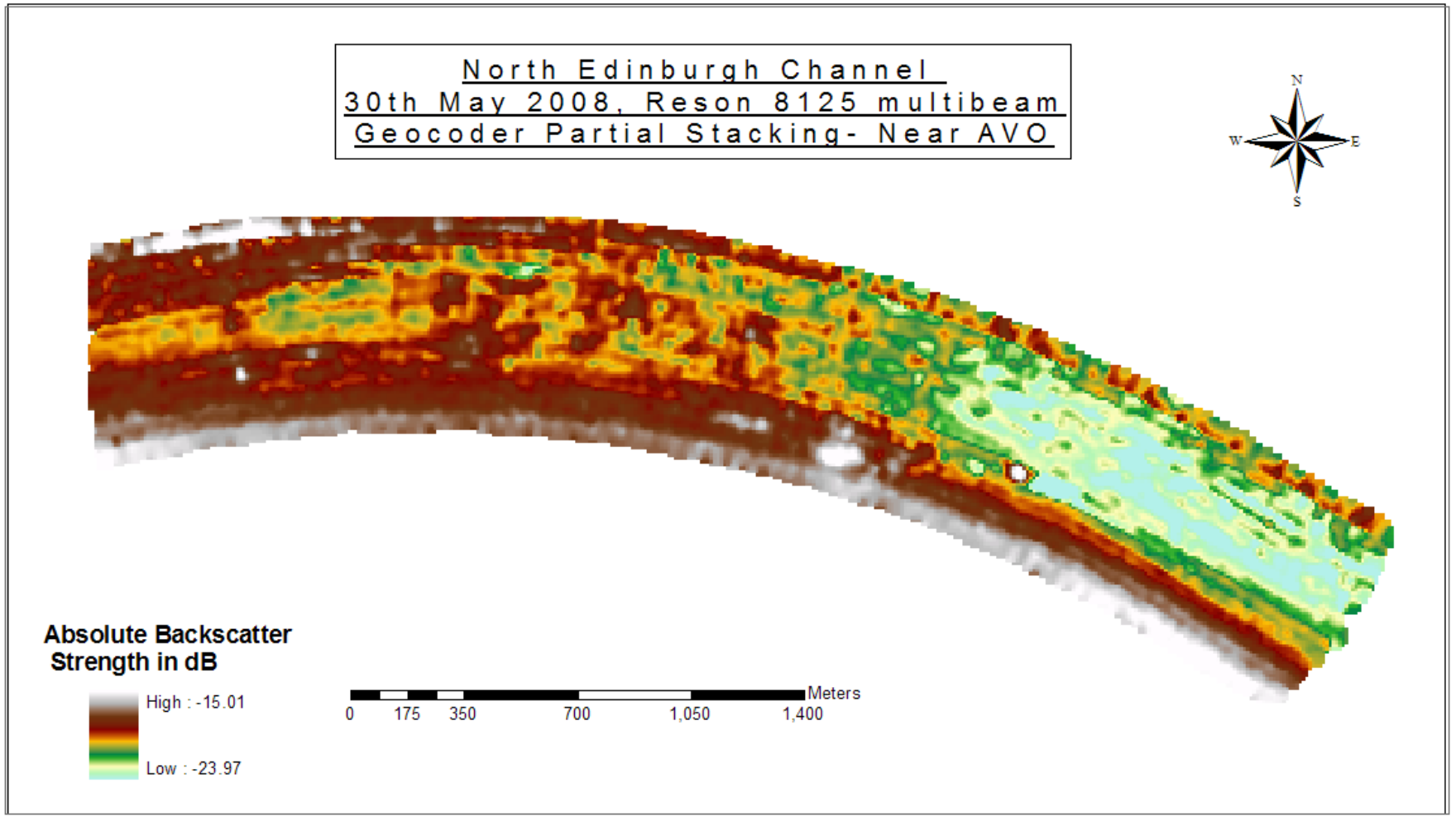

Figure 29: The Near AVO of the Reson 8125 data shows highlight features on the seabed, with lower values from the deeper region in the east. The area where sand placement has occurred is showing medium backscatter values in this domain.

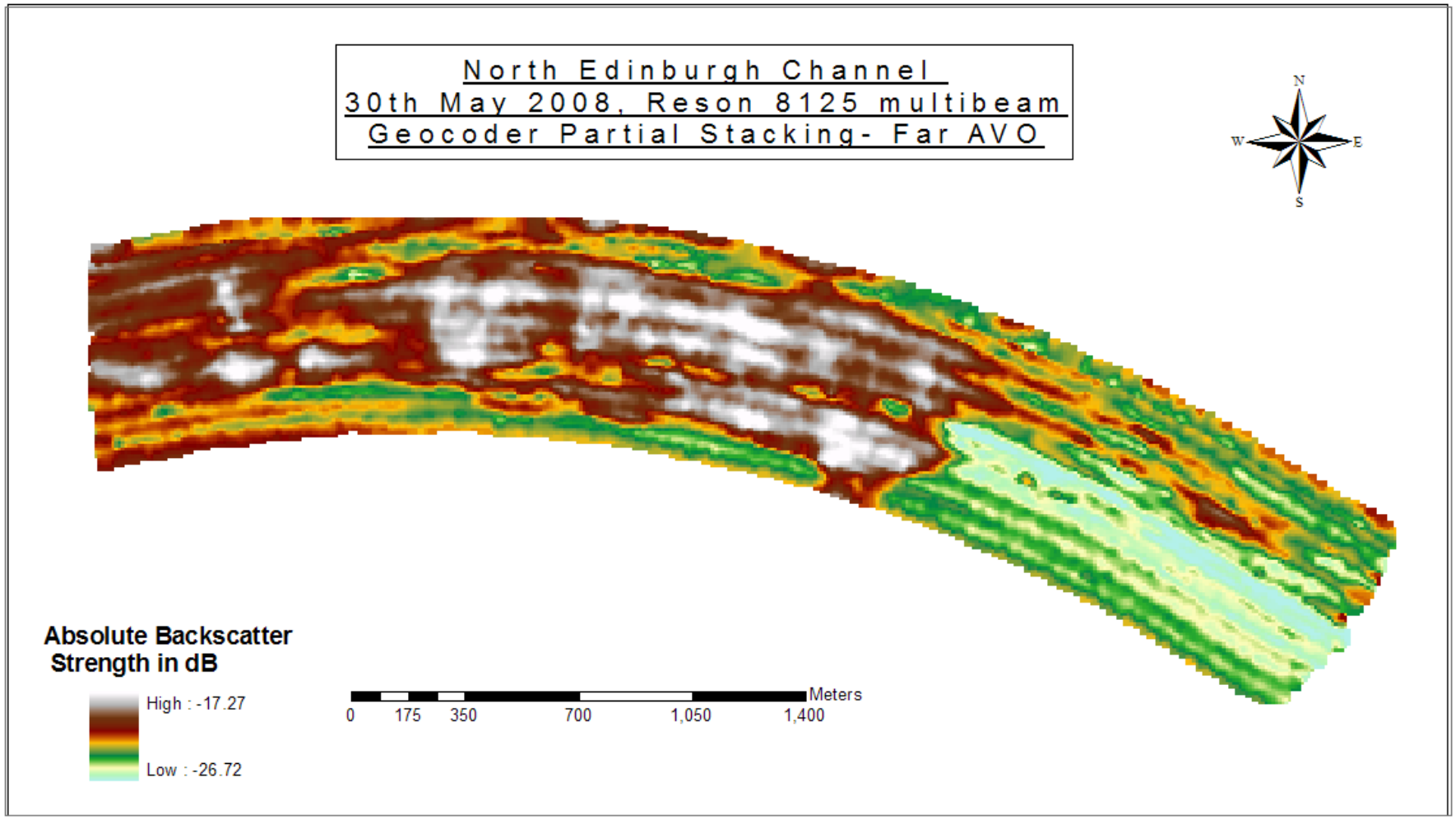

Figure 30: The Far AVO of the Reson 8125 data shows highlight different features on the seabed. The area where sand placement has occurred is showing the highest backscatter values in this domain, with the outer south east area with low values.

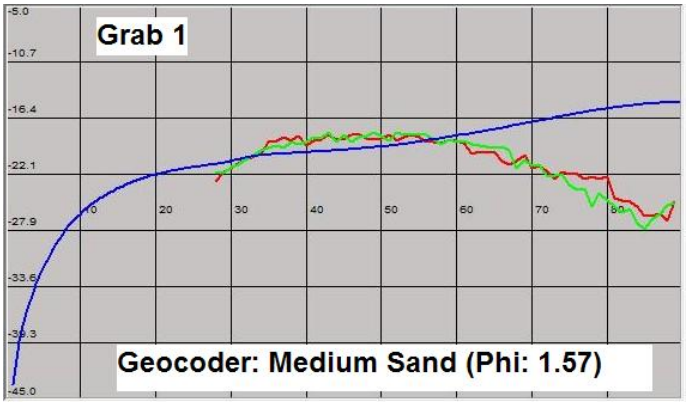

Figure 31: Patch AVO results for Grab 1, from the area potentially containing clay in the sand placement grid

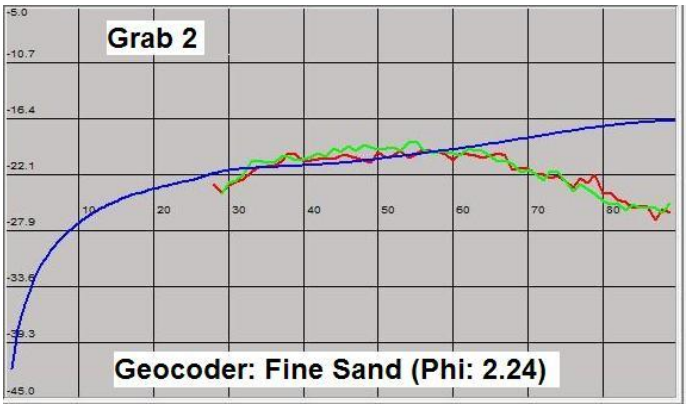

Figure 32: Patch AVO results for Grab 2, from the area of relocated sediment, as indicated by the bathymetry.

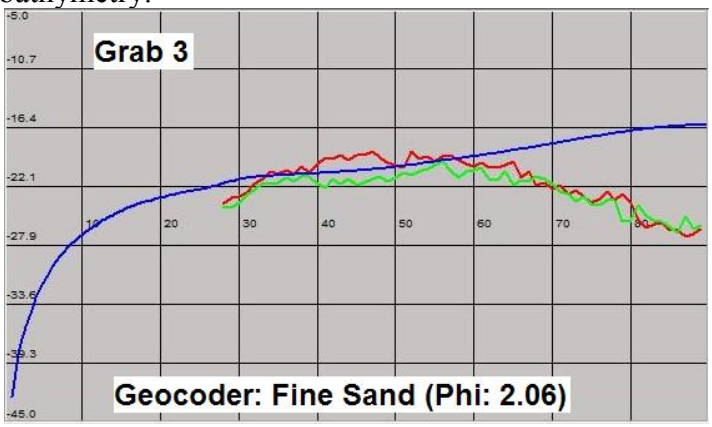

Figure 33: Patch AVO results for Grab 3, from the area of relocated sediment, based on the area of fine sand in the sand placement grid.

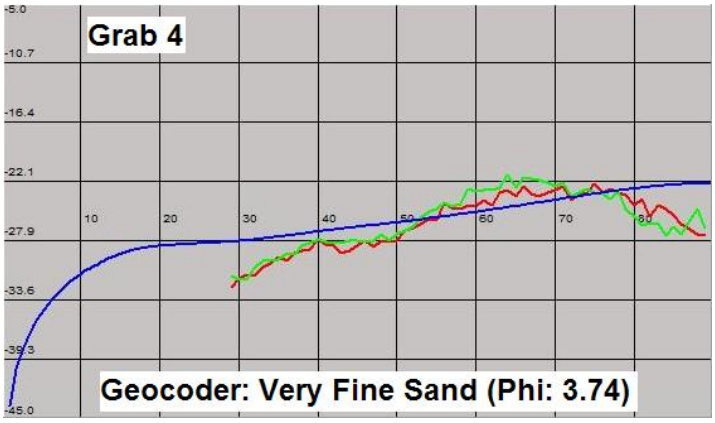

Figure 34: Patch AVO results for Grab 4, from the outer south east area (QTC class 13).

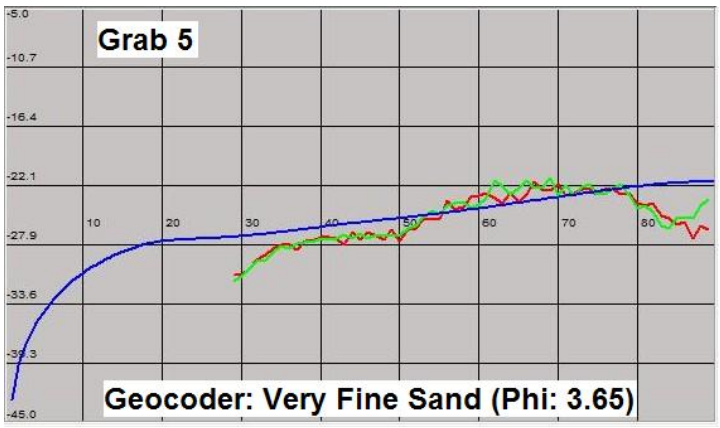

Figure 35: Patch AVO results for Grab 5, from the QTC class 7 located just west of the south eastern class.

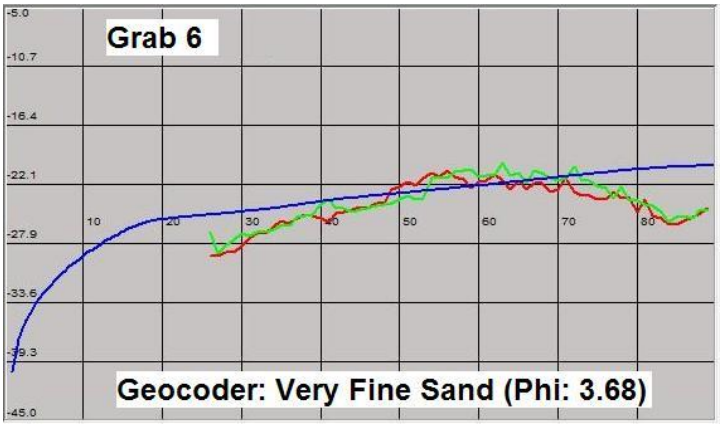

Figure 36: Patch AVO results for Grab 6, from QTC class 6 located in towards the north of the area of relocation.

Seabed Classification using QTC Multiview

The Reson 8101 hsx files were processed in QTC Multiview with unsupervised classification being carried out. Following raw load, cleaning was carried out by importing the Hypack .hs2 files and also using the internal tools available. The "Mask by beam grazing angle" tool calculates the true grazing angle, with use of the bathymetry. Returns from grazing angles outside 0 and 90 degrees were rejected as they do not originate from the seabed (QTC, 2007). Manual boarder editing in the Image Viewer also took place (Figure 37). It was apparent that there were some artefacts, resulting from the single beam echosounder running simultaneously (for bathymetric cross-checking purposes). The rectangle size was selected as being 33 x 33 using the rectangle size selection tool. This would give a high enough resolution, as well as reduce the possibility of a noisy classification output. The rectangle generation phase resulted in over 62 530 rectangles being generated on unmasked data. A compensation table to correct for the grazing angle dependence was also generated during the rectangle generation phase, prior to any feature extraction. Full Feature Vectors (FFVs) were generated and processed using the FFV editor, with manual editing to reject outliers (Figure 38). The FFVs from all the lines were merged and a catalogue was created. It is during this stage that the Principal Component Analysis is carried out, reducing the features to 3 Q values.

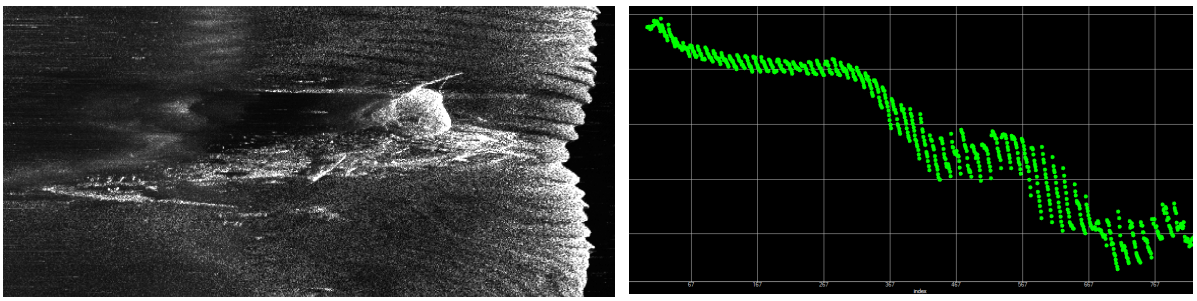

Figure 37 and 38: An image of the Hawksdale wreck in the Multiview Image viewer and FFV (Full Feature Vector) editing in the FFV Editor bathymetry editing mode is shown.

Cluster Analysis was then performed using the generated catalogue, using the Auto Cluster tool. This was an iterative process, with the user being required to select the number of iterations per class (i.e. 10) and the range of classes to test (i.e. 3 to 15). First, the pixels are clustered into three classes in Q space, with that iteration being assigning a BIC score (Figure 39). This process is then repeated 10 times for that number of classes. Following this, the process is repeated for the subsequent number of classes (Ie. 10 iterations for 4 classes). The iteration which gives the lowest BIC score is then used for updating the catalogue and subsequently gives the classified output (Figure 40).

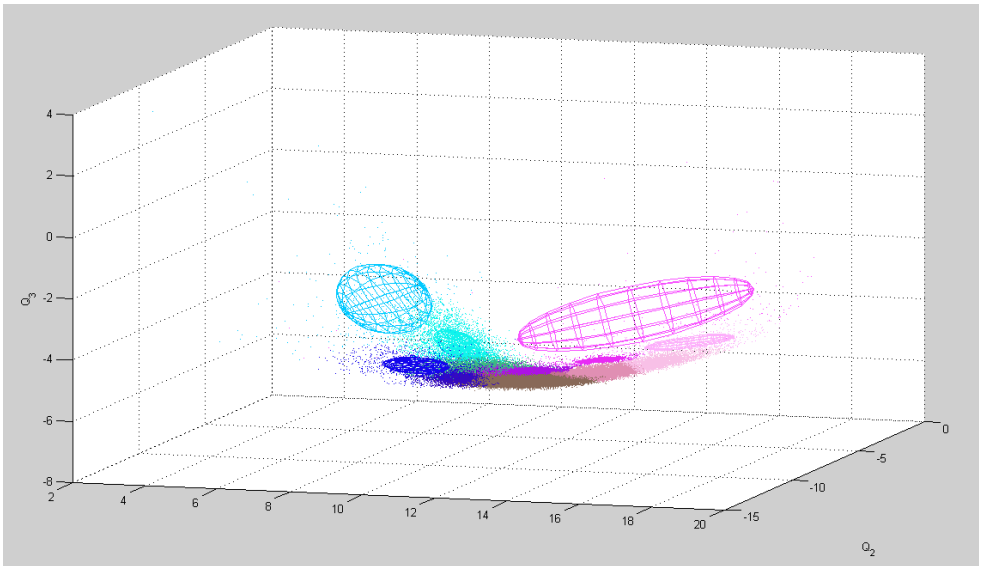

Figure 39: The 14 clusters from the North Edinburgh Channel are shown in the QTC feature space or Q Space, with the pink clusters representing the relocated class.

The final .seabed ascii file was created, with the UTM coordinates, class numbers, three Q values output from PCA (Q1, Q2, Q3) and the class confidence and probability. This file contained point data, which was then taken into QTC Clams for gridding and visualisation. The software performs categorical interpolation and post classification smoothing. Although, this alters the classified output, it does not necessarily degrade its accuracy if used appropriately. It can reduce classes which correspond to noise, common in unsupervised classification. Figure 41 shows the classification map with the sand placement grid overlaid (Figure 41).

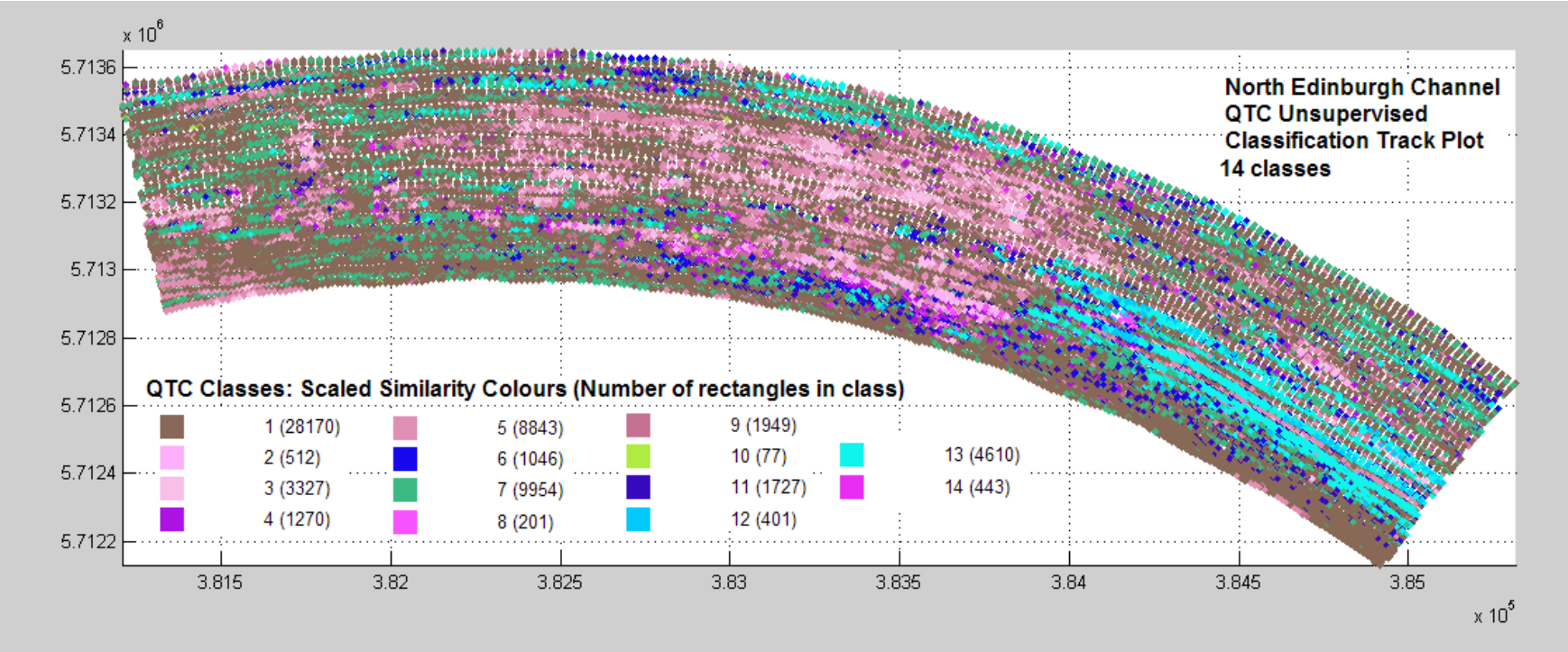

Figure 40: The Track plot of the classification with the rectangles output as an ascii .seabed file. Similarity colours are where a colour scale is assigned to each class depending on the distance that cluster from another cluster in feature space. This allows classes with a similar acoustic return to be of a similar colour etc.

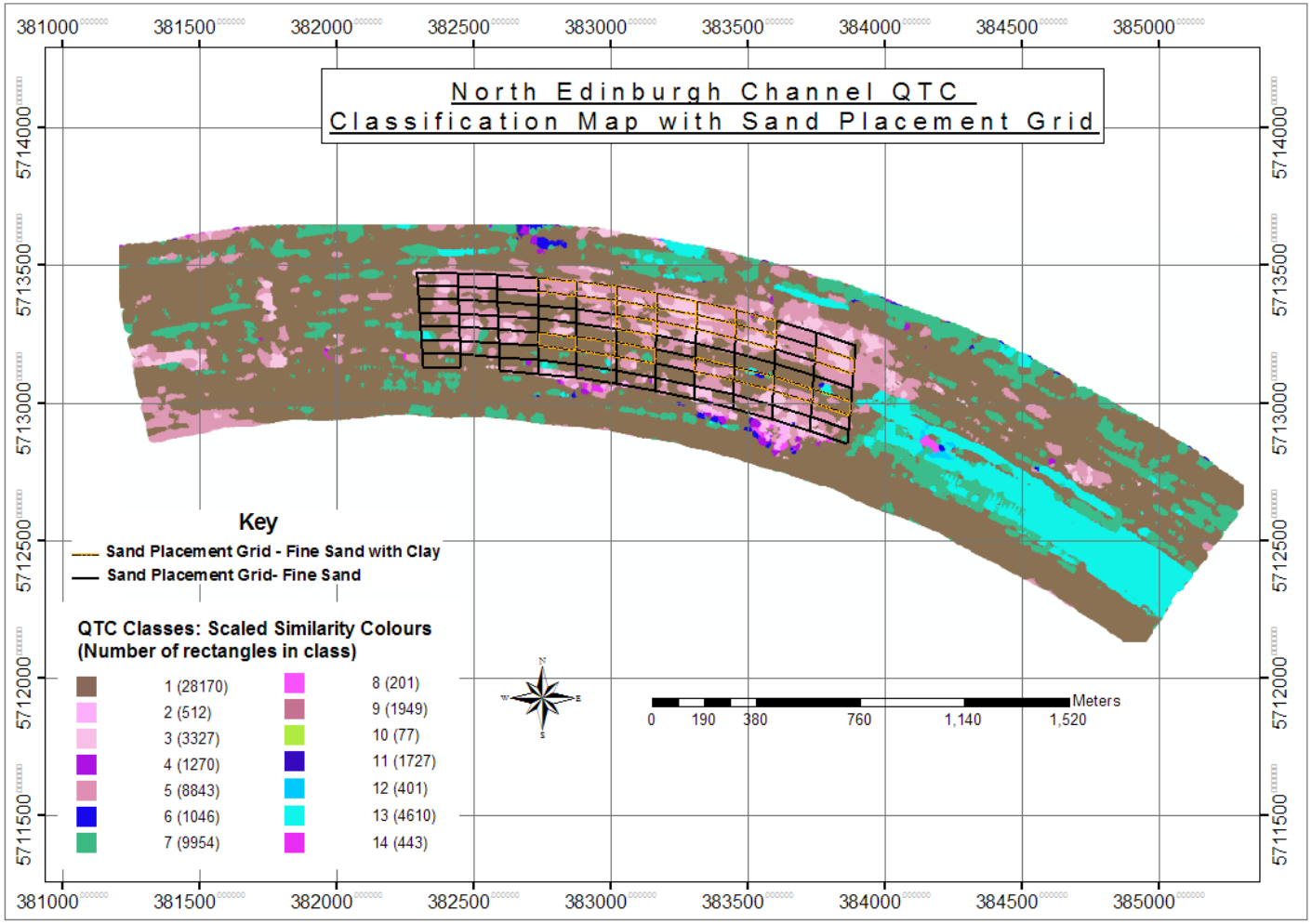

Figure 41: QTC Classification map with the Sand Placement Grid shows the presence of classes corresponding to the relocation area. There is also an eastward movement of these “relocated sediment” classes, in relation to the sand placement grid.

Grab Sample Results

Following the Particle Size Distribution analysis of the grab samples, Table 2 shows the groundtruthing results, together with Geocoder's estimates of the grain size and composition and the QTC classes for each grab (see also Appendix 3). The results show that the relocated material did not contain a significant amount of clay, with Grabs 1, 2 and 3 from the relocation area containing no more than 5% of silts or clays (Grab 1) (Figure 42). The Geocoder estimates of grain size are shown to match very well with the grab compositions. The results suggest that Geocoder can identify the composition of the relocated material as well as differentiate between different fractions of sand. Six different QTC unsupervised classes were identified, as shown in Figure 43. The identification of Class 1 should be treated with caution. This is because Grab 3, located in QTC Class 1, was sampled to obtain a representation of the sand placement grid –fine sand area. Although Grab 3 is in Class 1, most of the area in Class 1 is outside the sand placement grid.

Table 2: The results of the groundtruthing in the North Edinburgh Channel, with the corresponding QTC Classes and Geocoder remote estimates of the grain size.

Grab No	Grab Location Notes	Grab Basic Composition	Geocoder Composition	Geocoder Grain size	QTC Class
1	Sand Placement grid- fine sand with clay	Fine to coarse sand with abundant shell	Medium Sand	1.57	Class 3 (Light Pink)
2	Relocated sediment based on bathymetry	Fine to coarse sand with silt and shell	Fine Sand	2.24	Class 5 (Pink)
3	Sand Placement grid- fine sand	Fine to coarse sand with silt and shell	Fine Sand	2.06	Class 1 (Brown)
4	Outer south east - QTC class 13 (Light Blue)	Fine sand with silt	Very Fine Sand	3.74	Class 13 (Light Blue)
5	Near south east- QTC class 7 (Green)	Fine to medium sand	Very Fine Sand	3.65	Class 7 (Green)
6	Northern - QTC class 6 (Dark Blue)	Fine to medium sand with silt	Very Fine Sand	3.68	Class 6 (Dark Blue)

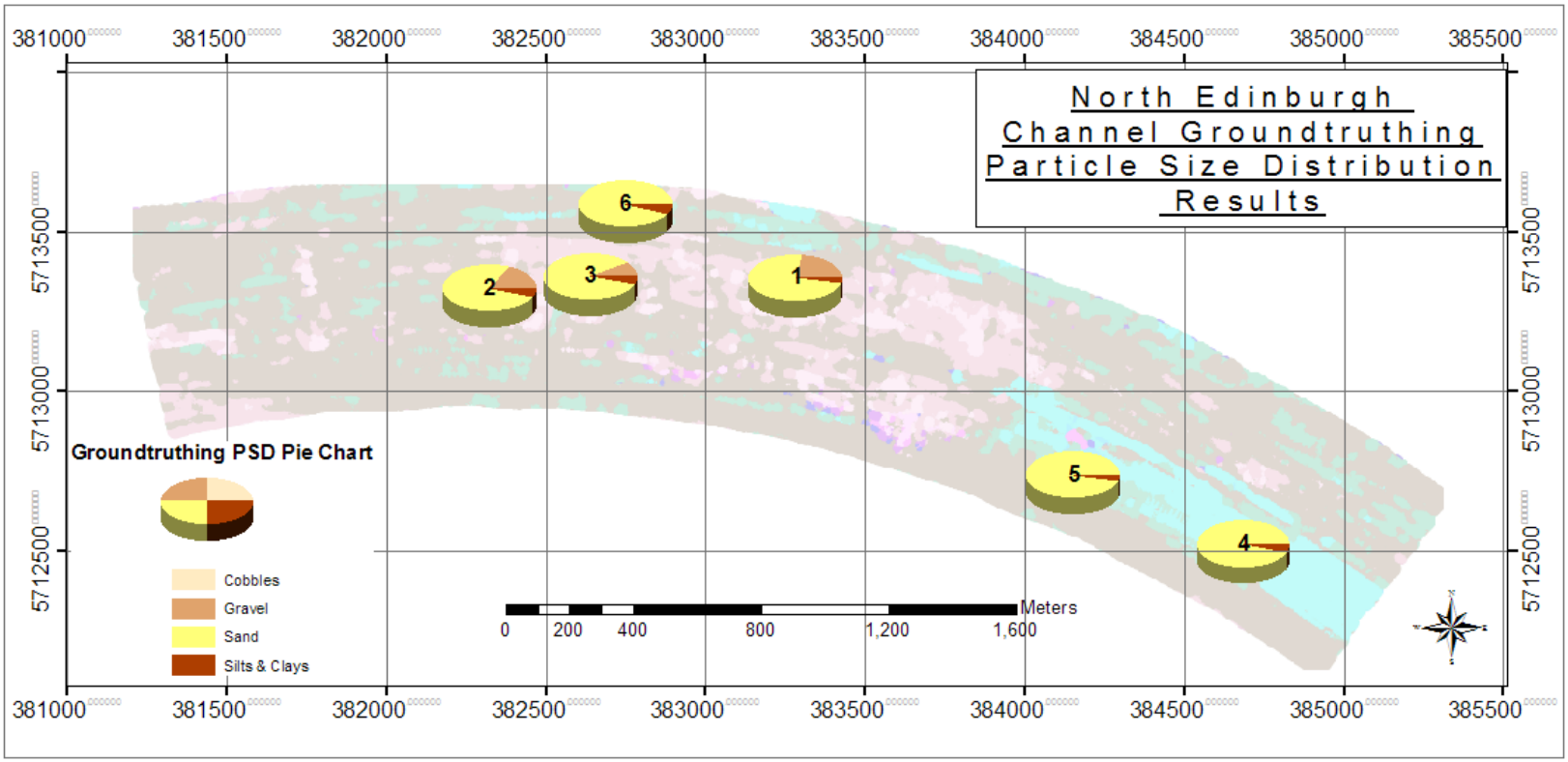

Figure 42: The results of the Particle size distribution shown as pie charts to show the compositions of the grab samples as being predominantly sand, with variable amounts of gravels (or gravel sized shell material), silts and clays.

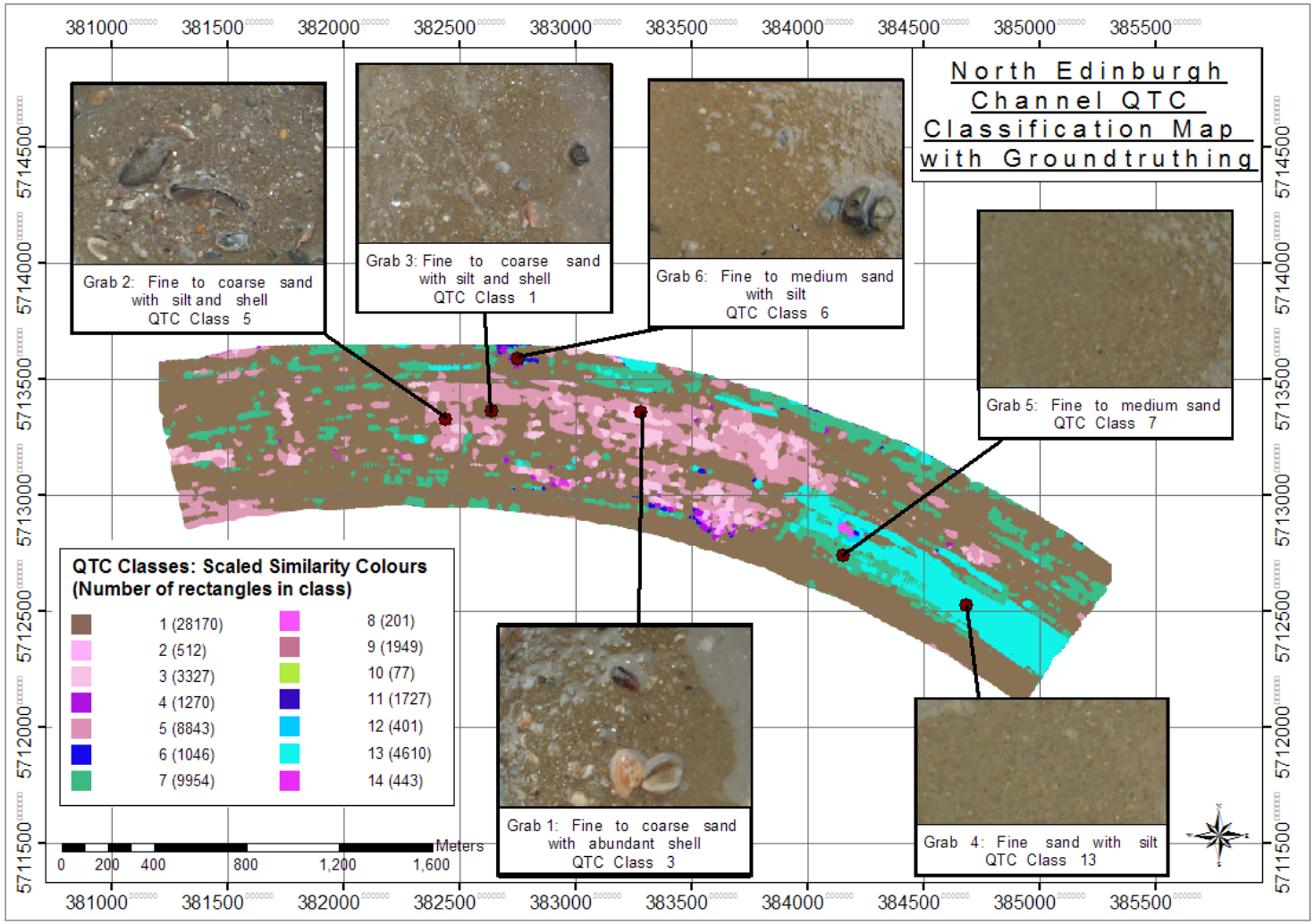

Figure 43: The QTC unsupervised classification map with groundtruthing based on the analysis of the grab samples.

Supervised Maximum Likelihood Classification

There are numerous available options of performing supervised classification after the unsupervised QTC classification stage. One option within the proprietary software is to use the catalogue generated from clustering of one data set and apply it to the features of another data set. Another previously used approach is to use the Q values from the unsupervised QTC classification (Boyd et. al. 2006). The Q values are the 3 intermediate outputs of the Principal Component Analysis (PCA) following feature extraction and account for a majority of the variance. These values can be clustered independently using the tools available in Geographic Information Systems (GIS) or image processing software designed to classify remote sensing images.

The first stage was to produce an image of the Q values in ArcGIS, by interpolating the point data, using the Inverse Distance Weighting (IDW) interpolation. This introduced an error, however this is an unavoidable cost of rasterisation. The introduced errors were predicted to be small, with a mean error value of -0.0042, 0.0568, 0.0095 respectively for Q1, Q2 and Q3 (Figure 44, 45 and 46). This produced three images for each principle component (Figure 47, 48 and 49). This was represented as a colour composite produced using the "Composite Band" tool in ArcGIS. The colour composite, with 3 bands corresponding to Q1 (red), Q2 (green) and Q3 (blue) is shown in Figure 50. The first stage of supervised classification is to develop training areas. This was carried out by using a 25m buffer around the locations of the grab samples, based on the assumption that the area within this buffer was of homogeneous composition.

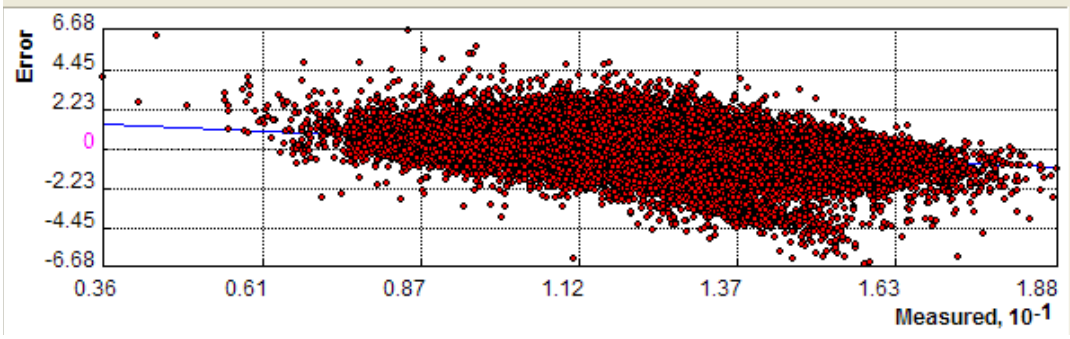

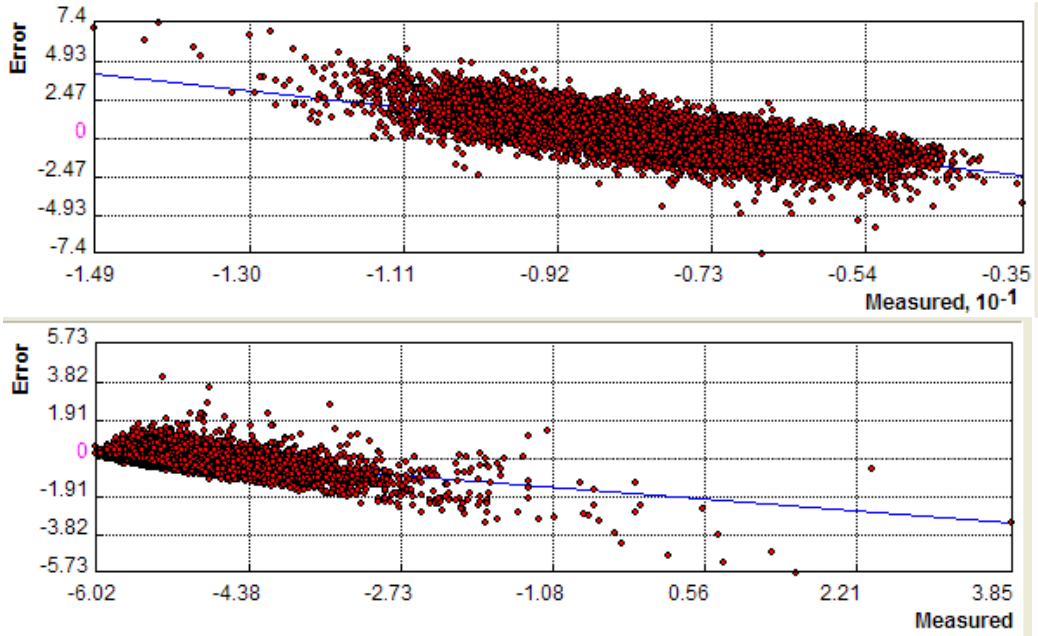

Figures 44, 45 and 46: The predicted errors of interpolation using the ArcGIS Geostatistical Analyst.

The unsupervised QTC classification map was examined with the training areas and this did not reveal any overlap between the training areas and determined class boundaries. The maximum likelihood classification method in ArcGIS was used to classify the colour composite. The six training areas would form the initial seeds for the clusters, with subsequent pixels assigned to a cluster based on the highest probability. This led to six classes being found in the classified output (Figure 51). No apriori probabilities were assigned. The classification was then smoothed using a 3 x 3 majority filter, the only filter suitable for post-classification smoothing (Liu and Mason, 2007, Figure 52). This classification was then compared with the Geocoder Patch AVO results (Figure 53).

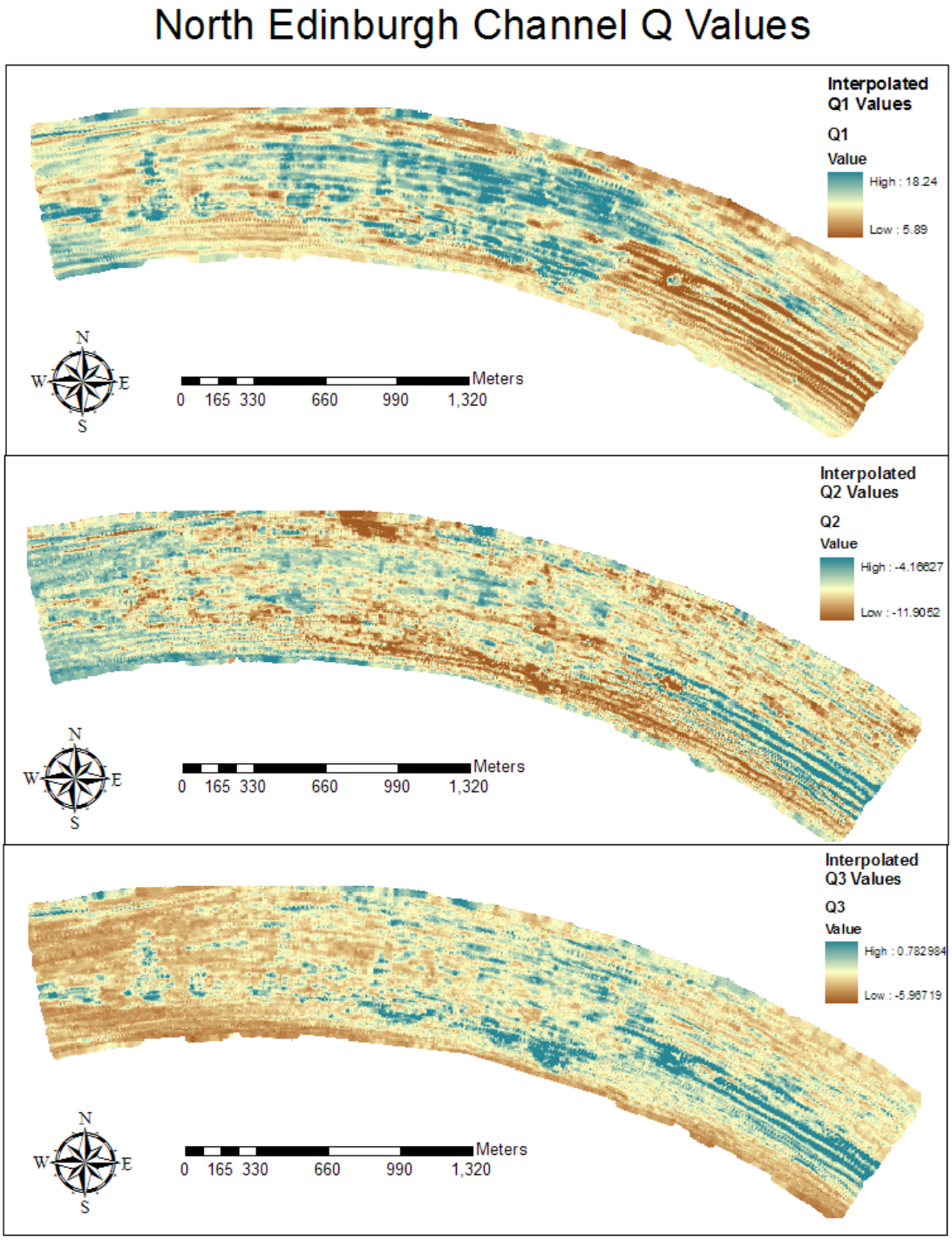

Figure 47, 48 and 49: The images representing the Q values output from the QTC unsupervised classification, for Q1, Q2 and Q3 respectively.

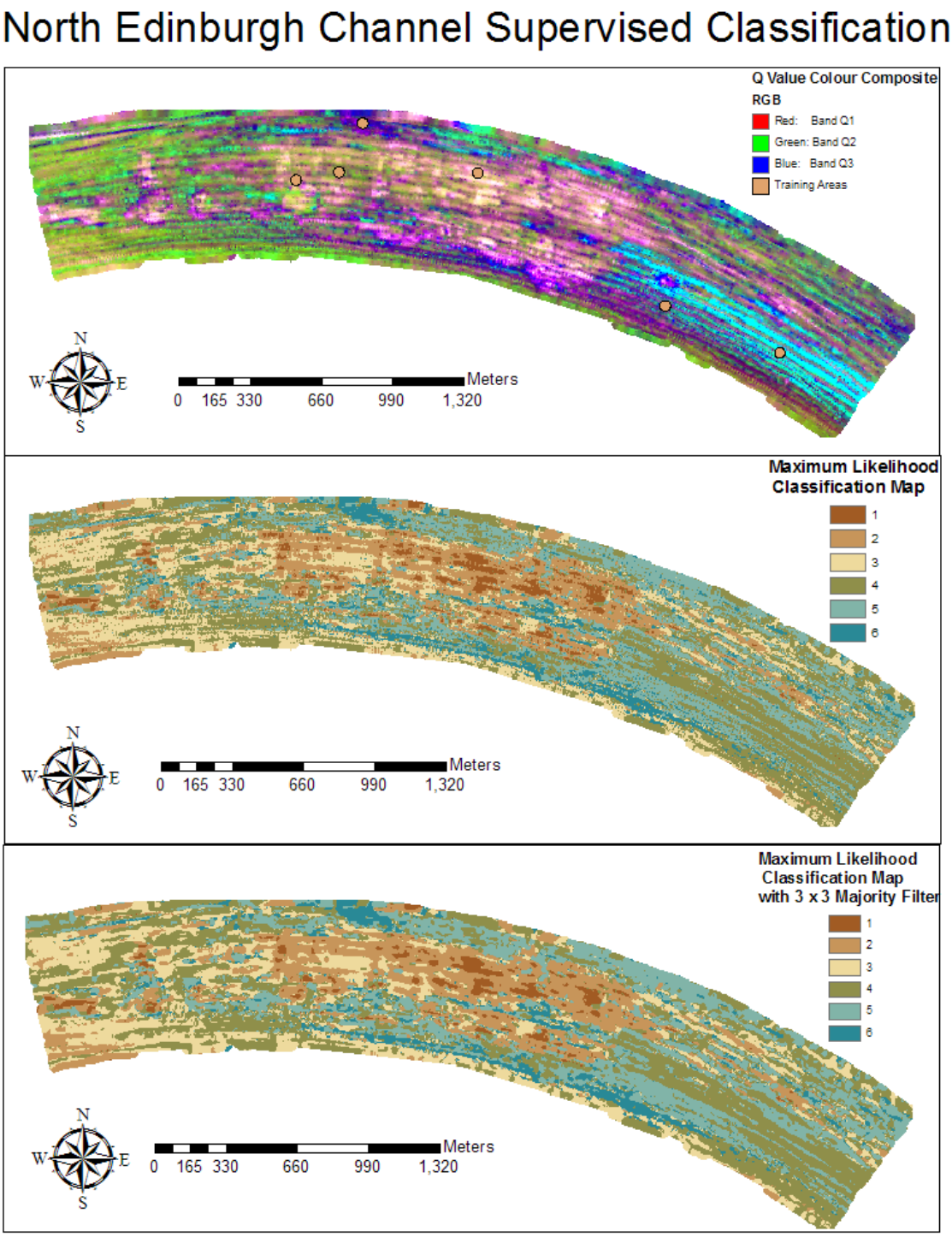

Figure 50, 51 and 52: The Q Value colour composite, the maximum likelihood supervised classification output and the smoothed output following filtering with a majority filter.

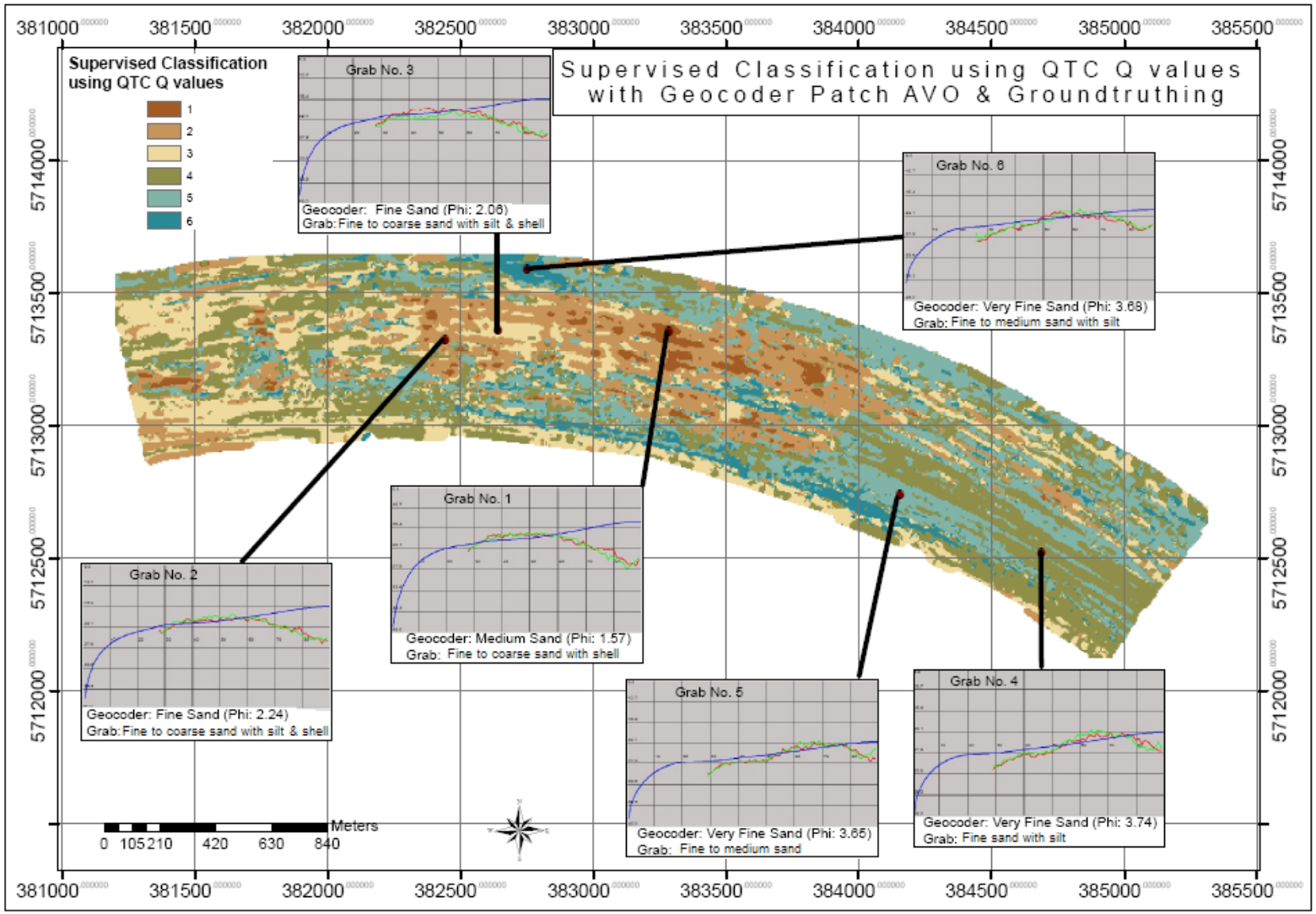

Figure 53: Maximum likelihood supervised classification using QTC Q values with Geocoder Patch AVO results.

Accuracy Assessment

The accuracy of Geocoder's remote estimate of grain size has been assessed by comparing with the results of the Particle Size Distribution (PSDs). Although it was not possible to do a full error matrix to assess the accuracy of the image-based classification quantitatively within ArcGIS, an attempt was made by comparing with groundtruthing. To assess the accuracy of the unsupervised classification, two previous grabs were found in known unsupervised classes were used to compare with the composition of the know classes. Note that although these two grab samples were collected prior to the relocation of the dredged material, they are not located within the relocation area sand placement grid (Figure 54).

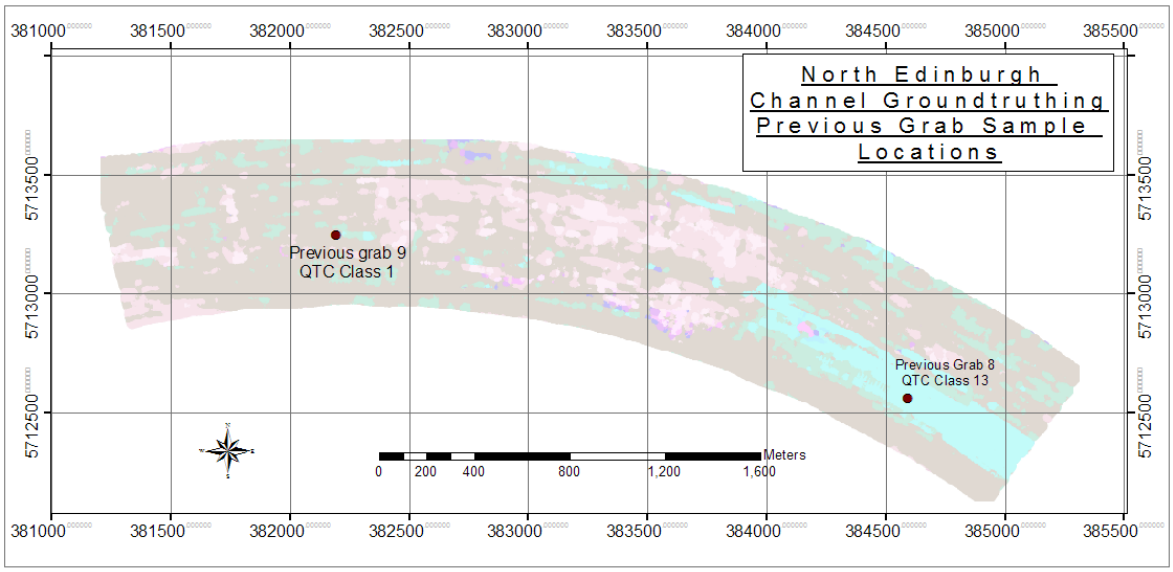

Figure 54: The locations of two previous grabs from the North Edinburgh Channel, with the respective QTC classes. For consistency, the numbering system is not changed.

Table 3: The results of the previous grab sampling, with the results from present grab samples located in the same QTC class.

Grab Number	Previous grab 8	Grab 4	Previous grab 9	Grab 3
QTC Class	13	13	1	1
Composition	Sand with minor silt fraction	Fine sand with silt.	Fine to medium sand	Fine to coarse sand with silt and shell.

In theory, two grabs in the same class should have a similar composition, as they are located a region with a similar acoustic return. Previous grab 8 from QTC Class 13 is composed of sand with silt, with Grab 4 from Class 13 also composing of sand and silt. This shows that there is consistency in the QTC classification map. Previous grab 9 was shown to be in QTC class 1. Judging from Grab 3, QTC class 1 should be composed of fine to coarse sand with silt and shell, suggesting this material originates from the Princes channel. The previous Grab 9 however is composed of Fine to medium sand and therefore this class 1 is less consistent. Still, Grab 4 was selected to study the sand placement grid area of fine sand, rather as basis to identify class 1. Ideally, more grab samples from previous data should be used to verify the classification accuracy and only a limited assessment can be made here. The Grab compositions from Grabs 4, 5 and 6, with locations selected so they can determine three different QTC classes, are all different in composition. This suggests that the QTC classification is able to differentiate between even small differences in the sediment composition.

The results of the backscatter mosaics, Geocoder results, the QTC unsupervised classification and supervised classification are fully discussed in Chapter 6. At first glance they suggest that both the QTC and Geocoder seabed classification methods can effectively discriminate between the dredged sediment from the Princes Channel and the original seabed.

Chapter 5: Regional Environmental Characterisation

5.1: Thames Regional Environmental Characterisation (REC)

This chapter compares the Geocoder's Angular Range Analysis (ARA) method with the QTC classification method using data collected as part of the Thames Regional Environmental Characterisation (REC) surveys. Some background information about the REC data and survey area is given, followed by the acquisition methodology and result. An assessment of the accuracy of Geocoder's remote estimates of the grain size is also made.

REC surveys are commissioned by Defra and being carried out around the country to help characterise larger regions such as the outer Thames estuary. This area is affected by aggregate extraction and seabed classification techniques can be used to assess the impacts on the existing seabed. The main aim of a seabed characterisation using the REC data is to obtain a broadscale idea of the composition of the seabed in a large region. The REC data is intended to be used to put data from more local Regional Environmental Assessment (REA) surveys into a broader regional context (Brown and Grove, 2008). As the regions where extraction is occurring changes on a regular basis, it is necessary to survey a larger region to be able to better assess the impacts.

The REC surveys of 2007 involved data collection from the South Coast and Thames region, with other regions such as the Humber Estuary and the East Coast to be covered this year (ALSF, 2008). A range of organisations were involved in the data collection from the Thames region, with Gardline Lankelma primarily involved with the data acquisition. Raw and processed data has been made available through the ALSF GIS website run by the Geodata Institute and ABP Mer (Moore, 2007). It highlights current initiatives to make marine geospatial data more publicly available. With the arrival of the INSPIRE directive, initiatives such as Marine Data Information Partnership (MDIP) aims to promote open access of data. The importance of seabed classification for marine spatial planning has also been realised in Ireland, with multibeam data being made publicly available by the Geological Survey of Ireland through the INFOMAR GIS (GSI, 2008).

The REC survey area covered a very large region, with over 1400km of lines being acquired. During the time of the survey, there were 8 licensed aggregate extraction sites in the Thames Estuary (BMAPA, 2007). The track lines from the survey are shown in Figure 55, with the aggregate extraction polygons also shown. The area studied is shown in greater detail in Figure 56. The areas with aggregate extraction licenses are regularly subject to review with new areas being granted a license to dredge in the area. The extraction areas are dredged by different companies and the polygons from July 2007 have been used here, as this corresponds to the survey period.

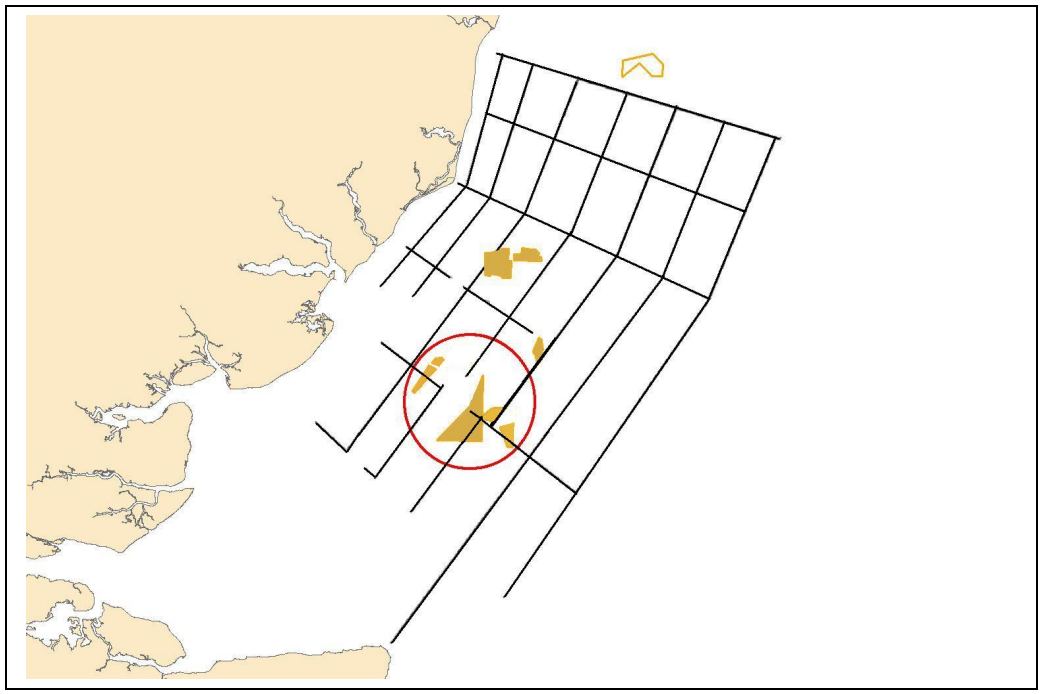

Figure 55: The Thames REC data track plot is shown. The yellow polygons define the licensed areas of aggregate extraction. The area examined in this study is circled (Courtesy of Cefas).

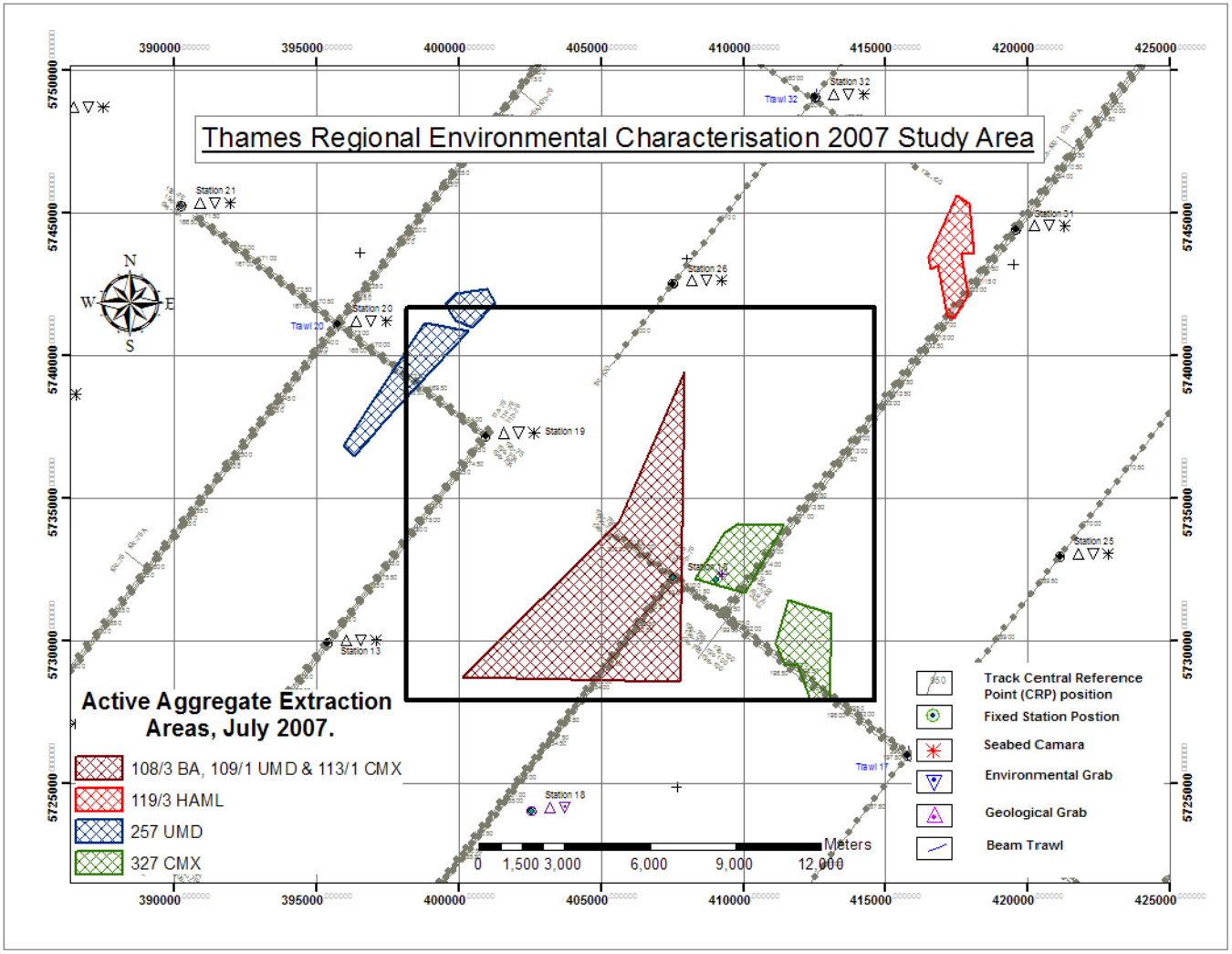

Figure 56: The licensed areas of aggregate extraction examined by this study, with the REC data trackplot (Extraction areas coordinates courtesy of Hanson Marine).

5.2: Data Acquisition Methodology

The reader is asked to consult the operations report produced by Gardline detailing the survey methodology in full, with a summary provided here (Brown and Grove, 2008). Gardline Lankelma led the geophysical data acquisition, with Marine Ecological Surveys (MES) carrying out the environmental sampling. Data collection took place aboard the THV Alert, a 39m vessel owned by the Trinity Lighthouse from between 7th July to 13th August 2007 (Figure 57). The Simrad EM 3002D (300kHz) dual head multibeam sonar was used to gather .all files. Data processing of the multibeam bathymetry and backscatter data was carried out in Fledermaus, by NetSurvey Limited with Geocoder's Angular Range Analysis being carried on the data set. The Edgetech 4200 sidescan sonar was also used to gather dual frequency sidescan data (100kHz and 500kHz). Other geophysical data collected here includes sub-bottom profiler data and magnetometer data. The groundtruthing in the area includes geological and environmental grab samples at 70 sites, beam trawl samples at 30 sites and extensive seabed photographs and visual imagery. The geological grab sample data was collected using a hydraulic clam shell grab and the environmental sampling was carried out using Hamon grab.

Figure 57: The THV Alert was used for data collection as part of the Thames Regional Environmental Characterisation surveys of 2007 (from Trinity House, 2008)

5.3: Data Processing Methodology and Results Analysis

Most of the data used here was obtained in processed form, although the processing of the raw Simrad EM 3002 .all files was carried out in QTC Multiview. Similar steps as outlined in Section 4.3 were followed for classification of Tracks 11, 12 and 19 (~200km). Parameters which differed included that the dual head multibeam system produced a separate line for each head, with editing of the port and starboard side carried out separately in the QTC Image Viewer. More boarder edits for masking were required, with some noise present in the data due to variable weather conditions during acquisition, although data quality otherwise was of a good overall standard (Figure 58). The rectangle size used was 129 x 129, with 131124 records classified. The results showed the presence of 11 classes, with the .seabed file processed in QTC Clams (Figure 59). The visual imagery has been used to help verify the QTC classes.

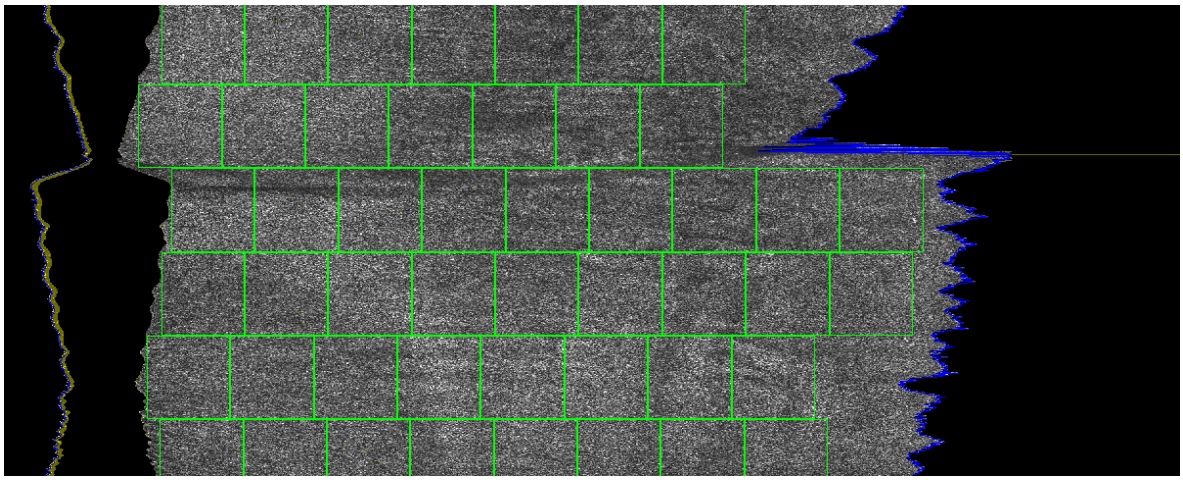

Figure 58: Rectangles generated in the QTC Multiview Image viewer, with boarder edits.

The Angular Range Analysis requires the partial stacking stage to be completed first, with the measured ARA parameters compared to the modelled ARA parameters. During the full model inversion, the roughness is calculated first, followed by the acoustic impedance (product of the bulk density and sound speed) and finally the grain size. The results are shown in Figures 60, 61 and 62 respectively, with Figure 63 comparing the remote estimates of the grain size with measured grain size based on the geological grabs.

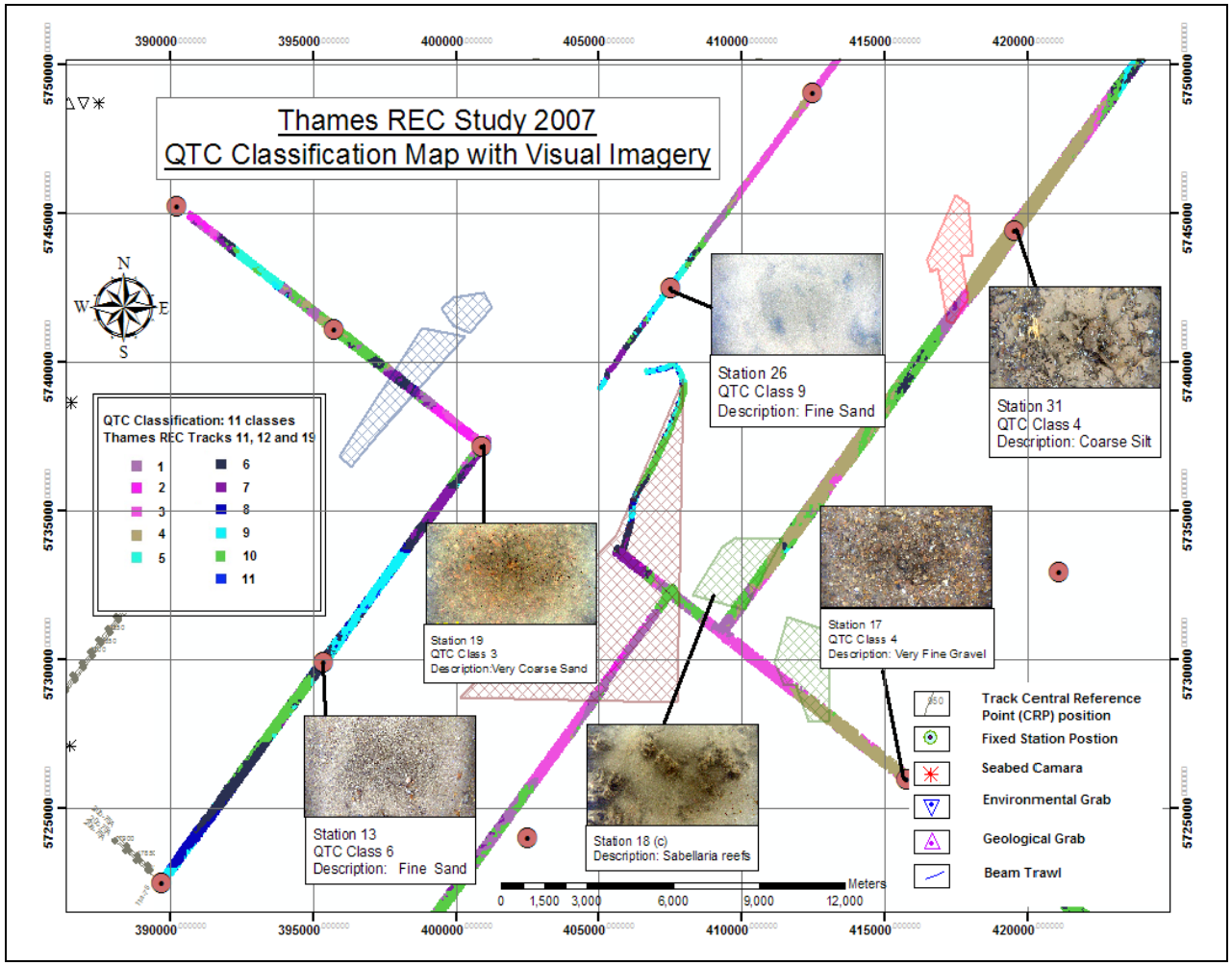

Figure 59: The QTC classification map of the Thames REC data with Visual imagery as groundtruthing. The aggregate extraction areas have separate classes, with the class boundaries corresponding to the polygons.

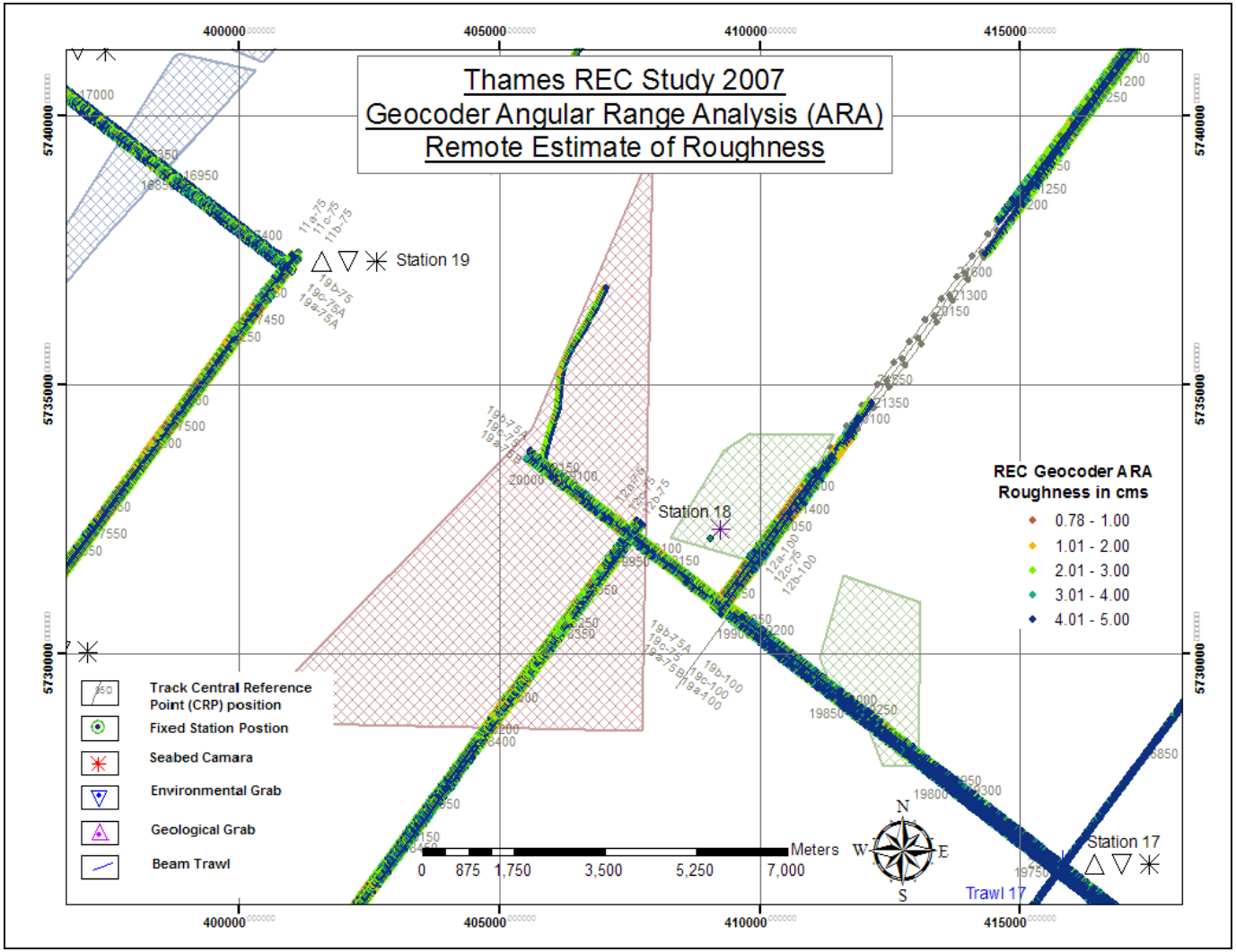

Figure 60: The remote estimate of roughness made by Geocoder's Angular Range Analysis for the study area.

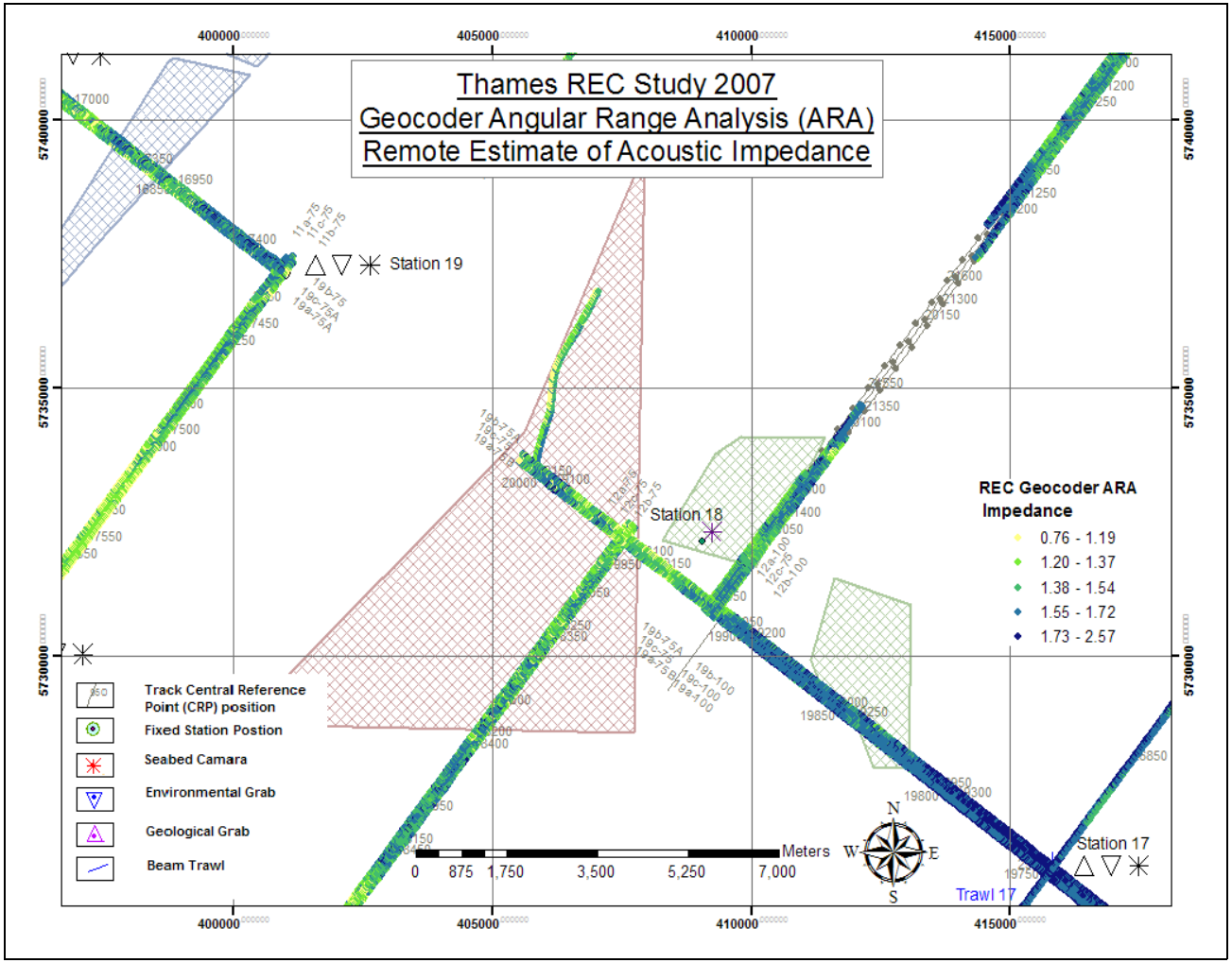

Figure 61: The remote estimates of impedance acquired using Geocoder's Angular Range Analysis for the study area.

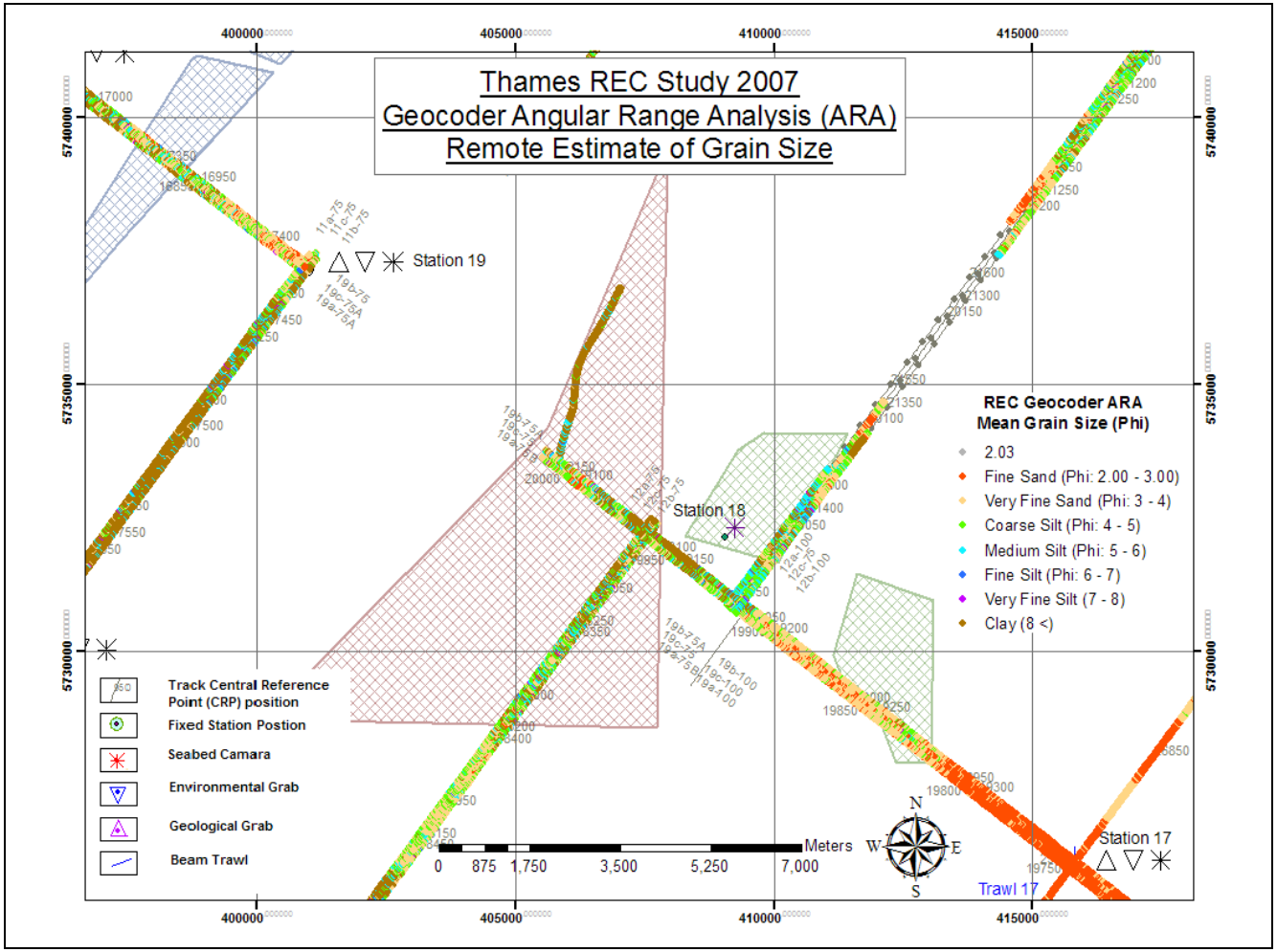

Figure 62: The remote estimates of the grain size made using Geocoder's Angular Range Analysis for the study area.

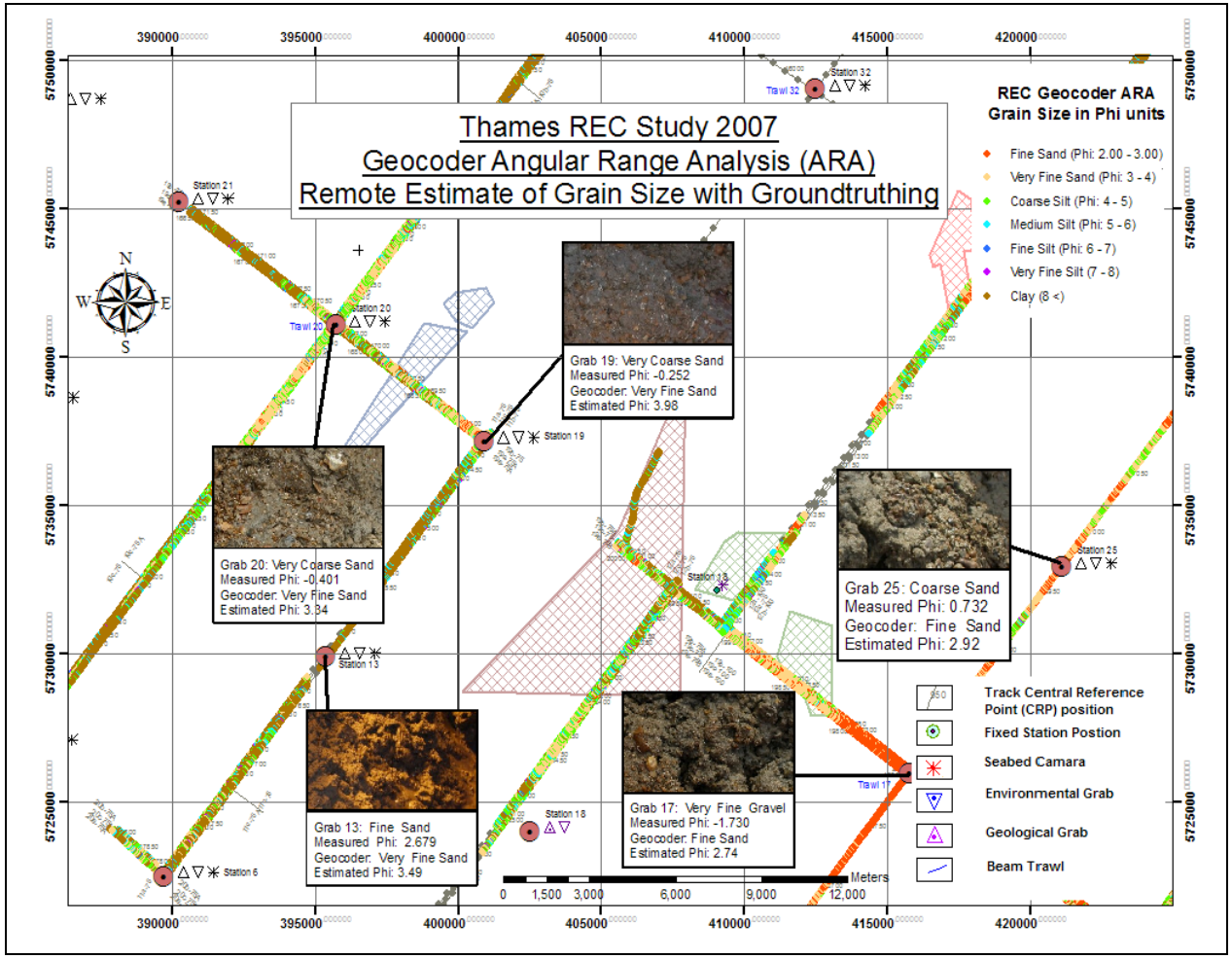

Figure 63: The remote estimates of grain size acquired using Geocoder's Angular Range Analysis with groundtruthing.

An assessment of accuracy of Geocoder's remote estimates of grain size

To assess the accuracy of Geocoder's grain size further, the measured grain sizes from 50 grabs were compared with the remote estimates. Twenty grabs did not have any multibeam coverage and hence were not used. This was carried out in ArcGIS, with Geocoder's estimates (point data) being gridded in a 25 x 25m grid, to enable comparison with the grab locations. The results of this were plotted against the measured Folk and Ward grain size and are shown in Figure 64. Examination of the Grain size data also showed the presence of one mode value, which is may be an artefact. This histogram revealed that there were a large number of pixels with 9 as the grain size, representing a seabed composed of clay (Figure 65). Although the Thames region contains numerous clay deposits, the groundtruthing at the grab sites do not verify the predicted presence of clay.

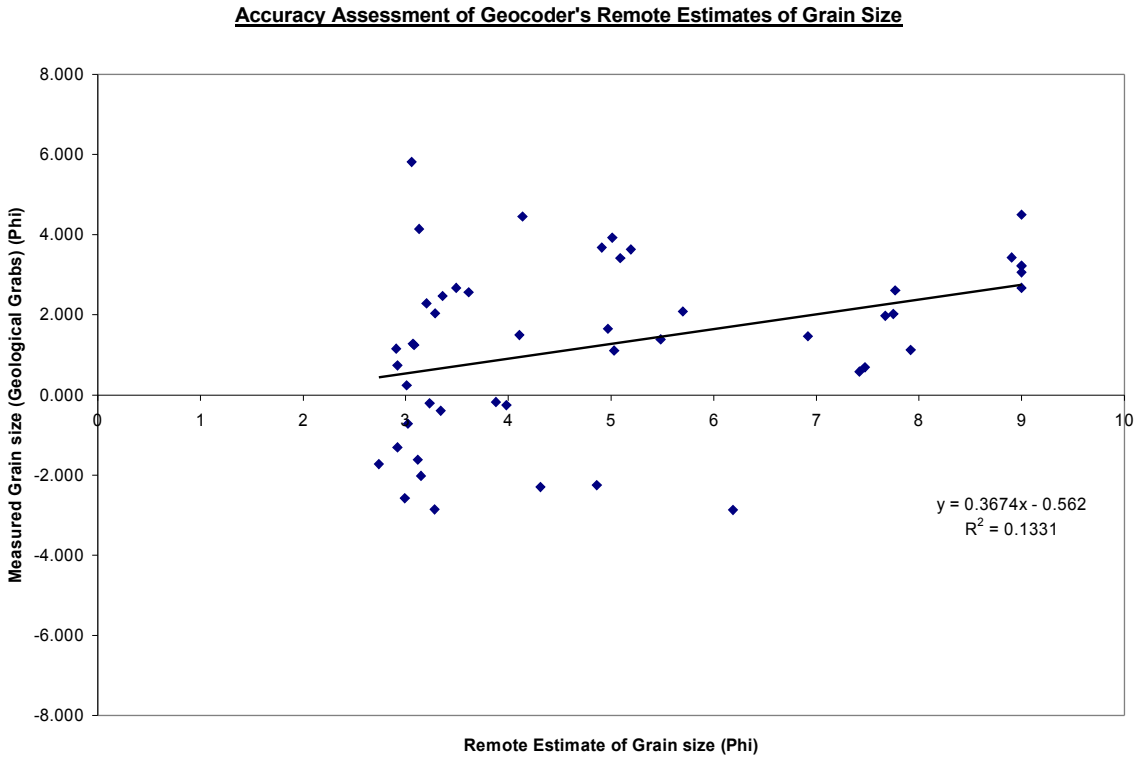

Figure 64: Scatter plot of the remote estimate of grain size and the measured grain size.

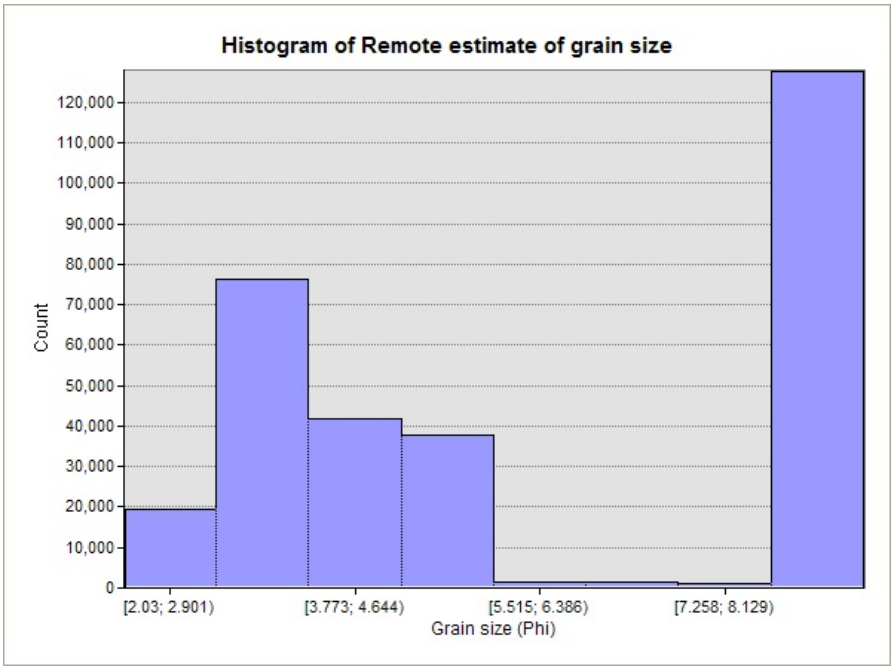

Figure 65: Histogram of the remote estimate of grain size of the Thames REC data shows the dominance of a grain size of 9.00 on the Phi scale.

In contrast with the North Edinburgh Channel Geocoder results, the results do not show good agreement with the groundtruthing. Nevertheless, examining Figure 61 and 62, the grain size results and the impedance results show the presence of a boundary at the aggregate extraction areas. This suggests that Geocoder is able to effectively differentiate between different classes or “themes” of sediment types, with further discussion in the next chapter.

Chapter 6: Discussion

The primary aim of this study has been to assess the potential of two different seabed classification methods for seabed characterisation and to compare and contrast the findings. Blondel, 2002 has made an important distinction between seabed classification and seabed characterisation. Seabed classification is the partitioning of an image into discrete physical entities, whereas seabed characterisation makes the link between the classified regions and the seabed physical, geological, chemical or biological properties (Blondel, 2002). The previous chapters have used the QTC image-based classification methods and the angular response characterisation approach used by Geocoder to obtain a range of results. Geocoder results discussed here including backscatter mosaics, partial stacking results, angular response curves and the Angular Range Analysis results. The QTC results include the Thames Regional Environmental Characterisation classification map, the unsupervised classification from the North Edinburgh Channel and the supervised maximum likelihood classification using the QTC eigenvectors. To conclude the study, the two methods are compared and contrasted, assessing the merits and limitations of each method for accurate seabed characterisation.

6.1. The Geocoder Approach

Geocoder is a primarily mosaicking software and its release has no doubt improved the quality of the multibeam backscatter mosaics. Backscatter mosaics are the first step to qualitative seabed characterisation and contain information about the spatial variability in the returns. Viewing the data also helps to assess its quality. Mosaics from the North Edinburgh Channel show differences in the output depending on the type of backscatter data logged, as well as the nature of the processing applied. The beam-average backscatter mosaic from the Reson 8125 data clearly shows the high values of backscatter strength from the relocated material (Figure 24). This corresponds very well to the difference model showing where the material has been disposed (Figure 23). Contrary to the expected findings, the snippet mosaic does not show as much of a contrast as the beam averaged data (Figure 25). Possible reasons include averaging of the high resolution data acquired, or the

way the gsf files are created in Hysweep. Also, work is still ongoing to improve Geocoder's method of constructing the snippet mosaics and it may be to do with how Geocoder's snippet routines are integrated into Hypack (Fonseca, 2008). Geocoder's mosaicking tools are a significant improvement to previously available mosaicking software, as demonstrated by the mosaic constructed using Hyscan (Figure 26). The pseudosidescan mosaic constructed in Geocoder is the most effective of all the mosaics at delineating the relocation area (Figure 27). Features visible include the mounds of dredged material, numerous sand waves and also the terraces in the North West (Figure 27 and 66).

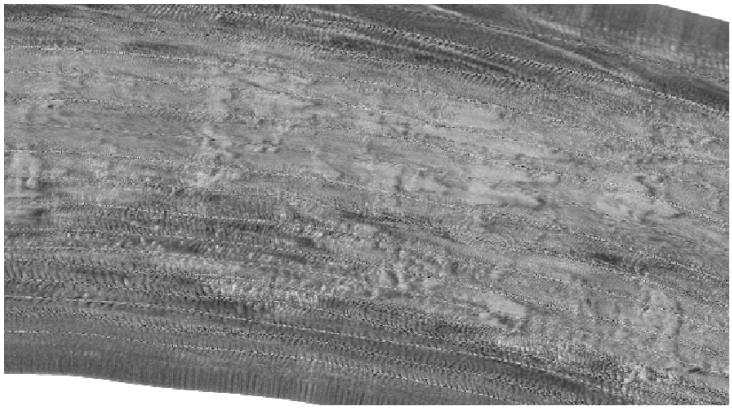

Figure 66: The relocated material is clearly visible in the Reson 8101 pseudosidescan mosaic constructed in Geocoder.

Additionally, this Reson 8101 mosaic shows better resolution than the Reson 8125 mosaics (Figures 24 and 27). Reson 8125 is a higher resolution system, which in theory obtains backscatter data of a higher quality. Still, the Reson 8101 pseudosidescan data originates from the Hypack hsx files and is the original raw data. The findings may be explained by the software used for logging the backscatter data. Hypack 2008 was used to log the Reson 8125 data, where as the Reson 8101 data was logged in Hypack Version 6. Due to the higher data volumes acquired by new multibeam systems, Hypack have had to decimate the files to make them more manageable in Hypack 2008 (Maddock, 2008). The previous version of Hypack does not carry out this decimation to the same extent.

The partial stacking stage from the North Edinburgh channel helps to demonstrate the theory behind the angular response characterisation method. The response from the same area varies in the different domains. This supports the idea that the angular response is affected by the seabed type. Overall, the near AVO gives higher absolute backscatter strength than the far-AVO (Figure 29). This is because the near-AVO shows the backscattered responses from the near-nadir domain of the angular response curve. The near AVO shows low values in the deep area in the east with some higher values in the area of relocation. Nevertheless, there is a notable absence of the return from the relocated material with only some medium values (Figure 29).

In contrast, the far-AVO response clearly shows the presence of the relocated material, corresponding again very well with the difference model (Figure 30 and Figure 23). The far-AVO also shows low values in south east, which corresponds to the QTC Class 13 composed of fine sand and silt. The physical processes affecting backscatter strength in this far-domain include the volume scattering contribution due to volume heterogeneities. These results demonstrate how the partial stacking approach helps to preserve the angular information provided by multibeam systems.

The angular response curve at each grab sample varies with seabed type, as recapped in Figure 67a and 67b. The response from grab 1, relocated material composed of fine sand with abundant shell, shows a higher value of backscatter strength than Grab 4, composed of fine sand with silt. Key ARA parameters which vary are the far-intercept and the far slope, corresponding to changes in the impedance and roughness (Fonseca and Mayer, 2007).

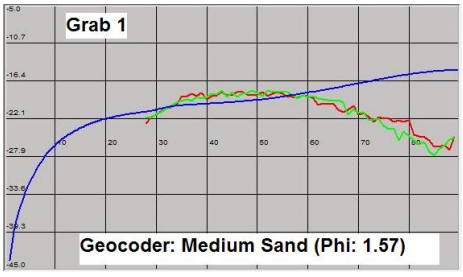

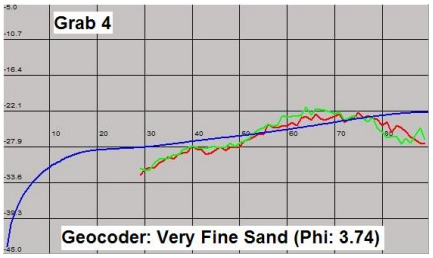

Figure 67a and 67b: The AR curves from Grabs 1 & 4 show the differences in the response.

The Patch AVO tool performs model inversion on the selected patch to obtain an estimate of the grain size and is possible in the Hypack 2008 version of Geocoder. The results of the estimate of the grain size from the Reson 8101 data match very well with the groundtruthing compositions as shown in Table 4. Table 4 contains the same data as in Table 2, only the grabs have been put in ascending order according to their grain size. This shows that Geocoder is effectively able to determine not only the composition of the patch, but also differentiate between smaller differences. For example, as the composition of the grabs becomes finer, the phi estimate also correspondingly increases.

Table 4: The results of the groundtruthing in the North Edinburgh Channel, with the corresponding QTC Classes and Geocoder remote estimates of the grain size.

Grab No	Grab Location Notes	Grab Basic Composition	Geocoder Composition	Geocoder Grain size	
1	Sand Placement grid- fine sand with clay	Fine to coarse sand with abundant shell	Medium Sand	1.57	Coarser
3	Sand Placement grid- fine sand	Fine to coarse sand with silt and shell	Fine Sand	2.06	
2	Relocated sediment based on bathymetry	Fine to coarse sand with silt and shell	Fine Sand	2.24	
5	Near south east- QTC class 7 (Green)	Fine to medium sand	Very Fine Sand	3.65	
6	Northern - QTC class 6 (Dark Blue)	Fine to medium sand with silt	Very Fine Sand	3.68	
4	Outer south east - QTC class 13 (Light Blue)	Fine sand with silt	Very Fine Sand	3.74	Finer

Both the Geocoder grain size and the measured grain size suggest that the relocated material is of a more coarse composition than the original seabed in the North Edinburgh Channel. Clay has not been relocated here as stated in the license. The material is composed of fine to coarse sand with shell fragments, with the Geocoder estimates for grabs 2 and 3 being quite similar (Figure 42). There are also some areas in the south east and north which contain different fractions of silt. The area in the outer south east of the North Edinburgh Channel contains material with the finest grain size.

The grab compositions are of greater detail than the description provided by Geocoder. For example, Geocoder approximates the Grab 1 composition to be medium sand, whereas the grab composition reveals that the relocated material is composed of a mixture of coarse to fine sand with abundant gravel sized shell material. Geocoder is determining an average value of the grain size in a particular patch, highlighting the issue of the resolution of the grain size estimate. The minimum possible patch size is half a swath width as this is by definition required to obtain the angular response. It is mandatory to average the angular response across 20-50 pings in order to get a representative sample of backscatter less affected by stochastic fluctuations. This lower resolution has previously restricted the practical application of the angular response characterisation method.

The resolution of ARA may be a possible reason for the lower agreement of the remote estimates with the grab grain sizes in the Regional Environmental Characterisation data set. The accuracy assessment shows poor agreement with the groundtruth, with a majority of the grabs not matching the measured value (Figure 64). This is likely to be due to the differences in the sampling scale of the remote estimate and that of the grab sample. Nevertheless, the dominance of one value in the histogram of the grain size suggests that this grain size estimate contains artefacts (Figure 65). Assessing the accuracy of the remote estimate of the grain size in this way is not the most suitable approach, due to this sampling scale difference. It is however the only feasible way of assessing Geocoder's accuracy.

All three ARA results from the Thames REC data do show the boundaries of the aggregate extraction area as shown in Figure 68. Figure 63 also shows the estimated fine sand areas being verified to be coarse sand areas for three grabs. This suggests that although the absolute value of the grain size estimates may not be correct, the relative accuracy may be higher. There is a possibility of a systematic error or bias affecting all the remote estimates, rather many random errors. If this is the case, this highlights the need for the angular response characterisation method to have calibrated and corrected values of backscatter strength. This is especially important when using the quantitative estimates from Geocoder on (continuous data) to classify discrete regions.

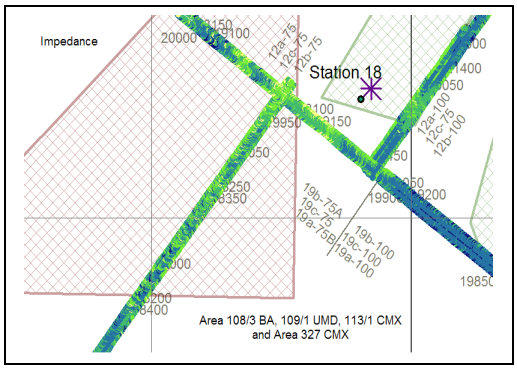

Figure 68: The impedance values in the REC data show changes corresponding to the area of aggregate extraction. An important point to note here is the quantitative estimates belong to a continuous distribution, and therefore would need to be "classified" by colour in GIS.

The impedance estimates give lower values within the dredged area, with higher values in the surrounding region, suggesting that the seabed is less hard in the dredged region (see also Figure 61). This may be due to finer layers being exposed as a result of the top layer of sediment structure being removed. Surprisingly, the roughness estimates also have smaller values within the extraction areas. Overall, the Geocoder results from the North Edinburgh Channel suggest that the ARA method has great potential for estimating the grain size and the full release of the characterisation software will have many new applications. The REC results show potential for the software to discriminate between areas of different sediment type, although it is felt that the relative accuracy of the quantitative estimates is higher than the absolute accuracy.

6.2: The Quester Tangent Classification Approach

Image-based classification methods obtain discrete classes corresponding to the areas of similar acoustic properties. With subsequent verification using groundtruthing, classification maps can be used to extrapolate groundtruthing information to a larger area. The QTC unsupervised classification results from the Thames REC data found 11 classes. It shows the aggregate extraction areas very effectively, with the class boundaries correspond closely with the polygon boundaries (Figures 69a and 69b). The results indicate that the QTC classification of the REC data can distinguish the boundaries where aggregate extraction is occurring more effectively than Geocoder's estimates of the grain size (Figures 59 and 62). The class boundaries are more in line with the aggregate extraction polygons and the discrete regions can be identified more clearly than with the grain size estimates. The classification map can also be used to monitor where aggregate extraction is occurring and distinguish between different degrees of impacts.

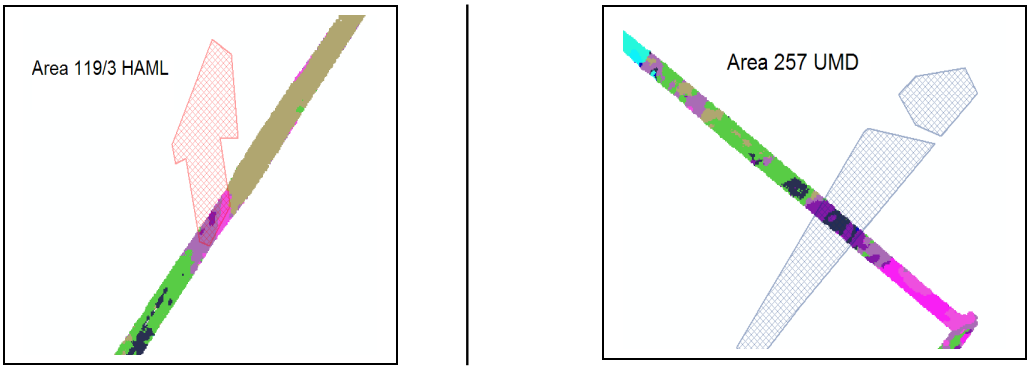

Figure 69a and 69b: The QTC classification is able to distinguish the dredged areas.

The comparison with the groundtruthing of the REC data identifies the classes as shown in Figure 59. Key points to note include the conflicting identification of REC Class 4. At station 17, this class has been identified as being composed of very fine gravel, whereas at station 31, it is identified as being composed of coarse silt. Unsupervised classification divides the classes depending on the features extracted from the image, rather than previous knowledge of the area. It can sometimes give one class which correspond to different

bottom types in different areas. Here, supervised classification is one possible alternative and this has been carried out in the North Edinburgh Channel.

The North Edinburgh Channel QTC unsupervised classification map clearly differentiates between the relocation area, with results recapped in Figure 70. The classification map found 14 classes, representing areas with different acoustic signatures. This is a large number of classes, with some classes distinguishing between finer differences in the sediment, as well as others corresponding to noise. This is one potential limitation of unsupervised classification, although the QTC software does allow manual clustering to merge (or split) similar clusters. The Auto-cluster option was used here, although manual clustering could also be carried out to improve the data processing strategy.

The relocated sediment has a group of classes, including classes 1, 3 and 5 (pink) and shows good agreement with the sand placement grid (Figure 41). There is some evidence of movement of the relocated material towards the east, suggesting the current is strongest in the direction of the ebb. The boundaries of the QTC relocated classes agree well with the bathymetric difference model, and also Geocoder's Far AVO results (Figure 23 and 30). By integrating the unsupervised classification results with the groundtruthing, the compositions of the relocated sediment classes can be identified to be fine to coarse sand with silt and shell (Table 2 & 4, Figure 43). The grabs with the sediment type mixtures show that the relocated sediment is of a more coarse composition than the surrounding region of fine to medium sand. The QTC Class 3 within the relocation area was identified to be composed of material with higher shell content, as opposed to higher clay content as hypothesised by the sand placement grid (Figure 42). With subsequent surveys, seabed classification can therefore be used to monitor the migration of the dredged material with time. The classification map and groundtruthing of the North Edinburgh Channel also show the extent of the finer more silty material located in the south east of the area (Figure 43). This is represented by QTC class 13 and QTC class 7. A summary of the QTC classes identified by the groundtruthing in are shown in Table 5.

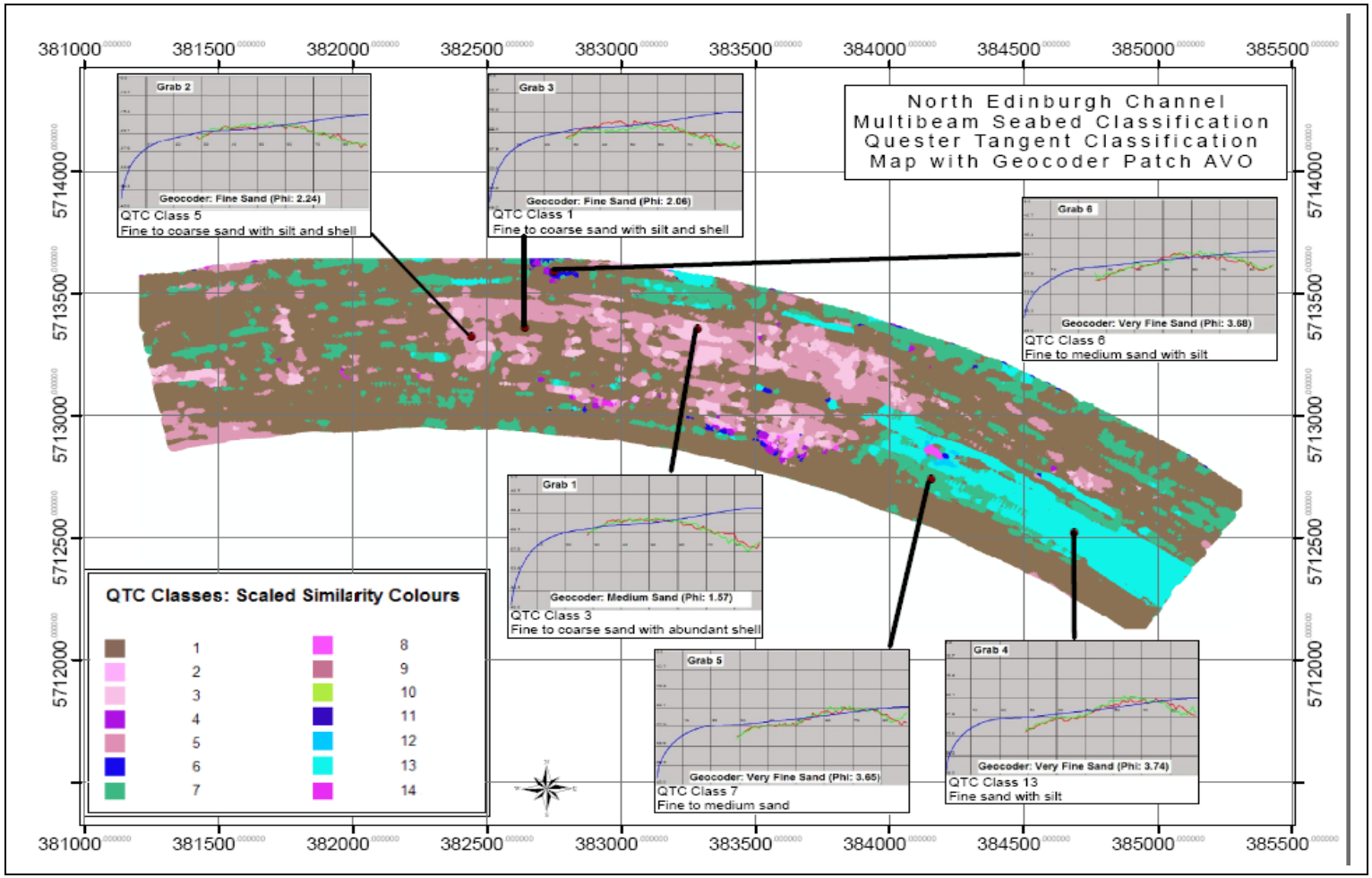

Figure 70: The QTC classification map with the angular response curves from Geocoder and groundtruthing results.

Table 5: The North Edinburgh Channel QTC classes with grab compositions.

QTC Class	Grab Basic Composition	Grab Location Notes
Class 3 (Light Pink)	Grab 1- Fine to coarse sand with abundant shell	Sand Placement grid- fine sand with clay
Class 5 (Pink)	Grab 2- Fine to coarse sand with silt and shell	Relocated sediment based on bathymetry
Class 1 (Brown)	Grab 3- Fine to coarse sand with silt and shell	Sand Placement grid- fine sand
Class 13 (Light Blue)	Grab 4- Fine sand with silt	Outer south east - QTC class 13 (Light Blue)
Class 7 (Green)	Grab 5- Fine to medium sand	Near south east- QTC class 7 (Green)
Class 6 (Dark Blue)	Grab 6- Fine to medium sand with silt	Northern - QTC class 6 (Dark Blue)

The QTC image based approach allows greater flexibility than the Geocoder approach, with data analysis possible at the intermediate stages. The Q values output of the Principal Component Analysis stage, show the 3 key features accounting for most of the variance and are the dimensions of feature space. Figures 47, 48, 49 and 50 shows that the Q1 value highlights the classes belonging to the area of relocation and the south east class, with Q2 showing the QTC class 6 in the north and Q3 also highlights the south east QTC class 13.

This output increases the range of processing options available, using other GIS or image processing systems. The training data set is based on the area around the grabs, and hence the results show 6 classes. The results shows similar trends as the unsupervised classification, only with the QTC Class 1, with the largest area in the classification map, further divided into subclasses. This class was concluded to be somewhat inconsistent with the previous groundtruthing during the accuracy assessment and hence this modified classification is thought to be more correct here. It could be argued that the supervised classification is in fact a hybrid classification as the grab sample locations used to determine the training areas have been selected based on the unsupervised classification map.

6.3: Conclusions of the Comparison

To conclude the study this section puts the results from the North Edinburgh Channel and the Thames REC areas in a broader context. The Quester Tangent image-based classification approach uses textural analysis algorithms for seabed classification. It has a different approach altogether from angular response characterisation, removing the angular information from the image. It does not depend on having absolute values of backscatter strength and the angular information provided by multibeam systems. Therefore this method is applicable to a wider range of systems, including sidescan sonar imagery. A key requirement is that thorough cleaning needs to be carried out on the data, to correct for the angular dependence of backscatter. The Geocoder approach makes use of this angular information and requires absolute values of backscatter strength to obtain the backscatter angular response curve.

A key difference between the Geocoder and the QTC approach to seabed classification is the type of results it determines. The QTC software classifies the area into discrete seabed types whereas Geocoder links the raw measurement of backscatter strength to the physical properties of the seabed. This has the advantage of being able to determine remote estimates of the grain size of the sediment quantitatively. Still, the software relies on the suitability of the acoustic backscatter model. For example, data processing in the North Edinburgh Channel shows that the frequency dependence of the backscatter models can sometimes be a limiting factor for the applicability of the software. The remote estimates of grain size from the North Edinburgh Channel shows promise with good agreement with groundtruth. The REC ARA results show good relative accuracy, although the absolute accuracy of the remote estimates of the grain size is not very high. This is thought to be due to the differences in resolution of the grain size estimates and the measurement. The resolution of angular response characterisation is restricted to half a swath width patch. Theme analysis is being incorporated into Geocoder, and will allow better estimates of the angular response.

The QTC software does not have this limitation and also is able to accept a wider range of data types. The Geocoder software is still in its developmental stages where as the QTC approach has been tried and tested. QTC results from the North Edinburgh Channel show that the software is able to discriminate between a range of complex sediment mixtures, including different fractions of shell material within the relocation area. The QTC classification map from the REC data also shows the boundaries overlaying with the aggregate extraction polygons more clearly.

Furthermore, the QTC classification results can be used in combination with the Geocoder Patch AVO results (Figure 70). The Patch AVO tool could even be used to identify the composition of a QTC class without groundtruthing. This combined approach using both methods simultaneously makes use of the merits of both software. Whereas the QTC software can effectively distinguish between discrete areas of different acoustic properties, Geocoder is able to give quantitative estimates of the sediment properties. Seabed classification increases the possible applications of multibeam data and should be considered a realistic option for organisations involved in seabed mapping.

Reference List

ALSF (2008). "Call for Expression of Interest Thames Regional Environmental Characterisation (REC) Programme - Data Analysis and Interpretation." Available online [http://www.alsf-mepf.org.uk]

Beaudoin, J., Hughes Clarke, J., van den Ameele, E. and Gardner, J. (2002). "Geometric and radiometric correction of multibeam backscatter derived from Reson 8101 systems." *Proceedings of the Canadian Hydrographic Conference* 2002, Canadian Hydrographic Association, Ottawa, Ontario, Available online: [http://ccom.unh.edu/publications/Beaudoin_2002_CHC_Geometric_Correction_Derived_from_Reson_8101.pdf]

Biot, M. (1956a). "Theory of Propagation of Elastic Waves in a Fluid-Saturated Porous Solid. I. Low-Frequency Range." The Journal of the Acoustical Society of America 28: 168.

Biot, M. (1956b). "Theory of Propagation of Elastic Waves in a Fluid-Saturated Porous Solid. II. High-Frequency Range." The Journal of the Acoustical Society of America 28: 173.

Blondel, P. (2000). "Automatic mine detection by textural analysis of COTS sidescan sonar imagery." International Journal of Remote Sensing 21(16): 3115-3128.

Blondel, P. (2002). Seabed Classification at Ocean Margins. Ocean Margin Systems. In G. W. e. al. Heidelberg, Springer: 125-141.

Blondel, P. and B. Murton (1997). Handbook of seafloor sonar imagery, *Chichester*. John Wiley and Sons.

Blondel, P. and L. Parson (1998). "Quantitative characterisation of geological processes using sidescan sonar imagery." Underwater Applications of Image Processing (Ref. No. 1998/217), IEE Colloquium on: 2.

BMAPA (2007). BMAPA website [http://www.bmapa.org/]

Boyd S.E., R.A. Coggan, S.N.R. Birchenough, D.S. Limpenny, P.E. Eastwood, R.L. Foster-Smith, S. Philpott, W.J. Meadows, J.W.C. James, K. Vanstaen, S. Soussi and S. Rogers, (2006). "The role of seabed mapping techniques in environmental monitoring and management." Sci. Ser. Tech Rep., Cefas Lowestoft, 127: 170pp. Available online: http://www.cefas.co.uk/publications/techrep/techrep127.pdf.

Brissette, M. and J. Hughes Clarke (1998). "Side Scan Versus Multibeam Echo Sounder Object Detection: Comparative Analysis." INTERNATIONAL HYDROGRAPHIC REVIEW 76(2): 21-34.

Brown, C. and V. Grove, (2008). "Thames REC Operations report." Available online [http://www.alsf-mepf.org.uk/survey]

Chu, D. and L. Hufnagle (2006). "Time varying gain (TVG) measurements of a multibeam echo sounder for applications to quantitative acoustics." Proceedings MTS/IEEE OCEANS 2006: 1-5.

Collier, J. and C. Brown (2005). "Correlation of sidescan backscatter with grain size distribution of surficial seabed sediments." Marine Geology 214(4): 431-449.

de Moustier, C. and D. Alexandrou (1991). "Angular dependence of 12-kHz seafloor acoustic backscatter." The Journal of the Acoustical Society of America 90: 522.

de Moustier, C. (1993). "Seafloor acoustic remote sensing with multibeam echo-sounders and bathymetric sidescan sonar system." Marine Geophysics Researches 15(1): 27-42.

Fish, J. and H. Carr (1990). Sound underwater images: a guide to the generation and interpretation of side scan sonar data, Lower Cape Pub.

Fonseca, L., L. Mayer, et al. (2002). "The high-frequency backscattering angular response of gassy sediments: Model/data comparison from the Eel River Margin, California." The Journal of the Acoustical Society of America 111: 2621.

Fonseca, L., L. Mayer, et al. (2004). "AVO Analysis of Multibeam Backscatter, An example from Little Bay, NH and Skjalfandi Bay, Iceland." American Geophysical Union, Fall Meeting 2004.

Fonseca, L. and B. Calder. (2005). Geocoder: An efficient backscatter map constructor. U.S Hydrogrphic Conference 1-9.

Fonseca L., (2006). Acoustic Backscatter and Remote Seafloor characterisation . Publication in International Marine Technicians Symposium, St Andrews, New Brunswick, Canada.

Fonseca L. B. R. Calder and M. Wetzler. (2006). "Experiments for multibeam Backscatter Adjustments on the NOAA Ship FAIRWEATHER". Americas IEEE Oceans, Boston, MA, USA., Sept06, 1-4

Fonseca L, and L. Mayer. (2007). "Remote estimation of surficial seafloor propeties through the application Angular Range Analysis to multibeam sonar data." Marine Geophysics Research 28: 119-126.

Fonseca L, (2008) Personal communication

Gilmour, N. (2008). "Advances in multibeam backscatter data processing and delivery of data product in a GIS Environment via Internet." Available online [http://www.fugro-pelagos.com/papers.asp]

Gubbay, S. (2005). A review of Marine Aggregate Extraction in England and Wales,1970-2005, BMAPA: 1-36. Available online http://*www.goodmarine.com/references*

Hamilton, E. (1974). "Prediction of deep-sea sediment properties: state-of-the-art." Deep-Sea Sediments: Physical and Mechanical Properties: New York (Plenum): 1-44.

Haralick, R. (1979). "Statistical and structural approaches to texture." Proceedings of the IEEE 67(5): 786-804.

Hughes-Clarke, J. E. H., (1996). "Shallow- water imaging multibeam sonars: A new tool for investigating seafloor processes in the coastal zone and on the continental shelf." Marine Geophysical Researches 18(607-629).

Hughes- Clarke, J. E. H., B. Danforth, et al. (1997). "Areal seabed classification using backscatter angular response at 95 kHz." SACLANTCEN Conf on High Frequency Acoustics in Shallow Water, Lerici, Italy: 243-250.

Jackson, D. and M. Richardson,. (2007). High-frequency seafloor Acoustics, Monograph series in Underwater Acoustics, Office of Naval Research. Springer.
Jackson, D. Winebrenner D.P,Ishamaru A (1986). "Application of the composite roughness model to high-frequency bottom backscattering." Journal of Acoustical Society of America 79(5): 1410-1422.

Johnson, H. and M. Helferty (1990). "The geological interpretation of side-scan sonar." Reviews of Geophysics 28(4): 357-380.

Lillisand T.M,, Keifer R.W,and_Jonathan W (2008)Remote Sensing and Image Interpretation, Sixth Edition Chipman: Books.

Liu, J.G., and P. Mason (2007) Image processing and GIS course notes. Earth Science and Engineering, Imperial College, London.

Lockhart, D et, al (2001). "New development in multibeam backscatter." Available online [http://www.fugro-pelagos.com/papers/newdevinmulitbeambackscatter/TGPI_Backscatter.htm.]

Lurton, X. (2002). An Introduction to Underwater Acoustics: Principles and Applications, Springer Praxis

Meurling, T, Baldwin M, Lockhart D and Malzone C (2008). "The Ultra High resolution future of Hydrography." Available online [http://www.fugro-pelagos.com/papers/High-Res_Future.pdf]

Moore (2007). "Marine ALSF GIS."[http://www.alsf-mepf.org.uk/downloads]

Parnum, I., P. Siwabessy, et al. (2004). Identification of seafloor habitats in coastal shelf waters using a multibeam echosounder, Acoustics.

Port of London Authority (2003). "Princes Channel Development, Recycling of Dredged Material in the Outer Thames Estuary, Environmental Scoping Report." Available online [http://www.pla.co.uk/pdfs/pe/EnvironmentalScopingReport.pdf]

Port of London Authority (2004). Princes Channel Development, Placement of Dredged Sand in the North Edinburgh Channel Environmental Characterisation Report. Available online: [http://www.pla.co.uk/pdfs/pe/EnvRep_Disposalv2_0.pdf]

Port of London Authority (2008). "Hydrographic Surveying vessels" Port of London Authority website [http://www.pla.co.uk/display_fixedpage.cfm/id/2211]

Port of London Authority, (2008b). Sand Placement Management Plan.

Pouliquen, E., M. T., P. Blondel, G. Canepa, F. Cernich, R. Hollet (2002). Multi-sensor Analysis of the seabed in shallow water areas: overview of the MAPLE'2001 experiment. 6th European conference of Underwater Acoustics.

Preston, JM, Christney, AC, Beran, LS, Collins, WT. 2004. Statistical seabed segmentation: from images and echoes to objective clustering. Proceedings of the Seventh European Conference of Underwater Acoustics, ECUA 2004 Delft, The Netherlands pp 813-818

QTC (2007). QTC Multiview user manual and reference.

QTC (2008). Quester Tangent Corporation Information CD.

Reed, T. and D. Hussong (1989). "Digital image processing techniques for enhancement and classification of SeaMARC II side scan sonar imagery." Journal of Geophysical Research 94(B6): 7469-90.

Robindoux L.(2008). "A Qualitative assessment of two MBES backscatter analysis approaches." Available online [http://pac.chs.gc.ca/files/session_8/P8-1_Robidoux_et_al.pdf.]

Trinity House. (2008). "Vessel services- Alert Information Sheet." Trinity House Website [http://www.trinityhouse.co.uk/pdfs/pdf_alert.pdf].

Tso, B. and P. Mather (2001). “Classification Methods for Remotely Sensed Data”, CRC Press.

Urick, R. (1967). Principles of underwater sound for engineers, 342 pp, McGraw Hill book company, New York.

Wessex Archaeology. (2004). "North Edinburgh Channel Dredging Disposal Area Archaeological Assessment." Technical Report. Available online [www.**wessex**arch.co.uk/]

Williams, K. (2001). "An effective density fluid model for acoustic propagation in sediments derived from Biot theory." The Journal of the Acoustical Society of America 110: 2276.

Wyatt G, (2008) Personal Communication

Appendix 1: Backscatter Models

Backscatter models aim to relate the factors affecting backscatter strength, with the measurement itself. Lambert's law is the simplest such model, which models the effect of angle of incidence on backscatter strength.

$$BS(\theta_i) = BS_0 + 20 \log \cos \theta_i \qquad \text{(Equation from Lurton, 2002)}$$

Equation: Lambert's Law links backscatter strength to angle of incidence.

Backscatter models and acoustic wave theory (Jackson and Richardson, 2007)

Most backscatter models are however much more complex and attempt to relate the sediment geophysical properties with the measured backscatter strength. Most backscatter models are also frequency specific and a particular backscatter model may not be applicable to the entire frequency range. Previous reviews have discussed the following framework as a useful way to group many of the different types of complex acoustic backscatter models (Jackson and Richardson, 2007). The acoustic wave theories upon which backscatter models are based can be divided into three types:

* Fluid Theory
* Elastic Theory
* Poroelastic Theory or Biot Theory

Each of these theories has different geophysical parameters included in the model. In turn, the geophysical properties of the sediments can be divided into two types; physical and the geoacoustic properties. The physical properties of the sediments include the mean grain size, permeability, porosity and bulk density. Geoacoustic properties include the acoustic impedance, compressional wave speed and attenuation. Fluid theory was used to form the basis of the oldest backscatter models and represents the sediment as a fluid medium. It uses the physical properties as input parameters and models the geoacoustic properties. The

simplest fluid model requires three geoacoustic parameters as inputs; the density ratio, sound speed ratio and the loss parameter. Hence, the main parameters accounted for in the backscatter models are the acoustic impedance, acoustic attenuation and also the roughness of the seafloor (Fonseca et. al, 2002).

The elastic theory takes into account the presence of shear waves and hence includes two additional parameters; the shear wave speed and the shear wave attenuation. This has been found to be a more useful model than the fluid model for seabed's composed of rock.

Models based on the poroelastic theory or Biot theory model the seabed as a porous media, as a fluid amongst a frame of grains (Biot, 1956a, Biot 1956b). It takes into account the seabed's elasticity as well as the porosity, resulting in many more parameters being required to model the nature of the seabed. The Biot theory makes the distinction that the displacement caused by acoustic waves, compression waves and shear waves has a different effect on the sediment frame and on the pore water fluid. Such models differ from the fluid models in that they require the physical parameter as inputs to model the geoacoustic parameters. This model is however difficult to apply in practice as it requires 13 parameters to be measured. The output parameters can then be used to estimate the backscatter strength, by applying the roughness approximations.

Effective Density Fluid Model (Williams, 2001)

The Geocoder software uses the Williams, 2001 "effective density fluid model." This combines the rigorous approach of models based on the Biot theory, only simplifying it to be more useful and widely applicable (Fonseca and Mayer 2007). It assumes two parameters, the frame modulus and the shear modulus to be negligible, with experiment results showing agreement with the full Biot model. Geocoder's ARA approach is based on the inversion of such a backscatter model and is discussed further in Chapter 3. A limitation of this backscatter model is that it should not be used to model backscatter acquired at frequencies greater than 300kHz.

Appendix 2: Assessing Classification Accuracy

A fundamental point to note when using any classification method is that, no classification map is 100% accurate. Hence, there is a need to assess the accuracy of the classification. The accuracy of a classification map is it's "closeness to truth" and hence this requires an independent method of verification using groundtruthing. One approach of assessing the relative accuracy of image based classification, is to form a confusion matrix of the classification output (Lillesand et. al., 2008). This involves resampling the training areas obtained at the first stage of supervised classification into two sets; one for supervised classification and the other for assessing the accuracy (Liu and Mason, 2007). Following this, a confusion matrix or contingency table is developed to compare the two datasets, with a row and a column for each class (Tso and Mather, 2001). It records the number of correctly identified pixels in each class and can be used for obtaining ratios for the number of correctly identified pixels vs. incorrectly identified pixels. Statistics which can be obtained include the overall accuracy, the producer's accuracy, the user's accuracy as well as the Kappa coefficient (Lillesand et. al., 2008). Nevertheless, this requires knowledge of what all the classes represent and is very dependent on the density of the groundtruthing. Groundtruthing is more difficult in the marine environment and therefore this can be a limiting factor when making quantitative estimates of the accuracy. Nevertheless, it should be stressed that all attempts practically feasible should be made to assess the accuracy. Also, a key consideration which needs to be made when designing a sampling strategy is the quality of the groundtruthing acquired.

Appendix 3: North Edinburgh Channel Groundtruthing

This appendix contains the photographs and particle size distribution analysis results of the grab sample collected from the North Edinburgh Channel.

Grab Number	Description	Photograph
1	Brown fine to coarse sand with abundant fine to coarse gravel sized shell fragments	
2	Grey-brown very slightly silty fine to coarse sand with occasional fine to coarse gravel sized shell fragments	

3	Grey-brown very slightly silty fine to coarse sand with occasional fine to coarse gravel sized shell fragments	
4	Grey very slightly silty fine sand	

5	Grey fine to medium sand	
6	Brown very slightly silty fine to medium sand	

BS1377 : Part 2 : Clause 9 : 1990

Determination of Particle Size Distribution

Sample Number: 001	Description: Brown fine to coarse SAND with abundant fine to coarse gravel sized shell fragments

BS1377 : Part 2 : Clause 9.3 : 1990 Dry Sieving Method

SIEVE	
Sieve	% pass
200 mm	100
125 mm	100
90 mm	100
75 mm	100
63 mm	100
50 mm	100
37.5 mm	98
28 mm	96
20 mm	95
14 mm	93
10 mm	90
6.3 mm	85
5 mm	83
3.35 mm	82
2 mm	78
1.18 mm	74
600 µm	72
425 µm	70
300 µm	64
212 µm	49
150 µm	19
63 µm	2

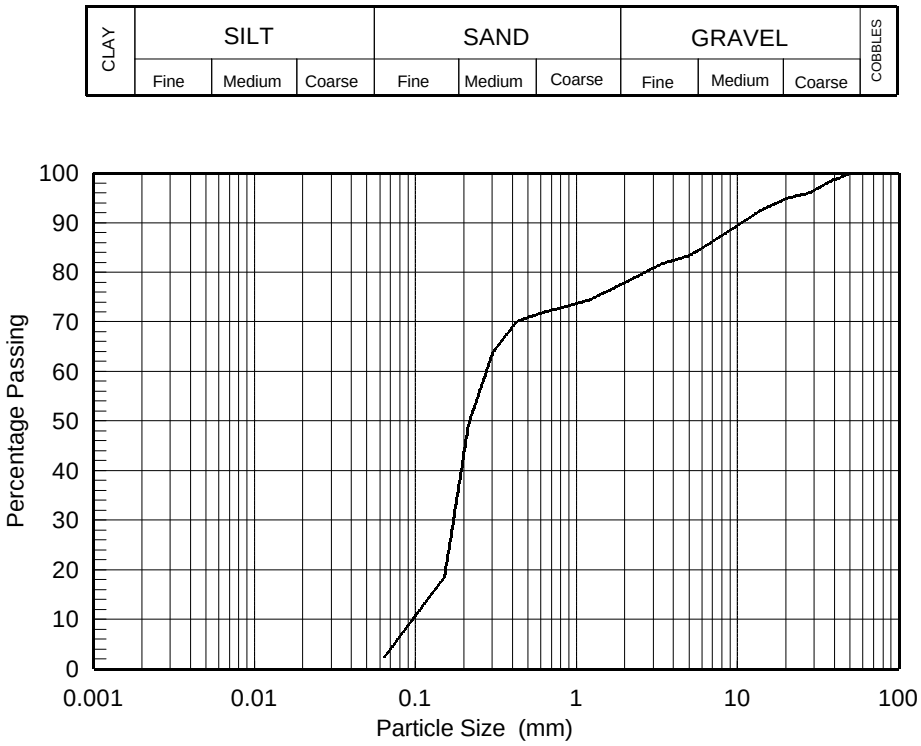

Particle Proportions		
Cobbles	0.0	%
Gravel	22.0	%
Sand	75.8	%
Silt & Clay	2.3	%

Checked and Approved	Project Number:	
Initials: JS	Project Name:	**GEO / 13653** **NORTH EDINBURGH CHANNEL**
Date: 27/08/2008		GEOLABS

BS1377 : Part 2 : Clause 9 : 1990

Determination of Particle Size Distribution

Sample Number: 002	Description: Grey-brown very slightly silty fine to coarse SAND with occasional fine to coarse gravel sized shell fragments

BS1377 : Part 2 : Clause 9.3 : 1990 Dry Sieving Method

SIEVE	
Sieve	% pass
200 mm	100
125 mm	100
90 mm	100
75 mm	100
63 mm	100
50 mm	100
37.5 mm	100
28 mm	100
20 mm	98
14 mm	97
10 mm	94
6.3 mm	91
5 mm	89
3.35 mm	88
2 mm	84
1.18 mm	80
600 µm	76
425 µm	75
300 µm	69
212 µm	51
150 µm	24
63 µm	5

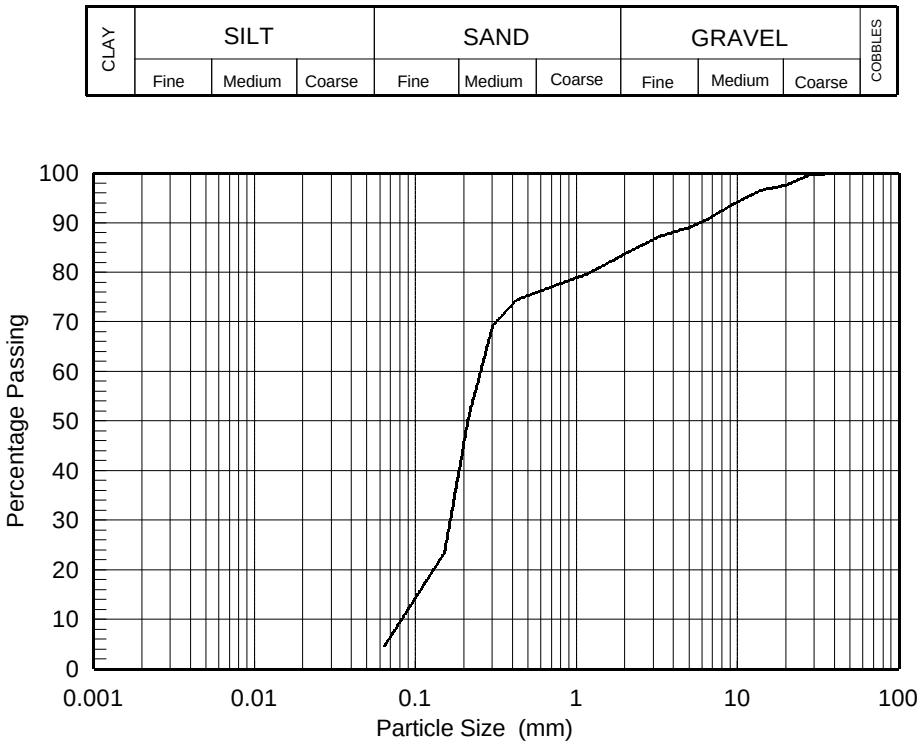

Particle Proportions		
Cobbles	0.0	%
Gravel	16.1	%
Sand	79.4	%
Silt & Clay	4.5	%

Checked and Approved	Project Number:	
Initials: JS	Project Name:	**GEO / 13653**
Date: 27/08/2008		**NORTH EDINBURGH CHANNEL**

GEOLABS

BS1377 : Part 2 : Clause 9 : 1990

Determination of Particle Size Distribution

Sample Number: 003	Description: Grey-brown very slightly silty fine to coarse SAND with very occasional fine to coarse gravel sized shell fragments

BS1377 : Part 2 : Clause 9.3 : 1990 Dry Sieving Method

SIEVE	
Sieve	% pass
200 mm	100
125 mm	100
90 mm	100
75 mm	100
63 mm	100
50 mm	100
37.5 mm	99
28 mm	98
20 mm	97
14 mm	97
10 mm	96
6.3 mm	95
5 mm	95
3.35 mm	94
2 mm	92
1.18 mm	90
600 µm	88
425 µm	86
300 µm	80
212 µm	55
150 µm	26
63 µm	4

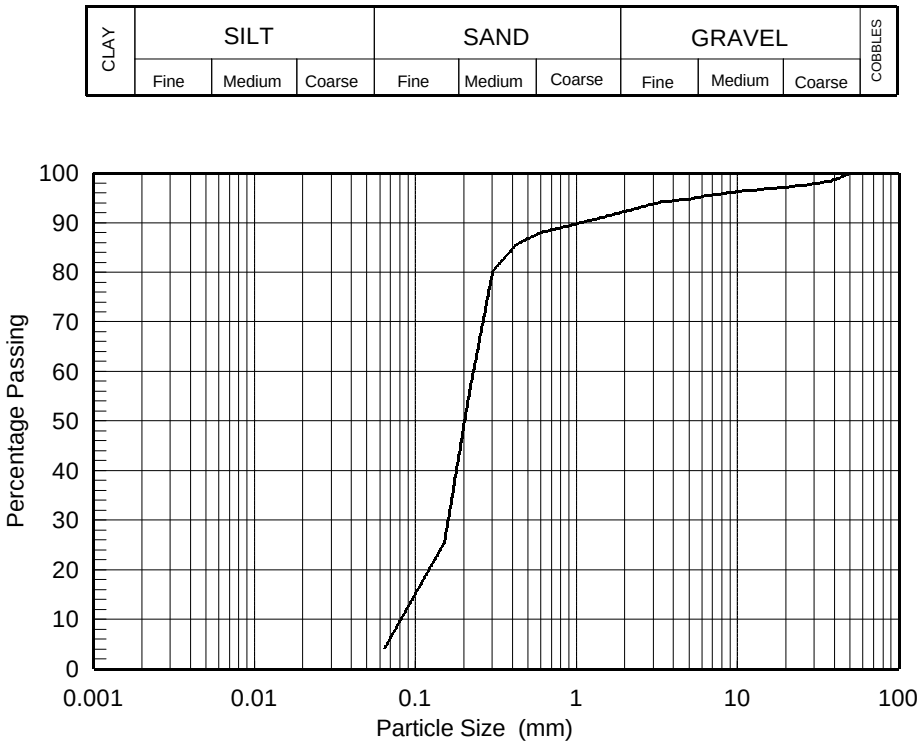

Particle Proportions		
Cobbles	0.0	%
Gravel	7.6	%
Sand	88.5	%
Silt & Clay	3.9	%

Checked and Approved	Project Number:	
Initials: JS	Project Name:	GEO / 13653 NORTH EDINBURGH CHANNEL
Date: 27/08/2008		GEOLABS

BS1377 : Part 2 : Clause 9 : 1990

Determination of Particle Size Distribution

Sample Number: 004	Description: Grey very slightly silty fine SAND

BS1377 : Part 2 : Clause 9.3 : 1990 Dry Sieving Method

SIEVE	
Sieve	% pass
200 mm	100
125 mm	100
90 mm	100
75 mm	100
63 mm	100
50 mm	100
37.5 mm	100
28 mm	100
20 mm	100
14 mm	100
10 mm	100
6.3 mm	100
5 mm	100
3.35 mm	100
2 mm	100
1.18 mm	100
600 µm	100
425 µm	100
300 µm	100
212 µm	99
150 µm	66
63 µm	5

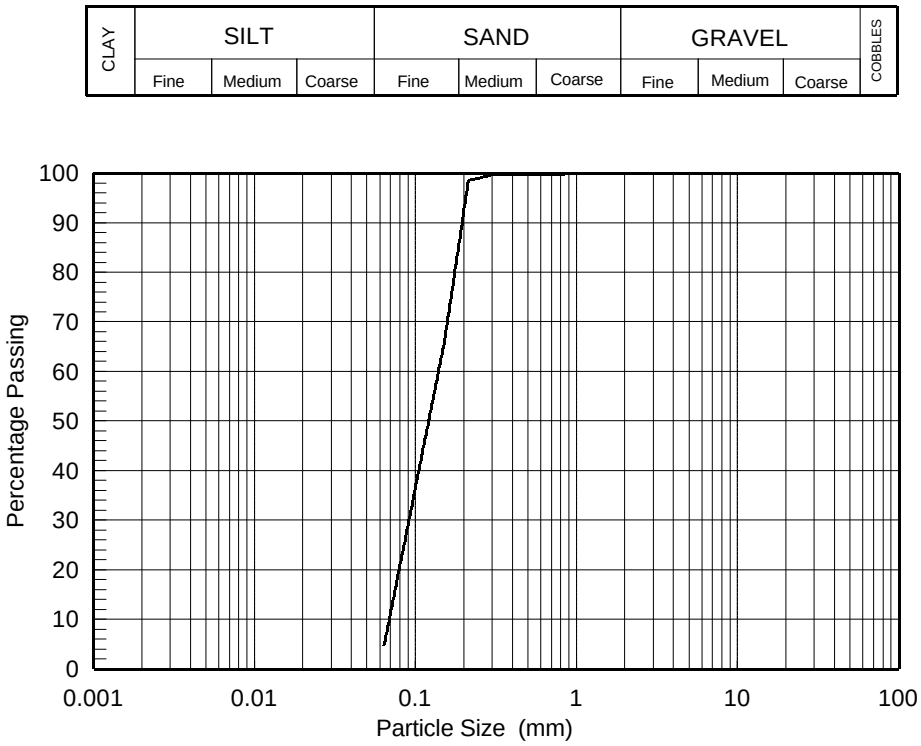

Particle Proportions		
Cobbles	0.0	%
Gravel	0.0	%
Sand	95.4	%
Silt & Clay	4.6	%

Checked and Approved	Project Number:	
Initials: JS	Project Name:	**GEO / 13653**
Date: 27/08/2008		**NORTH EDINBURGH CHANNEL**

GEOLABS

BS1377 : Part 2 : Clause 9 : 1990

Determination of Particle Size Distribution

Sample Number: 005	Description: Grey fine to medium SAND

BS1377 : Part 2 : Clause 9.3 : 1990 Dry Sieving Method

SIEVE	
Sieve	% pass
200 mm	100
125 mm	100
90 mm	100
75 mm	100
63 mm	100
50 mm	100
37.5 mm	100
28 mm	100
20 mm	100
14 mm	100
10 mm	100
6.3 mm	100
5 mm	100
3.35 mm	100
2 mm	100
1.18 mm	100
600 µm	100
425 µm	100
300 µm	100
212 µm	95
150 µm	48
63 µm	3

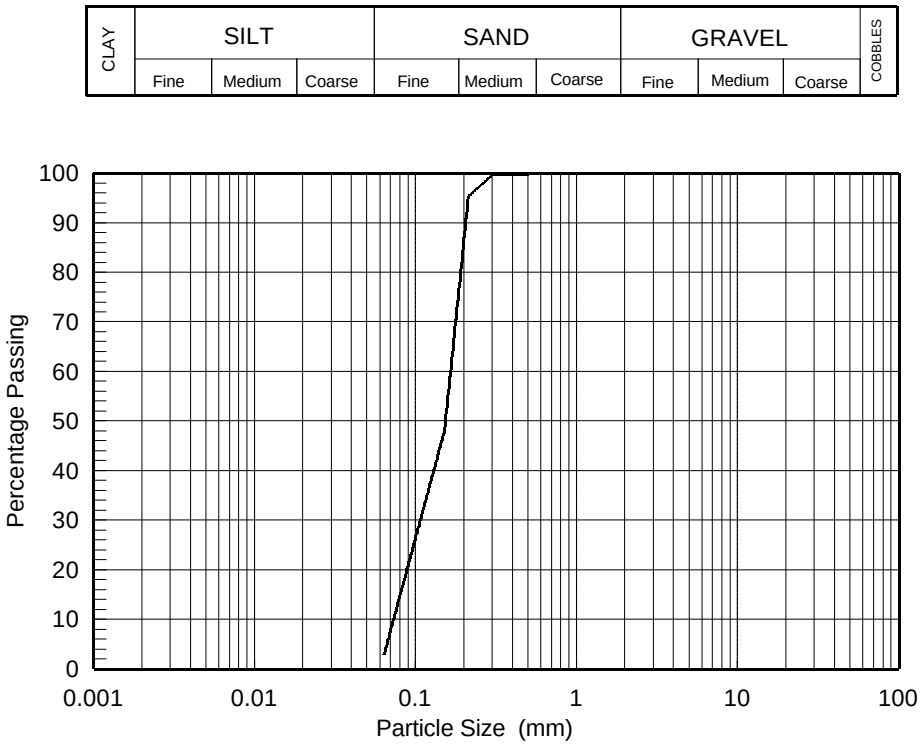

Particle Proportions		
Cobbles	0.0	%
Gravel	0.0	%
Sand	97.2	%
Silt & Clay	2.8	%

Checked and Approved	Project Number:	
Initials: JS	Project Name:	**GEO / 13653**
Date: 27/08/2008		**NORTH EDINBURGH CHANNEL**

GEOLABS

Authorised Signatories: • J R Masters (Qual Mgr) • C F Wallace (Tech Mgr) • G J Corio (Tech Mgr) [X] J Sturges (Tech Mgr) • S Burke (Snr Tech)

Client: Port of London Authority, London River House, Royal Pier Road, Gravesend, Kent DA12 2BG

BS1377 : Part 2 : Clause 9 : 1990

Determination of Particle Size Distribution

Sample Number: 006	Description: Brown very slightly silty fine to medium SAND

BS1377 : Part 2 : Clause 9.3 : 1990 Dry Sieving Method

SIEVE	
Sieve	% pass
200 mm	100
125 mm	100
90 mm	100
75 mm	100
63 mm	100
50 mm	100
37.5 mm	100
28 mm	100
20 mm	100
14 mm	100
10 mm	100
6.3 mm	100
5 mm	100
3.35 mm	100
2 mm	100
1.18 mm	100
600 µm	100
425 µm	99
300 µm	97
212 µm	52
150 µm	16
63 µm	5

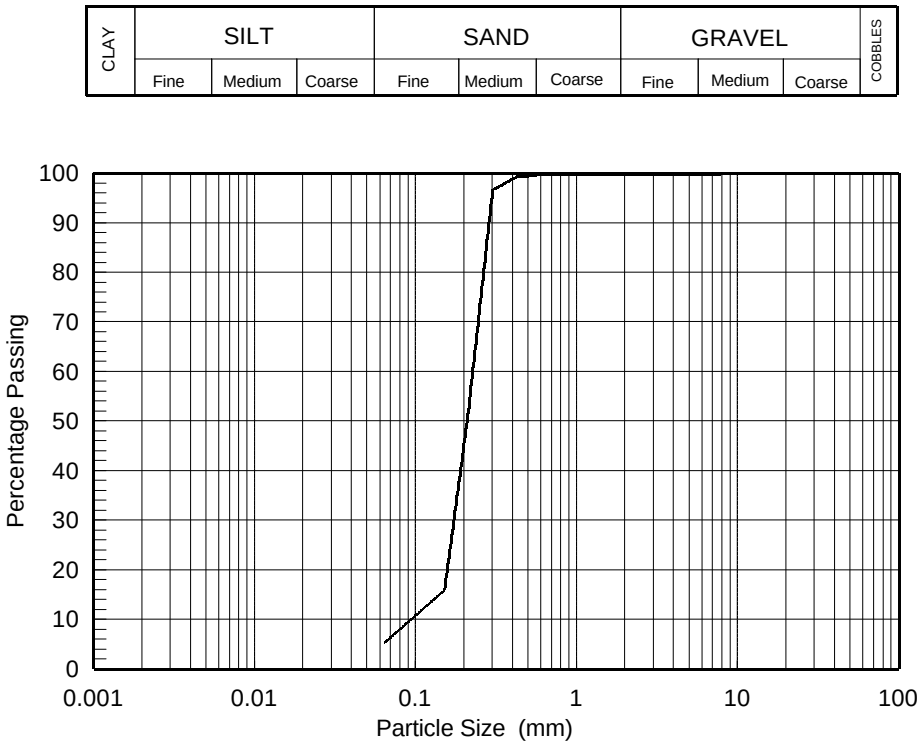

Particle Proportions		
Cobbles	0.0	%
Gravel	0.1	%
Sand	94.7	%
Silt & Clay	5.2	%

Checked and Approved	Project Number:	
Initials: JS	Project Name:	**GEO / 13653**
Date: 27/08/2008		**NORTH EDINBURGH CHANNEL**

GEOLABS